UNIVERSITY OF CALIFORNIA
SANTA CRUZ

SEASONAL DYNAMICS OF SEAWEED PRODUCTION IN A CHANGING OCEAN: IMPLICATIONS FOR BOTTOM-UP EFFECTS IN MARINE FOOD WEBS

A dissertation submitted in partial satisfaction
of the requirements for the degree of

DOCTOR OF PHILOSOPHY

in

ECOLOGY AND EVOLUTIONARY BIOLOGY

by

Lauren E. Bell

June 2023

The Dissertation of Lauren E. Bell is approved:

_____
Professor Kristy J. Kroeker, chair

_____
Professor Peter T. Raimondi

_____
Douglas B. Rasher, Ph. D.

_____
Professor Catriona L. Hurd

_____
Peter Biehl
Vice Provost and Dean of Graduate Studies

TABLE OF CONTENTS

LIST OF FIGURES

LIST OF TABLES

ABSTRACT

SEASONAL PRODUCTION DYNAMICS OF HIGH LATITUDE SEAWEEDS IN A CHANGING OCEAN: IMPLICATIONS FOR BOTTOM-UP EFFECTS ON TEMPERATE COASTAL FOOD WEBS

by Lauren E. Bell

As the oceans absorb excess heat and CO_2 from the atmosphere, marine primary producers face significant changes to their abiotic environments and their biotic interactions with other species. Understanding the bottom-up consequences of these effects on marine food webs is essential to informing adaptive management plans that can sustain ecosystem and cultural services. In response to this need, this dissertation provides an in-depth consideration of the effects of global change on foundational macroalgal (seaweed) species in a poorly studied, yet highly productive region of our world's oceans. To explore how seaweeds within seasonally dynamic giant kelp forest ecosystems will respond to ocean warming and acidification, I employ a variety of methods: year-round environmental monitoring using an in situ sensor array, monthly subtidal community surveys, and a series of manipulative experiments. I find that a complementary phenology of macroalgal production currently characterizes these communities, providing complex habitat and a nutritionally diverse energy supply to support higher trophic levels throughout the year. I also find that future ocean warming and acidification will lead to substantial shifts in the phenology, quantity and quality of macroalgal production in these systems. My results suggest that the giant kelp *Macrocystis pyrifera* may be relatively resilient to the effects of

global change in future winter and summer seasons at high latitudes. In contrast, the calcifying coralline algae *Bossiella orbigniana* and *Crusticorallina* spp. and the understory kelps *Hedophyllum nigripes* and *Neoagarum fimbriatum* will experience a suite of negative impacts, especially in future winter conditions. The resulting indirect effects on macroalgal-supported coastal food webs will be profound, with projected reductions in habitat and seasonal food supply on rocky reefs. Coming at a time of heightened interest in seaweed production potential at high latitudes, this dissertation provides a comprehensive evaluation of the future of these foundational organisms in a changing environment.

Dedicated to Lione Rae,

who was formed in tandem with this work.

May the world continue to be a wild, wonderous place for you to explore.

ACKNOWLEDGEMENTS

This research took place within Lingít Aaní, or Tlingit land, near Sheet'ká Kwáan, also known as Sitka, Alaska. My understanding of these ecosystems has been informed by the relationships that Lingít Peoples have developed with these lands and waters over millenia, and I endeavor to learn from and honor their knowledge, stewardship, and leadership.

I am grateful to a wide network of mentors, collaborators, and supporters for their support of this work. My deepest thanks go to my advisor, Kristy Kroeker. Thank you for providing me with such a generous, beautiful opportunity for professional and personal growth. I have gained so much from observing your approaches to teaching, mentorship, and research over the years. I aspire to be as grounded, compassionate, and creative in my career ahead as you have been in your leadership. I also value your friendship dearly, and I look forward to many years of adventure and laughter ahead.

During my time in this program, the Kroeker Lab has been an ever-evolving group of grad students, undergraduates, technicians and post-docs who have worked incredibly hard to accomplish truly fantastic things. Despite the challenges, I will forever hold positive memories of the marathon weeks (and months!) of field and lab work because of the genuinely wonderful people I worked alongside. This group has also faced significant hardship and tragedy during these last six years. I would not have finished this program if it weren't for the care and love provided by my Lab Family. Thanks to each of you for always being there right when I most needed it, even when we were separated by thousands of miles of Pacific coastline.

I was fortunate to have a truly enjoyable and engaged dissertation committee. Doug, Catriona and Pete, I appreciate your flexibility, advice and support throughout this multi-year journey. I hope that future collaborations will ensure that we stay connected across the globe. My heartfelt thanks to Diana Steller, Kristen Heady, and Robin Dunkin – you have each inspired me greatly with the passion and joy that you bring to your work. You three also demonstrated to me that motherhood was not only a possibility within my career trajectory, but that it could greatly enrich my relationship with my science and teaching. I see the hard work that you all do, and I am encouraged by your strength. To Christie McCullen, Kendra Dority, and others involved in UCSC's Center for Innovations in Teaching and Learning: thank you for opening my eyes to inclusive and equity-minded pedagogy during my time at UCSC. My considerable growth as an educator is due in large part to CITL's high-quality workshops, courses, and exceptional Graduate Pedagogy Fellowship.

To the staff at the Sitka Sound Science Center: thank you for graciously hosting me as your on-site graduate student for these years. I recognize the incredible amount of time (many of it after-hours) that staff put in to ensure the success of my research. Sometimes this came at the expense of SSSC's ability to operate smoothly, or at the very least, without the stench of drying seaweed in the air. I am so very appreciative of your patience, your kindness, and your good humor.

To the employees of the Sitka Tribe of Alaska's Resource Protection Department and SEATOR, past and present: thank you for the myriad ways you have supported my work over the years. From conversations about Sitka's carbonate chemistry dynamics,

to critical Milli-Q top-offs, to hosting me in your offices for several months, I've been grateful for your collaborative generosity. At the University of Alaska Southeast, Sitka Campus, I am grateful to Greg George for providing me with a superb office space for several critical months of data analysis. Thank you to Kitty LaBounty for allowing me and my mentees to make use of the excellent lab space at UAS over the years. And a huge hug of thanks to Angie Bowers for being my local phycophile friend, and for collaborating on an ambitious and creative research project together during my graduate program. I regret that I was ultimately unable to include that work within this dissertation, given the implications of our findings and how impactful the experience was to my growth as a scientist. I look forward to many years of algal adventures together!

Many significant life events occurred for me within the span of this Ph.D., and I leaned heavily on my network of friends and family for support. I won't attempt to name everyone here, but please know that I share this achievement with each of you – because it couldn't have happened without you. A special thanks to my in-laws and my parents for the all-star grandparent support. It was a true gift to know Lione was being lovingly cared for while I submerged into uninterrupted hours of deep work. Finally, to my husband, Dane, and my daugher, Lione: I love you. Thank you for believing in my ability to pull this off, and for putting up with my long absences. Thank you for reminding me that scientific names and equations and manuscripts pale next to an afternoon spent exploring the marvelous universe within a tidepool.

We did this! Together! My heart is so full.

The text of this dissertation includes reprints of the following previously published material:

Chapter 1 is reproduced from the following published article:

Bell, L. E., & Kroeker, K. J. (2022). Standing crop, turnover, and production dynamics of *Macrocystis pyrifera* and understory species *Hedophyllum nigripes* and *Neoagarum fimbriatum* in high latitude giant kelp forests. *Journal of Phycology, 58*(6), 773–788. https://doi.org/10.1111/jpy.13291

Chapter 3 is reproduced from the following published article:

Bell, L. E., Gómez, J. B., Donham, E., Steller, D. L., Gabrielson, P. W., & Kroeker, K. J. (2022). High-latitude calcified coralline algae exhibit seasonal vulnerability to acidification despite physical proximity to a non-calcified alga. *Climate Change Ecology, 3*, 100049. https://doi.org/10.1016/j.ecochg.2022.100049

INTRODUCTION

Anthropogenic emissions of greenhouse gases into the atmosphere over the last century have set in motion dramatic changes to the temperature and carbonate chemistry of the world's oceans (Orr et al. 2005, Doney et al. 2009, IPCC 2018). Seawater has absorbed more than 90% of the excess heat trapped in the atmosphere in the last 50 years (Durack et al. 2018, Cheng et al. 2019). In addition, the oceans have taken up more than 30% of human-produced CO_2 gas, resulting in a several hundred-fold increase in aqueous CO_2 and a nearly 50% reduction of carbonate in the marine environment over the last 150 years (IPCC 2018). These changes to oceanic carbonate chemistry result in decreased seawater pH and increased corrosive conditions, collectively termed 'ocean acidification'. Even with a best-case scenario return to pre-industrial global CO_2 emission levels, these changes are predicted to continue through 2100 due to the energetic imbalance between the world's atmosphere and oceans (IPCC 2018).

In addition to the direct effects that these environmental changes are expected to have on marine organisms at every trophic level, emergent effects within marine ecosystems will depend on the connectivity and relative interaction strength among species (Bernhardt & Leslie 2013). For example, negative direct effects of elevated pCO_2 or temperature on consumer energetics can be mitigated through access to sufficient quantities or quality of food (Gaylord et al. 2015, Bruno et al. 2015,

Rosenblatt & Schmitz 2016, Vizzini et al. 2017, Doubleday et al. 2019). On the other hand, higher trophic level organisms that are resilient to the direct effects of global change may still be vulnerable to changes in the availability and natural phenology of their basal resources (Edwards & Richardson 2004, Sydeman & Bograd 2009). Alongside trophic resource effects, shifting interactions among species may also affect relative access to critical abiotic resources (Harley et al. 2006, Burek et al. 2008, Burnell et al. 2014). Therefore, it is imperative that global change research incorporates ecological knowledge of community structure and species interactions to properly account for both the direct and indirect effects of environmental change.

In coastal ecosystems worldwide, macroalgae (seaweeds) are foundational primary producers that provide both complex habitat and food supply that promote marine biodiversity (Steneck et al. 2002, Graham 2004, Hurd et al. 2014, von Biela et al. 2016). Macroalgal species will differ in their vulnerability to the direct effects of ocean warming and acidification. Calcifying seaweeds consistently exhibit reduced growth and condition under ocean acidification (Kroeker et al. 2010, Roleda et al. 2012), whereas some non-calcifying macroalgae can increase their production in elevated pCO_2 conditions (Koch et al. 2013, Cornwall et al. 2017). Other seaweeds experience reductions in their growth, nutritional quality, or chemical defenses under the combined effects of ocean acidification and warming (Gao et al. 2021, Kinnby et al. 2021). Such interspecific variation in seaweeds' responses will alter interactions and competitive hierarchies among the macroalgae, and ultimately lead to dramatic

shifts in the composition and productivity of many seaweed communities (Kroeker et al. 2013b, Harley et al. 2012, Connell et al. 2013).

For marine food webs that depend on macroalgal-derived energy and habitat, the emergent implications of these future community changes will hinge on the environmental context in which they occur. Many temperate to sub-polar rocky reef environments where seaweeds dominate are naturally characterized by substantial temporal variability in temperature, pCO_2, light and nutrients (Schiel & Foster 2015, Koweek et al. 2017, Pessarrodona et al. 2022). Interactions among these fluctuating abiotic drivers on diel and seasonal time scales shape seaweed physiology and production through the year (Hurd et al. 2014, Menge et al. 2021). Further, variability in temperature and pH influence consumer metabolism and grazing, so that top-down pressures on seaweed communities also vary over time (Werner et al. 2016, Donham et al. 2021, Kroeker et al. 2021). Research that links this natural variation in environmental drivers with community dynamics of production, consumption, and energy flow is essential to predicting how environmental change will manifest at an ecosystem level (Harley et al. 2017, Kroeker et al. 2020). This is particularly true where abiotic variables already vary asynchronously, as marine climate change will lead to novel combinations of physiological stressors at different times of the year. Yet, few biological studies of macroalgal-based systems have integrated such oceanographic information into scenarios of ocean warming and acidification, due in part to the increased difficulty of this approach. Where such research has occurred, it

is evident that underlying environmental variability within a system interacts with elevated temperatures and pCO_2 to affect the strength and direction of the community's response (Celis-Plá et al. 2015, Graiff et al. 2015, Wahl et al. 2020).

Considering that the most productive macroalgal forests in the world are found in environmentally variable environments, there is an urgent need to expand global change research to include natural variation in, and interactions among, both biotic and abiotic factors in these systems. **The goal of my dissertation is to address this knowledge gap by exploring how the production dynamics of temperate, macroalgal-based communities in a seasonally dynamic environment will respond to ocean warming and acidification.** I focus my research within high latitude giant kelp (*Macrocystis pyrifera*) forest ecosystems, on the rocky reefs of coastal southeast Alaska. The diverse marine communities of macroalgae and their consumers that constitute giant kelp beds provide relatively accessible and spatially manageable domains in which to explore the emergent effects of global change within a highly interconnected ecosystem. Global change is occurring rapidly in these high latitude marine environments, where pronounced warming and persistent calcium carbonate undersaturation of polar and sub-polar surface waters are anticipated within the next 50 years (Feely et al. 2004, Steinacher et al. 2009). These changes are expected to have far-reaching impacts across marine phyla (Kroeker et al. 2013a, Lotze et al. 2019). Consequently, productive sub-polar fisheries sectors face considerable risk (Himes-Cornell & Kasperski 2015, Mathis et al. 2015, Holsman et

al. 2019). This present-day vulnerability indicates these regions can function as bellwethers for impending impacts of global change to mid-latitude marine systems (Fabry et al. 2009).

In this dissertation, I spotlight a selection of calcified and fleshy seaweeds that dominate the macroalgal communities within giant kelp forests of Sitka Sound, Alaska: *Macrocystis pyrifera*, *Hedophyllum nigripes*, *Neoagarum fimbriatum*, *Bossiella orbigniana*, and *Crusticorallina* spp. Together, these co-existing, foundational species provide the majority of macroalgal-derived habitat and food supply within these ecosystems. I start by describing the current seasonal production dynamics of the three canopy-forming kelp species in the context of natural environmental variability in this high latitude region (**Chapter 1**). I then use manipulative experiments to test how projected ocean acidification and warming will interact with seasonal variability to impact the production and nutritional value of these kelps (**Chapter 2**). Finally, I consider how ocean acidification will interact with seasonal light availability to affect the production of the two coralline algae species, and whether these species' responses are influenced by their interaction with a non-calcifying alga (**Chapter 3**). By integrating a robust understanding of the current drivers and dynamics of community structure into the design of sophisticated global change experiments, this collection of work provides a comprehensive picture of how environmental change in dynamic environments can affect coastal marine ecosystems from the bottom-up.

Chapter 1: Standing crop, turnover, and production dynamics of *Macrocystis pyrifera* and understory species *Hedophyllum nigripes* and *Neoagarum fimbriatum* in high latitude giant kelp forests

This chapter was originally published in a peer reviewed journal and is reproduced here for inclusion in this dissertation. The citation for the original publication is:

Bell, L. E., & Kroeker, K. J. (2022). Standing crop, turnover, and production dynamics of *Macrocystis pyrifera* and understory species *Hedophyllum nigripes* and *Neoagarum fimbriatum* in high latitude giant kelp forests. *Journal of Phycology, 58*(6), 773–788. https://doi.org/10.1111/jpy.13291

Abstract

Production rates reported for canopy-forming kelps have highlighted the potential contributions of these foundational macroalgal species to carbon cycling and sequestration on a globally relevant scale. Yet, the production dynamics of many kelp species remain poorly resolved. For example, productivity estimates for the widely distributed giant kelp *Macrocystis pyrifera* are based on a few studies from the center of this species' range. To address this geospatial bias, we surveyed giant kelp beds in their high latitude fringe habitat in southeast Alaska to quantify foliar standing crop, growth and loss rates, and productivity of *M. pyrifera* and co-occurring understory kelps *Hedophyllum nigripes* and *Neoagarum fimbriatum*. We found that giant kelp beds at the poleward edge of their range produce ~150 g C $\cdot$ m^{-2} $\cdot$ yr^{-1} from a standing biomass that turns over an estimated 2.1 times per year, substantially lower rates than have been observed at lower latitudes. Although the productivity of high latitude *M. pyrifera* dwarfs production by associated understory kelps in both winter and summer seasons, phenological differences in growth and relative carbon and nitrogen content among the three kelp species suggests their complementary value as nutritional resources to consumers. This work represents the highest latitude consideration of *M. pyrifera* forest production to date, providing a valuable quantification of kelp carbon cycling in this highly seasonal environment.

Introduction

Increasing anthropogenic carbon emissions have sharpened the worldwide focus on natural carbon sinks (de Coninck 2018, Lecocq et al. 2022). Terrestrial woody forests and vegetated coastal habitats (mangroves, seagrass meadows, salt marshes) have received the majority of attention due to their capacity to sequester carbon through standing crop and burial. More recently, marine macroalgal (seaweed) ecosystems have been highlighted for their potential as a substantial, climate-relevant carbon sink (e.g., Krause-Jensen and Duarte 2016, Laurens et al. 2020, Duarte et al. 2022a). Seaweeds - and canopy forming kelp forests in particular - may contribute substantially to 'blue carbon' storage through their rapid growth, large standing crop, and the allochthonous burial of their detrital export (Ortega et al. 2019, Queirós et al. 2019, Filbee-Dexter and Wernberg 2020, Smale et al. 2021). However, the paucity of quality data on kelp production rates (as g Carbon $\cdot$ m^{-2} $\cdot$ yr^{-1}) is cited as one of the major obstacles to practical estimates of kelp's carbon sequestration capacity (Reed and Brzezinski 2009, Krause-Jensen et al. 2018).

Research on kelp production is difficult because of the intensive sampling necessary to capture growth and turnover dynamics (Hurd et al. 2014, Schiel and Foster 2015). Production rates of the giant kelp *Macrocystis pyrifera*, a globally abundant and high biomass macroalga, have primarily come from well-studied regions in the center of this species' latitudinal range (Pessarrodona et al. 2022). Much less is known about carbon cycling within *M. pyrifera* in fringe habitats, particularly at its polar extents (but see Wheeler and Druehl 1986, van Tussenbroek

1989, Attwood et al. 1991). Understanding kelp production capacity in these habitats is needed to correct the geospatial bias of the data that currently inform global estimates of seaweed productivity. High latitude environments are seasonally dynamic, where variation in seawater temperature, pCO_2, storms, light and nutrient availability impact macroalgal physiology (Graham et al. 2007, Kroeker et al. 2020). The long photoperiod of the high latitude spring and summer contributes to seasonally high rates of production for some macroalgal species (Druehl and Wheeler 1986, van Tussenbroek 1989, Brown et al. 1997, Nielsen et al. 2014). Yet, the duration and magnitude of this production may be constrained by intense competition for nutrients and light with phytoplankton blooms and other macroalgae (Kavanaugh et al. 2009, Miller et al. 2011, Pfister et al. 2019, Bell et al. 2022). Additionally, the physiological tolerance of *M. pyrifera* is likely challenged at certain times of the year near the edge of the range, which may also restrict its overall productivity (e.g., King et al. 2020). Year-round measurements of giant kelp growth, loss, and foliar standing crop (FSC) from higher latitude regions are therefore necessary to understand the carbon production associated with *M. pyrifera*-dominated ecosystems worldwide.

While surface-canopy forming kelp genera (e.g., *Macrocystis, Nereocystis, Eklonia, Laminaria*) have received the most attention for their carbon production potential, these kelps frequently co-occur with substantial macroalgal subcanopies. Total production by understory algae has been estimated to rival production by *M. pyrifera* in kelp forests within the center of its range, and it can increase to compensate for production lost if the surface canopy is removed (Miller et al. 2011,

Castorani et al. 2021). In higher-latitude giant kelp forests, understory algal communities are often dominated in biomass by a few species of large, fast-growing stipitate kelps, such as *Hedophyllum nigripes*, *Neoagarum fimbriatum*, *Agarum clathratum* in the north Pacific (Schiel and Foster 2015, Kroeker et al. 2020). Some of these subcanopy kelp species may have more poleward distributions than the primary canopy forming species (Wulff et al. 2009, Grant et al. 2020), which could influence their relative production capacity in these regions. Studies resolving the comparative ecological performance of subcanopy versus canopy kelps in these regions of overlapping range distributions will provide valuable context ahead of anticipated environmental and species distribution changes (Krumhansl et al. 2016).

In addition to understanding the relative production capacity of different kelp species, investigations of the temporal nature of this relationship in seasonally driven ecosystems may be essential for predicting their vulnerability to global change. As ocean acidification and warming overlay onto current environmental variability at high latitudes, the responses of marine producers may vary by season (Graiff et al. 2015, Wahl et al. 2020). Further, consumers in these systems will experience heightened susceptibility to stressful conditions in particular seasons (Kroeker et al. 2020). Ecological theory suggests that the resilience of these ecosystems will hinge on both the abundance and diversity of basal production that is available to support consumers under such enhanced stress (Bernhardt and Leslie 2013, Gaylord et al. 2015, Doubleday et al. 2019). Although some seasonal complementarity in macroalgal production may already occur due to natural variation in different species'

growth phenologies, such fundamental knowledge is still lacking for many high latitude environments. Yet, we know that it is very likely that coexisting macroalgal species will be differentially affected by global change stressors (Phelps et al. 2017, Pessarrodona et al. 2019). Therefore, to predict how future changes could alter the temporal availability of basal energy resources in high latitude coastal marine ecosystems, it is essential that we first understand the current seasonal timing of production for the dominant macroalgal species of the region.

In this study, we provide a novel, multi-year time series of canopy and subcanopy kelp production in a seasonally dynamic high latitude system. Our research focuses on *M. pyrifera* beds in Sitka Sound, southeast Alaska, near the northernmost continuous edge of this species' range (Druehl 1970, 1981). Similar to other high latitude regions, temporal variation in the FSC of kelp beds in southeast Alaska is expected to be driven by seasonal variation in temperature, nutrient supply, disturbance from winter storms, and irradiance (Calvin and Ellis 1981, Druehl and Wheeler 1986, Stekoll 2019). However, observations from outer coast areas such as Sitka Sound are sparse. In our study of three of the most common subtidal kelps of this region (*M. pyrifera, H. nigripes, N. fimbriatum*), we expect to see increased growth and FSC of all species in late winter and early spring, followed by substantial FSC declines in fall and early winter due to physical stress from storm swell. We previously observed that *M. pyrifera* canopies in Sitka Sound begin to degrade and foul by mid-summer (~July), perhaps due to low nutrient concentrations during this period (Brown et al. 1997, Rodriguez et al. 2016). To investigate the local

relationship between kelp production and nutrient supply, we also conduct year-round sampling to capture the temporal availability of seawater nitrogen in Sitka Sound. In other systems exhibiting seasonal trends in nutrient availability, the nitrogen content of kelps is observed to generally mirror temporal patterns in seawater inorganic nitrogen supply (Wheeler and Srivastava 1984, Brzezinksi et al. 2013, Stephens and Hepburn 2016) though bulk seawater samples don't necessarily reflect all nitrogen sources or supply available to algal tissues (Hurd et al. 1994). Therefore, we also sample a variety of kelp tissues to determine temporal and spatial variability in thallus carbon and nitrogen concentrations. Finally, two of our three sites undergo a phase shift from lush kelp forest to urchin barrens during our study, ostensibly caused by changes in top-down control (Raymond et al. 2019, Gorra et al. 2022). These unexpected changes facilitate observations of how growth, loss, and production rates of three dominant, interacting kelp species respond to declines in their FSC associated with enhanced grazing pressure.

Methods

Plant biomass and foliar standing crop

We conducted monthly surveys of *Macrocystis pyrifera* for FSC estimation in Sitka Sound, Alaska from January 2017 to February 2018 at Breast Is. (57.039 N, 135.333 W) and Harris Is. (57.032 N, 135.277 W), and seasonally in July 2018, January 2019, and July 2019 at Breast Is., Harris Is., and Samsing Pinnacle (56.988 N, 135.357 W). We surveyed all unique *M. pyrifera* sporophytes (hereafter, "plants" (Bolton 2016)) within two permanent 30 · 2 m transects at the 5 - 7 m depth (MLLW) contour and counted the total number of fronds extending > 1 m above the holdfast (hereafter, "frond density"). To determine the relationship between frond density and total wet mass (g), we collected and measured *M. pyrifera* plants (excluding their holdfasts) in summer 2017 ($N = 16$) and winter 2018 ($N = 10$) (Kroeker et al. 2020). We used a linear model to test the effect of season (winter and summer) on the relationship between frond density and wet mass. *M. pyrifera* frond density explained 94% of the variability in total plant wet mass (g) excluding its holdfast, regardless of season ($p = 0.594$; see Table S1.1 for all regression parameter results). In January 2022, we collected *M. pyrifera* stipe and blade tissue collected from the surface canopy, mid canopy, and 1 m above the holdfast ($N = 12$ unique plants) to capture within-plant variation in tissue dry mass composition (% wet mass). We used the slopes of the zero-intercept linear regression lines generated from these relationships as conversion factors to calculate wet and dry mass for each surveyed plant from its frond density. Across all *M. pyrifera* tissue samples, wet biomass explained 96% of

the variation in dry biomass. Although mean dry mass composition of *M. pyrifera* tissues varied by location along the frond, the range of total variation (8.8-12.6% of wet mass) was small. We chose to use a mean conversion value (10.3% of wet mass) to estimate dry mass for all *M. pyrifera* tissues, as we did not consistently collect the canopy length data necessary to incorporate within-plant variation in dry mass composition. We summed the estimated dry mass of each plant and divided by surveyed area to calculate *M. pyrifera* FSC as dry mass ($g \cdot m^{-2}$) at each site for each survey,

We performed seasonal surveys of the understory stipitate kelp community, including *Neoagarum fimbriatum* and *Hedophyllum nigripes,* in July 2018 - 2020, January 2019 - 2020, and March 2019 at Breast Is., Harris Is., and Samsing Pinnacle. At each site, we counted individuals of these species within two permanent $30 \cdot 2$ m transects at the 5 - 7 m depth (MLLW) contour. Starting in March 2019, we also measured a subset of individuals for total blade length and maximum blade width. When we encountered > 10 individuals of either species within a $10 \cdot 1$ m swath of a transect, we used the blade morphometrics calculated for the first 10 plants over a subsampled area to estimate total biomass for that species in the rest of that swath. To estimate total dry biomass from blade morphometrics, we collected > 10 individuals of each understory kelp species from each site in August 2018, measured each blade for maximum length and width to estimate surface area (cm^{-2}) and weighed for wet mass (g). We dried collected *N. fimbriatum* and *H. nigripes* individuals at 60 ℃ for at least 24 hrs and reweighed for dry mass (g). For each relationship (blade surface area

to wet mass, and blade wet mass to dry mass), we used the slopes of the zero-intercept linear regression lines as conversion factors to calculate a dry mass for each surveyed plant. Blade surface area explained 96% of the variability in thallus wet mass for *N. fimbriatum* and 97% of the variability in thallus wet mass for *H. nigripes* (Table S1.1). Thallus wet mass explained 99% of the variability in dry mass for both *N. fimbriatum* and *H. nigripes.*

We summed plant dry masses and divided by surveyed area to obtain the total dry mass FSC ($g \cdot m^{-2}$) of each understory species at each site for each survey. In instances where we performed surveys of both stipe counts and blade morphometrics during the same month, we used these calculated season-specific relationships to estimate total dry mass FSC of each species from their stipe densities ($stipes \cdot m^{-2}$) prior to March 2019. We also used seasonal relationships between stipe counts or blade morphometrics and the season-specific average wet mass of each understory kelp species to estimate the percent composition of understory FSC represented by each species in a survey. Stipe density in January 2020 explained 83% (*N. fimbriatum*) and 97% (*H. nigripes*) of the variability in total dry mass present in the transect, whereas stipe counts in July 2019 and 2020 explained 53% (*N. fimbriatum*) and 98% (*H. nigripes*) of the variability in total thallus dry mass during these periods.

Macroalgal growth and loss

We monitored monthly growth and loss of dominant kelp species in Sitka Sound from January 2017 to February 2018 at Breast Is. and Harris Is. (*M. pyrifera*

only), and from July 2018 to July 2019 at Harris Is., Breast Is., and Samsing Pinnacle (*M. pyrifera*, *N. fimbriatum, H. nigripes).* At each site, we identified 12 - 15 "adult" individuals of each species (*M. pyrifera*: at least one frond reaching the surface; *N. fimbriatum* and *H. nigripes*: maximum blade length > 20 cm) along a 5 - 6 m depth (MLLW) contour with numbered tags. Each month, we re-surveyed tagged *M. pyrifera* plants for frond density, with zip ties loosely bound around new fronds exceeding 1 m in height to distinguish new growth. For tagged *N. fimbriatum* and *H. nigripes* plants, each month we punched a new hole through the thallus at 10 cm from the intercalary meristem (Parke 1948), and we measured blade morphometrics (maximum blade length and width) and distance from meristem to the previous month's punched hole. When previously tagged individuals were not re-sighted after two consecutive months, we assumed they had been physically removed from the substrate, either through grazing or abiotic factors.

We determined size-specific growth and loss rates using an approach modified from Rassweiler et al. (2008, 2018). We use the term "size" broadly here, as we utilize either frond density (*M. pyrifera*) or blade length (understory species) to estimate sporophyte size as a proxy for sporophyte biomass. Because we use single conversion factor to calculate each species' sporophyte biomass from its size, size-specific and mass-specific growth rates are equivalent. Thus, hereafter we refer to them simply as "specific" rates. We calculated the specific frond loss or blade erosion rate (f_i; d^{-1}) of each plant during a survey period using the equation:

$$f_i = \frac{1}{T} ln(\frac{F_T}{F_0})$$

where T is the number of days between surveys, F_0 is the frond density (*M. pyrifera*) or the maximum blade length (*N. fimbriatum, H. nigripes)* at the start of the survey period (time *0*), and F_T is the number of fronds > 1 m that had zip ties at time 0 that remain at time T (*M. pyrifera*) or the maximum blade length at time *0* plus the difference between the total blade increase (maximum blade length at time T minus maximum blade length at time *0*) and the linear blade growth (*N. fimbriatum, H. nigripes).*

We calculated the specific growth rate (g_i; d^{-1}) of each plant during a survey period using the equation:

$$g_i = \frac{1}{T} ln(\frac{B_T}{B_0}) + f_i$$

where T is the number of days between surveys, B_0 is the frond density (*M. pyrifera*) or the maximum blade length (*N. fimbriatum, H. nigripes)* at the start of the survey period (time *0*), and B_T is the total frond density or the maximum blade length at time *T*.

We calculated the per capita plant loss rate (p; d^{-1}) for each species during a survey period using the equation:

$$p = \frac{1}{T} ln(\frac{P_T}{P_0})$$

where T is the number of days between surveys, P_0 is the total number of individual plants of a species at the start of the survey period (time 0), and P_T is the number of plants at time 0 that remain at time *T*.

To determine a net rate of change (n; d^{-1}) for all individuals of a species during a survey period, we calculated the difference between each individual's specific growth rate and the sum of the individual and species' loss rates: $n_i = g_i - (f_i + p)$. We then averaged n_i among all individuals to get n. Similarly, we averaged g_i among individuals of each species during each survey period to calculate a mean specific growth rate (g).

Growth and loss equations were not defined in cases when all fronds were lost (*M. pyrifera*), or when the punched hole from time 0 was not re-sighted at time T (*N. fimbriatum, H. nigripes)*. In the case of *M. pyrifera*, we substituted a value of ½ frond to enable an approximation of growth and loss rates as they approached zero (per Rassweiler et al. 2018). We did not observe any *M. pyrifera* plant to recover from a complete loss of fronds, and thus these individuals were accounted for in plant loss rates during a later survey period. When a punched hole was not re-sighted on a tagged understory kelp species, we did not include the individual in our analyses for that survey period. Following our observations of multi-year declines in *M. pyrifera* populations at two of our sites, we used regression analysis (R Core Team, 2022) to test if the number of elapsed days in the study period was a significant predictor of *M. pyrifera* net growth rates at Harris and Breast Islands.

Nutrient monitoring

To capture the annual variation in nutrient concentrations around a high latitude giant kelp bed, we sampled seawater monthly (July 2018 to July 2019) from

the water column adjacent to Breast Is. in Sitka Sound, Alaska. We collected seawater using a surface-deployed Niskin bottle at 0.5 m and 4.5 m depth at each of four locations: in the middle of the Breast Is. giant kelp bed canopy, at the canopy edge, 150 m away from canopy edge, and 600 m away from the canopy edge towards the open ocean (Gulf of Alaska). In addition, we collected benthic seawater samples monthly (June 2016 to July 2017) and opportunistically (fall 2017 to summer 2020) using a diver-deployed Niskin bottle at 8 - 10 m depth at Breast Is., Harris Is., Samsing Pinnacle and Talon Is. (57.073 N, 135.414 W). We brought collected water to the surface, immediately filtered each sample through a 0.2 μm filter and kept it frozen until analysis for dissolved inorganic nitrogen content as NO_x (NO_3 + NO_2) on a Lachat QuikChem 8000 Flow Injection Analyzer at the University of California Santa Cruz Marine Analytical Laboratory (detection limit < 0.28 μM NO_x, average run measurement error < 0.1 μM NO_x). To assess spatial variability in monthly seawater NO_x concentrations collected near Breast Is., we used a linear mixed-effects model (R Core Team, 2022) with *depth*, *location,* and *the interaction of depth and location* as fixed factors and *date* as a random intercept using restricted maximum likelihood. With log transformation of seawater NO_x, we used plots of model residuals and Q-Q plots to confirm that our final model satisfied assumptions of homoskedasticity and normality (Winter 2013). We determined p-values for the effects of fixed factors and their interactions using the Sattertwaithe's method for t-tests ($\alpha = 0.05$).

Macroalgal carbon and nitrogen content

Coincident with monthly sampling of seawater for nutrient concentrations, we collected surface blades from *M. pyrifera* in the Breast Is. giant kelp bed from July 2018 to July 2019 to analyze for carbon (C) and nitrogen (N) content. On one frond from each plant ($N = 3$), we identified and removed the second intact blade closest to the frond's scimitar blade. To capture seasonal variation in C and N content in kelp species in July 2018, January 2019, and August 2019, we collected blades from *M. pyrifera* plants ($N = 5$) at ~1 m above their holdfasts and blades ($N = 5$) of *N. fimbriatum* and *H. nigripes* between 4 - 7 m depth (MLLW) at Samsing Pinnacle. We also opportunistically collected blades ($N = 3$-5) representing all kelp species present at Harris Is. in summer 2018 and 2020 and at Samsing Pinnacle in summer 2020. For all macroalgal tissue field collections, we immediately drained collected samples of excess seawater and kept them on ice in a covered cooler for transport to the lab. Within 2 hours of collection, we cleaned collected tissue of epiphytes and rinsed it briefly in fresh seawater. From all collected blades we excised 1 - 5 g of tissue immediately adjacent to the intercalary meristem where the blade meets the stipe. We spun tissue samples 10 times in a salad spinner before drying at 60 ℃ for at least 24 hrs. Dried samples were analyzed for C and N content (% dry mass) by the University of California Santa Cruz Stable Isotope Laboratory using a CE Instruments NC2500 elemental analyzer coupled to a Thermo Scientific DELTAplus XP isotope ratio mass spectrometer via a Thermo-Scientific Conflo III (routine measurement error ≤ 1.0 %C and ≤ 0.2 %N).

To assess the relationship between *M. pyrifera* surface blade N content and seawater NO_x concentration at Breast Is., we used a Spearman's rank correlation to compare blade tissue and seawater samples from 4.5 m depth (all seawater samples were pooled together by sampling date). We used two-factor analysis of variance tests (ANOVA; R Core Team, 2022) to analyze the effects of fixed factors *season* and *algal species* and the *interaction of season and species* on the C and N content of *M. pyrifera*, *H.nigripes*, and *N. fimbriatum* tissue collected at Samsing Pinnacle in 2018 and 2019. We confirmed assumptions of normality were met with Q-Q plots of model residuals, and used residual plots to verify the absence of heteroskedasticity (Winter 2013). Where fixed factors or their interaction were significant ($\alpha = 0.05$), we used the Tukey's honest significant difference (HSD) method to test pairwise differences among means.

Production estimates

We estimated macroalgal production rates in terms of dry mass, carbon mass and nitrogen mass produced per square meter per day using a similar approach to Rassweiler et al. (2008, 2018). Calculations of giant kelp bed productivity in southern California were found to be robust to the type of growth model employed (Rassweiler et al. 2018). We chose to use an exponential growth model, which assumes that any new growth or erosion of a kelp sporophyte during a survey period occur in constant proportion to its starting size. For each survey period where we could estimate the starting dry mass FSC (S_0; $g \cdot m^{-2}$) of a species at a site, we used the specific growth

rate (g) and the specific net rate of change (n) to estimate the daily average dry mass production (P; $g \cdot m^{-2} \cdot d^{-1}$) that occurred during this sampling interval:

$$P = \frac{g \cdot S_0}{n}(e^n - 1)$$

We used the equation to calculate P in terms of carbon mass (i.e., net primary production or NPP) and nitrogen mass, except we first defined S_0 in units of carbon or nitrogen mass by multiplying by the average carbon and nitrogen content of each species during that time period: $S_{0(C\ or\ N)} = S_0 \cdot$ (%C or %N). We recognize the significant variation in C and N content that can exist within kelp thalli (Gevaert et al. 2001) and have confirmed inter-thallus variability in elemental content for our monitored kelps in Sitka Sound that differs by species and season (Bell and Kroeker, unpublished data). Incorporation of this level of macroalgal elemental content variation into our productivity estimates was beyond the scope of this paper. We chose to use the average C and N content of the 'newest' blade tissue (sampled closest to the intercalary meristem) as the sole conversion factor for each species in each time period. To calculate the error around our estimates of macroalgal production rates for each species at a site in a survey period, we used Monte Carlo methods to propagate uncertainty from measured variability in the actual data (Harmon et al. 2007). We generated 1,000 randomly simulated normal distributions for each variable used in each calculation of P (as dry mass, C mass, and N mass) to create a normally distributed range of 1,000 estimates of P. We then used the standard deviation of these values as the standard error in each of our estimates of P.

Results

Plant biomass and foliar standing crop

From January 2017 to February 2018, *M. pyrifera* FSC was lowest in January (combined sites mean ± SE: 174 ± 24 g dry mass · m^{-2}), but began to rise by April to reach an annual maximum around June (468 ± 47 g dry mass · m^{-2})(Fig. 1.1a). By July, FSC had begun to decline again towards its winter minimum. At one site (Harris Is.), FSC was noticeably lower in July 2018 than had been observed during the same months in the prior year and continued to decline over the course of our study. By July 2019, giant kelp were absent along the surveyed transects at this site. A similar trend in declining *M. pyrifera* FSC was observed at a second site (Breast Is.) starting in slightly later (January 2019). Within one year of the noted decline (January 2020), there was a total loss of giant kelp from the surveyed area at this site (Bell and Kroeker, unpublished data). Concurrent with decreasing FSC, *M. pyrifera* mean plant density and average plant size (as number of fronds) also decreased at both sites.

Estimated dry mass FSC of both *H. nigripes* (Fig. 1.2a) and *N. fimbriatum* (Fig. 1.3a) were highest at all sites in July 2018. At Harris Is., *H. nigripes* and *N. fimbriatum* declined to local extinction over the course of our study (Table S1.1). Similarly, at Breast Is. *H. nigripes* was locally extinct from surveyed transects by January 2020 and *N. fimbriatum* had disappeared by January 2021 (Bell and Kroeker, unpublished data). Within the communities of understory kelps surveyed at each site, the species *Agarum clathratum* was consistently present in higher biomass than either *H. nigripes* and *N. fimbriatum*, but together these three species composed > 97% of

estimated total understory kelp FSC (as wet mass) during each survey at each site (Table S1.2).

Macroalgal growth and loss

At all sites, tagged *M. pyrifera* plants demonstrated new frond growth as well as frond loss in every surveyed period of this study (Fig. S1). The one exception was at Harris Island in the final two months prior to site-level extinction, where no new growth was observed on the few remaining *M. pyrifera* plants. Size-specific growth rates of *M.pyrifera* appear to peak in the spring (during March and April; ~1.6% per day) and again in the early fall (~October) (Fig. 1.1b). High frond and plant loss rates in the fall resulted in a mean negative net rate of change at all sites during October to December (Figs. 1c, S1). Net rates of change of *M. pyrifera* decreased over the duration of this study (February 2017 to August 2019) at both Harris Is. (simple linear regression model: $F_{1,15} = 16.8$, $p < 0.001$) and Breast Is. (simple linear regression model: $F_{1,16} = 14.5$, $p = 0.002$)(Table S1.3).

Both *H. nigripes* and *N. fimbriatum* exhibited the highest specific growth rates in April-May (*H. nigripes:* ~2.8% per day; *N. fimbriatum:* ~1.6% per day) at all sites. The majority of *H. nigripes*' annual growth was observed in the first half of the calendar year (January to June) (Fig. 1.2b). Compared to *H. nigripes*, tagged *N. fimbriatum* individuals sustained relatively higher specific growth rates through the late summer and fall (July to October) (Fig. 1.3b). Both species experienced high erosion and plant loss rates in the late summer and fall (Figs. S2, S3), resulting in

mean negative net rates of change at all sites during this period (Figs. 2c, 3c). We confirmed perennial recovery of both species from substantial grazing: tagged individuals that were observed in January with near-complete blade loss and bearing characteristic grazing scars were re-sighted in March with new growth of intact healthy blade tissue.

Seawater nutrients

Seawater NO_x concentrations in Sitka Sound, Alaska followed a regular seasonal cycle, reaching their annual peak of 17-22 μM from December to February and remaining under 3 μM from April to August in each year of sampling (Fig. 1.4a). Water column NO_x concentrations sampled near the Breast Is. kelp bed were consistently higher at 4.5 m depth compared to 0.5 m (mixed linear model: $F_{1,84} = 12.8$, $p < 0.001$), but there was no relationship between nutrient concentration and location relative to the bed (mixed linear model: $F_{1,84} = 0.67$, $p = 0.570$) or the interaction between factors (mixed linear model: $F_{1,84} = 1.49$, $p = 0.224$)(Table S1.4).

Macroalgal carbon and nitrogen content

The nitrogen (N) content of *Macrocystis pyrifera* surface canopy blades at Breast Is. in 2018 - 2019 were positively correlated with near-surface seawater NO_x concentrations (Spearman's $\rho = 0.72$, $p = 0.009$)(Fig. S4). Outliers from samples collected in March, however, suggest that N content of *M. pyrifera* blades was decoupled from seawater nutrient concentrations in the spring for at least 1 month

after NO_x began to decline (Fig. 1.4b). Surface blade N content reached its annual high in March (mean ± SE = 3.5 ± 0.1% dry mass) and an annual low in August (0.7 ± 0.1% dry mass). In contrast, *M. pyrifera* surface blade carbon (C) content remained relatively stable throughout the year at 29.0 ± 0.3% dry mass (Fig. 1.4c).

Nitrogen content of macroalgal tissue collected in 2018-2019 at Samsing Pinnacle was significantly impacted by the interaction between the effects of species and season (two-way ANOVA: $F_{2,39} = 15.5$, $p < 0.001$)(Tables S5, S6). Blade tissue N was higher in winter than summer for all three species (Tukey's HSD: $p < 0.006$). *M. pyrifera* had lower N content in the winter than either *H. nigripes* (Tukey's HSD: $p < 0.001$) or *N. fimbriatum* (Tukey's HSD: $p < 0.001$), but the understory kelp species did not differ in N content from each other (Tukey's HSD: $p = 0.406$). In the summer, *N. fimbriatum* N content was higher than both *H. nigripes* (Tukey's HSD: $p < 0.001$) and *M. pyrifera* (Tukey's HSD: $p < 0.001$), whose N content did not differ from each other (Tukey's HSD: $p = 0.851$). Carbon content of kelp blade tissue collected during this period was impacted by season (two-way ANOVA: $F_{1,39} = 14.6$, $p < 0.001$) and species (two-way ANOVA: $F_{2,39} = 11.2$, $p < 0.001$), but we did not detect an interaction between these factors (two-way ANOVA: $F_{2,39} = 6.10$, $p = 0.005$)(Tables S5, S7). Tissue C did not differ between winter and summer seasons for *M. pyrifera* (Tukey's HSD: $p = 0.582$) or *N. fimbriatum* (Tukey's HSD: $p = 0.999$), but was higher in the summer compared to winter for *H. nigripes* (Tukey's HSD: $p < 0.001$). *M. pyrifera* had marginally lower C content in the winter than *N. fimbriatum* (Tukey's HSD: $p = 0.044$), as well as lower C content in the summer than

H. nigripes (Tukey's HSD: $p < 0.001$), but otherwise within-season blade C content did not differ among species (Tukey's HSD: $p > 0.05$).

Production and turnover

Monthly monitoring of *M. pyrifera* beds in 2017 - 2018 indicated that annual dry mass productivity rates were maximal around June (mean ± SE: Harris Is.: 2.04 ± 0.70 g dry mass · m^{-2} · d^{-1}; Breast Is.: 3.05 ± 0.86 g dry mass · m^{-2} · d^{-1}) and minimum rates occurred around January (Fig. 1.1d). Giant kelp bed production rates at both Harris Is. and Breast Is. were comparatively lower in subsequent years and had dropped to zero at Harris Is. by July 2019. The highest productivity rate of *H. nigripes* (0.11 ± 0.04 g dry mass · m^{-2} · d^{-1}) was recorded in April 2019 at Samsing Pinnacle (Fig. 1.2d), whereas maximum productivity of *N. fimbriatum* (0.07 ± 0.02 g dry mass · m^{-2} · d^{-1}) was observed in August 2018 at Samsing Pinnacle (Fig. 1.3d).

Estimated annual net primary production (C mass) in 2017 was ~142 g C · m^{-2} · yr^{-1} at Harris Is. and ~156 g C · m^{-2} · yr^{-1} at Breast Is. Using a ratio of total annual net primary production to the mean foliar standing crop at these sites in 2017 (Harris Is.: ~68 g C · m^{-2}; Breast Is.: ~75 g C · m^{-2}), we estimate the turnover of FSC in both of these *M. pyrifera* beds was approximately 2.1 times in that year. During seasonal sampling at Samsing Pinnacle in 2018-2019, mean C production rates of *M. pyrifera* ranged from 0.21-0.32 g C · m^{-2} · d^{-1}, whereas estimated C production of *H. nigripes* and *N. fimbriatum* combined did not exceed 0.03 g C · m^{-2} · d^{-1} in either season (Fig. 1.5a). In both winter and summer 2019, the total carbon mass production of the two

understory kelp species represented less than 3.2% of *M. pyrifera* C production. The combined N mass production rates of *H. nigripes* and *N. fimbriatum* were 4.3% of estimated *M. pyrifera* N productivity in winter 2019, and 4.0% in summer 2019 (Fig. 1.5b). In summer 2018 there was a smaller relative difference in mass production rates between understory species and giant kelp, with C and N production by both *H. nigripes* and *N. fimbriatum* reaching 13.3% and 17.5%, respectively, of *M. pyrifera* C and N production.

Discussion

Here, we present the dry mass, carbon mass, and nitrogen mass production dynamics of three kelp species in a highly seasonal marine system. This work reveals the relative production rates of the surface canopy forming *Macrocystis pyrifera* and the two spatially dominant subcanopy kelps *Hedophyllum nigripes* and *Neoagarum fimbriatum* in giant kelp beds during periods of macroalgal persistence, as well as during phase shifts to urchin barrens. We calculate that the annual net primary production (g C $\cdot$ m^{-2} $\cdot$ yr^{-1}) of *M. pyrifera* in its polar fringe habitat is up to an order of magnitude lower than productivity estimates from the center of its range (Rassweiler et al. 2008, 2018, Reed et al. 2008, 2009). Foliar standing crop (FSC) and turnover rates are also nearly 2-3 times lower for *M. pyrifera* beds in Sitka Sound than mean values from southern California giant kelp forests. These results indicate that even 'conservative' estimates of *M. pyrifera* production in fringe habitats are currently too high and may therefore lead to overestimates of carbon flux through giant kelp forests in these regions (Reed and Brzezinski 2009, Wilmers et al. 2012, Duarte et al. 2022b). Even so, production rates of giant kelp in this high latitude system dwarf total biomass contributions from co-occurring understory kelp species *H. nigripes* and *N. fimbriatum*. These data are a valuable contribution to the limited year-round studies of kelp growth and loss rates around the world and represent the highest latitude (N or S) consideration of *M. pyrifera* production rates yet (Pessarrodona et al. 2022).

Productivity of *M. pyrifera* in its fringe habitat compared to range center populations is likely primarily constrained by light availability (Stekoll and Else 1990, Graham et al. 2007, Stekoll et al. 2021), although seasonal nutrient limitation may also play a role (van Tussenbroek 1989). Our monthly seawater nutrient monitoring confirms that subtidal macroalgae in this system have access to high NO_x concentrations (> 5 μM) from October through March. However, nutrient depletion from enhanced water column production in the spring brings these concentrations below 1 μM, the putative minimum concentration necessary to sustain *M. pyrifera* growth (Gerard 1982a). Our sampling of *M. pyrifera* surface blades indicates a 2-month lag between the decline in seawater NO_x and a decrease in the nitrogen content of their tissues. Unlike giant kelp in southern California that maintain reserves of nitrogen in their tissues throughout the year (Stewart et al. 2009, Brzezinksi et al. 2013), *M. pyrifera* in Sitka Sound experience a 2-month period in the late summer during which their blade nitrogen reserves are depleted (blade % N below 1% dry mass; Gerard 1982b). This seasonal nutrient deficiency corresponds with seasonal lows in specific growth and productivity rates of *M. pyrifera* in Sitka Sound, similar to giant kelp ecosystems in coastal waters of New Zealand and the Falkland Islands (van Tussenbroek 1989, Brown et al. 1997).

Monthly tagging of *H. nigripes* and *N. fimbriatum* reveals that the annual growth cycles for these understory species also follow seasonal variation in light and nutrient availability in this system. Although external NO_x sources have declined by March, these understory kelps are likely able to draw on internal nitrogen reserves

accumulated during winter for up to 1-2 months before this source is depleted (Korb and Gerard 2000, Pueschel and Korb 2001). Relative nitrogen storage capacity and rate of utilization may underlie slight differences in annual growth regime between the two species. In January at Samsing Pinnacle, both *H. nigripes* and *N. fimbriatum* had similarly high tissue nitrogen content ahead of notable spring increases in their growth and production rates. However, by summer, *N. fimbriatum* individuals maintained both higher relative tissue nitrogen content than *H. nigripes* as well as higher relative growth from July to October. Further, decreased carbon content in *H. nigripes* in winter relative to summer may indicate that this species utilizes a substantial proportion of its carbohydrate reserves for growth as early as January, at a time that loss of carbon through respiration exceeds assimilation of new carbon via photosynthesis (Gómez and Wiencke 1998, Gevaert et al. 2001). Such species-specific differences suggest that these co-occurring understory kelps employ distinct 'strategies' in the timing and magnitude of their resource mobilization for growth. In this system, these phenological differences in basal production may be critical to sustaining certain consumers' energetic demands during the more physiologically stressful winter season (Kroeker et al. 2020).

Variability in relative carbon and nitrogen production rates among kelp species suggests that the importance of understory kelps as a potential food source to marine consumers may also vary markedly inter-annually. Regardless of season, *M. pyrifera* dominated total C and N production by kelp at Samsing Pinnacle. However, both understory species exhibit equal or higher relative C and N concentrations per

tissue mass than *M. pyrifera*. As a result, when understory kelp FSC was relatively high (such as during summer 2018), the relative proportion of C and N production by these species compared to giant kelp was notably increased. Prior work in this system has shown that pinto abalone (*Haliotis kamtschatkana*), a common rocky reef grazer, experience higher growth rates when fed a mixed algal diet consisting of several kelp species than when fed a diet of *M. pyrifera* alone (Kroeker et al. 2020). Given that *M. pyrifera* dwarfed understory kelp species in terms of both FSC and productivity at sites not undergoing phase shifts, even modest increases in the relative productivity of any understory kelp species would provide a valuable, diverse source of nutrition to the primary consumer community.

Our consideration of only two understory kelp species means that our results certainly underestimate total dry mass production by understory kelps in this system. Based on our community surveys, *H. nigripes* and *N. fimbriatum* only composed 30% of total understory kelp wet mass FSC in some seasons. Inclusion of the biomass-dominant, C- and N-rich understory kelp *Agarum clathratum* in our study would have provided a more complete picture of understory kelp production dynamics. We have observed that *A. clathratum* is not readily consumed by grazers, perhaps due high polyphenolic concentrations or tissue toughness affecting its palatability relative to other kelps (Alstyne et al. 1999, Dubois and Iken 2012). It is consistently the last kelp species to be grazed on rocky reefs undergoing phase shifts from kelp beds to urchin barrens in Sitka Sound (Bell, pers. obs.). Therefore, although C and N production represented by *H. nigripes* and *N. fimbriatum* accounts for the bulk of the understory

kelp production important to rocky reef grazers, future work considering the production of *A. clathratum* will be essential to predicting the potential C cycling and sequestration capacity of understory kelp communities in this region.

Our estimates of frond, blade, and whole-plant loss rates highlight the year-round turnover of macroalgal biomass in this system. In addition, we confirm that the late fall and early winter seasons represent a regular period of enhanced net tissue loss for all three kelp species. Winter storm swell in the North Pacific is high during this time and can drive whole plant losses via mechanical stress on holdfasts (Druehl and Wheeler 1986, Pedersen et al. 2020). We also observed substantial blade loss via grazing during the late fall and early winter. Unfortunately, we are unable to tease apart how much of the net tissue loss at this time of year is due to increased grazing pressure versus decreased algal growth. On tagged understory kelps, such intense grazing frequently extended past the prior survey's punched hole, making it challenging to quantify blade growth and loss rates during these seasons. Even so, our calculations of high loss rates of detrital and particulate matter appear to be on par with kelp from other high latitude regions, representing substantial carbon supply to the surrounding marine ecosystem (Krause-Jensen and Duarte 2016, Pedersen et al. 2020, Smale et al. 2021). And our study did not account for losses of macroalgal tissue released as dissolved organic carbon, which can represent an estimated 13-35% of fixed carbon in kelps (reviewed by Paine et al. 2021). Because we did not track the fate of all 'lost' macroalgal production, we cannot accurately assess the carbon sequestration potential of these kelp species (Hurd et al. 2022).

We acknowledge that our seaweed survey methods could not capture all new tissue growth, which would explain how these populations could persist despite our calculations of negative net rates of change during the majority of the year. For tagged *M. pyrifera* individuals, our periodic surveys would have missed any new fronds that grew and were subsequently lost in between sampling periods. For *N. fimbriatum* and *H. nigripes*, our hole-punch method could not account for any growth that occurred beyond the punched hole, which is known to occur in stipitate kelps (Calvin and Ellis 1981, Gagne and Mann 1987, Miller et al. 2011). Furthermore, kelps can invest new growth in increasing blade width and thickness (Calvin and Ellis 1981, Druehl et al. 1987) as well as stipe mass (Gagne and Mann 1987), and none of these metrics were captured in our tagged understory surveys. Lastly, we did not incorporate any temporal or spatial variation in the conversion factors used to calculate each species' tissue dry mass from wet mass and blade surface area measurements. Our assumption of low variability in these relationships is supported by prior studies in certain kelp species (Rassweiler et al. 2018, Wickham et al. 2019) but not others (Gagné et al. 1982, Gevaert et al. 2001). For that reason we advise that our coarse estimates of species' net rates of change at each site be interpreted alongside a consideration of the variation in species' FSC over time.

At two of our monitored sites, FSC of *M. pyrifera* and *H. nigripes* did unexpectedly decline over the course of our study. By 2021, all kelps except for *A. clathratum* had disappeared from these sites. Previous studies in this area suggest that these site-level phase shifts occurred due to changes in top-down pressures (Raymond

et al. 2019, Gorra et al. 2022). Recent marine heatwaves and sea star wasting in this region may have also influenced the structure of these rocky reef communities (Burt et al. 2018, Ross et al. 2021). However, environmental and invertebrate community monitoring data collected at these sites do not indicate notable differences in annual temperatures or sea star abundances that correlate with patterns of macroalgal loss (Bell and Kroeker, unpublished data). The spatial pattern of kelp forest declines that we've recently observed in Sitka Sound (e.g., kelp forests transitioning to barrens predominantly in areas of high human activity) suggests that human-influenced trophic cascades were a primary driver of change at our sites. At Harris Is., where we first noticed the net rate of change of *M. pyrifera (*and later, *H. nigripes)* becoming unusually negative, there appeared to be a simultaneous increase in the mean and variability of these species' specific growth rates. This short-term pattern may have arisen from decreased competition for resources (e.g., light and nutrients) as FSC of canopy-forming conspecifics declined (Gerard 1976, Reed et al. 2008). Although increased resource availability following removal of a *M. pyrifera* surface canopy can enhance understory kelp production in some cases (Miller et al. 2011, Castorani et al. 2021), we did not observe such a response at our sites. This finding is consistent with research in southern California showing that high herbivore densities can suppress the response of understory algae to surface canopy loss (Castorani et al. 2021). Net loss rates of each kelp species eventually overwhelmed any temporary increases in their specific growth rates, and the majority of the kelp carbon mass lost during these phase shifts was likely consumed and remineralized as CO_2 (Krause-Jensen and

Duarte 2016, Filbee-Dexter and Wernberg 2020). The complete eradication of the *M. pyrifera* population at both Harris Is. and Breast Is. represents approximately 150 g C $\cdot$ m^{-2} $\cdot$ yr^{-1} of lost production from giant kelp alone. While the loss of canopy-forming macroalgal species can benefit local phytoplankton productivity, phytoplankton are unable to fully compensate for the production capacity of these biomass-rich kelp beds (Pfister et al. 2019). Therefore, the loss of these macroalgal communities represents a net decrease in the carbon sequestration capacity of these coastal rocky reef areas (Wilmers et al. 2012, Gorra et al. 2022).

Current debate over the relevance of macroalgae to global blue carbon stocks has resulted in a demand for more robust accounting of carbon flows through seaweed beds (Macreadie et al. 2019, Bach et al. 2021, Gallagher et al. 2022, Hurd et al. 2022). Our results underscore the importance of integrating productivity estimates for each species from a diversity of environments in order to accurately assess its aggregate potential contribution to carbon and nitrogen storage and cycling. We calculate that the production rates of the globally distributed foundational kelp *M. pyrifera* are substantially lower at the poleward fringe of its range compared to populations from its range center. We also provide the first estimates of production capacity for the subcanopy kelps *H. nigripes* and *N. fimbriatum* associated with high latitude giant kelp beds, which represent only 3-18% of *M. pyrifera* production in winter or summer. These findings indicate that the kelps composing high latitude *M. pyrifera* beds may not contribute substantially to global kelp production, as their

productivity falls substantially below even the lower-bound estimates for this ecosystem (Reed and Brzezinski 2009).

Our consideration of kelp production capacity in high latitude *M. pyrifera* beds comes at a time of dramatic change in these marine environments. Polar regions are experiencing some of the fastest rates of ocean warming and acidification in the world (Fabry et al. 2009, Mathis et al. 2015, IPCC 2018). The global geographic distribution of kelp communities is shifting, with some of the most dramatic changes to kelp abundance projected at species' poleward edges (Krumhansl et al. 2016, Smale 2020). Concurrently, there is heightened interest in seaweed mariculture and macroalgal carbon sequestration potential in these high latitude regions (AMTF 2018, Stekoll 2019, Smale et al. 2021). Understanding the relative timing and magnitude of production among kelp species in naturally occurring beds is an essential first step to predicting how future global change could affect these significant basal energy sources. Although not considered in our study, the bull kelp *Nereocystis luetkeana* may currently have higher carbon fixation and dissolved carbon release than *M. pyrifera* where they co-occur in the north Pacific (Weigel and Pfister 2021). However, if the warm-temperate adapted *M. pyrifera* increases in abundance due to favorable environmental changes, it may be better poised to outcompete and outperform cold-temperate adapted kelp assemblages in production capacity (as has been seen in climate-driven kelp community changes in the NE Atlantic (Pessarrodona et al. 2019)). Additionally, future increases in ocean temperatures and pCO_2 have the potential to alter the assimilation and elemental composition of these

macroalgae as well as their rates of organic matter release (Pessarrodona et al. 2018, Close et al. 2020, Paine et al. 2021, Wright et al. 2022). Research investigating how such changes in the marine environment will impact the carbon and nitrogen mass productivity of these coastal primary producers will be a crucial next step for predicting the future carbon sequestration potential of high latitude kelp forest communities (Harley et al. 2012, Gilson et al. 2021).

Acknowledgements

This research took place within Lingít Aaní, or Tlingit land, near Sheet'ká Kwáan, also known as Sitka, Alaska. We acknowledge and understand that our work is dependent on the land and waters that Lingít Peoples have stewarded since time immemorial, and we are grateful to be guests in this region. We thank E. O'Brien, C. Gray, D. Steller, H. Damron, Z. Kitchel, A. Ravelo, E. Donham, G. Dionne, C. Carney and B. Dreyer for assistance in the field and in sample processing, and J. Straley and L. Wild for use of their microbalance. We also thank C. Hurd, M. Kilpatrick, P. Raimondi and J. Metzger for their guidance of our analysis and framing. We greatly appreciate the Sitka Sound Science Center for their support of our field and laboratory work. This research was supported by the National Science Foundation (OCE 1752600), the North Pacific Research Board's Graduate Student Research Award (1748-01), and The David and Lucile Packard Foundation.

Figures

Figure 1.1. Site-level estimates (mean ± SE) by survey period of *Macrocystis pyrifera* (a) foliar standing crop (g dry mass · m^{-2}), (b) specific growth rate (d^{-1}), (c) net rate of change (d^{-1}), and production rate (g dry mass · m^{-2} · d^{-1}). A missing bar indicates no data for that particular site and survey period except where noted by "(0)", in which case the data point was zero. Shaded panels indicate the months with the shortest photoperiod (October – March).

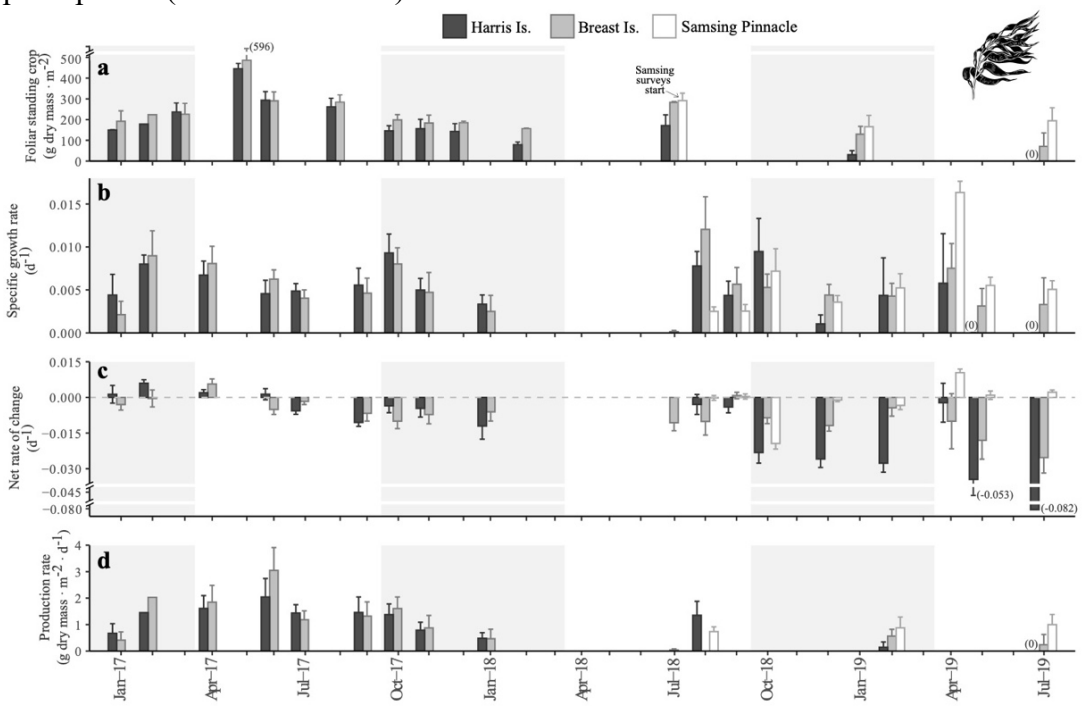

Figure 1.2. Site-level estimates (mean ± SE) by survey period of *Hedophyllum nigripes* (a) foliar standing crop (g dry mass · m^{-2}), (b) specific growth rate (d^{-1}), (c) net rate of change (d^{-1}), and production rate (g dry mass · m^{-2} · d^{-1}). A missing bar indicates no data for that particular site and survey period except where noted by "(0)", in which case the data point was zero. Shaded panel indicates the months with the shortest photoperiod (October – March).

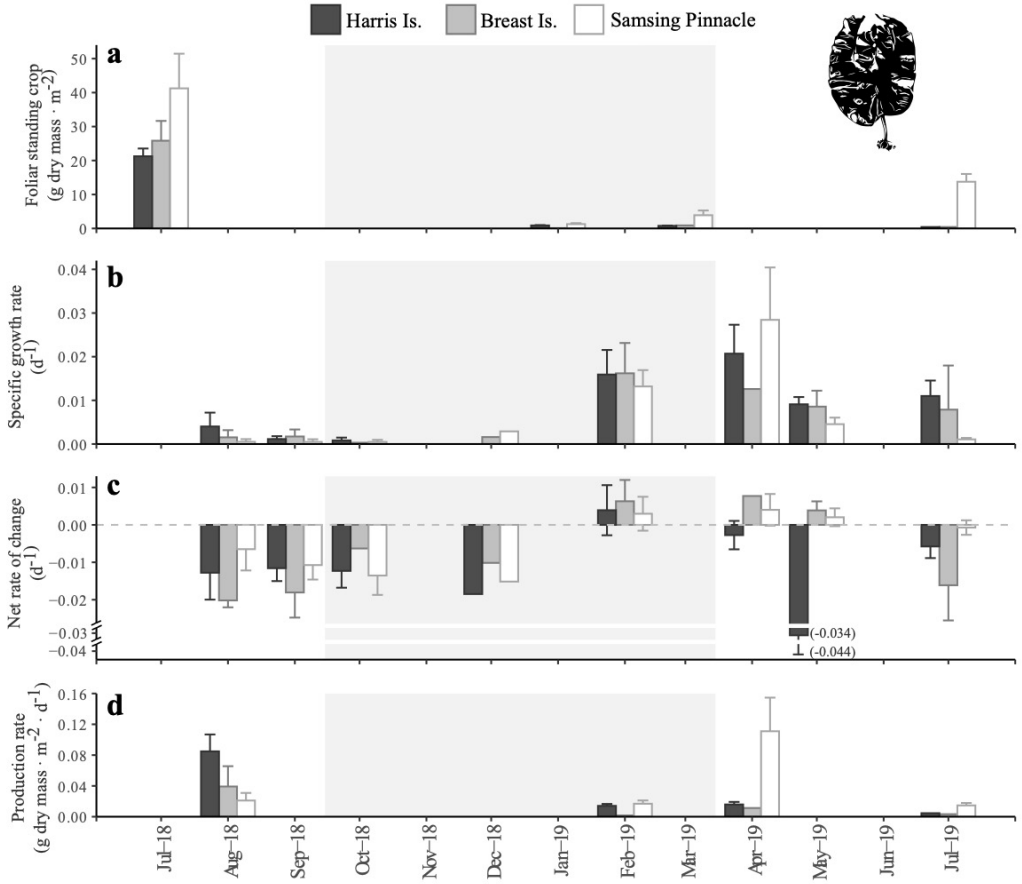

Figure 1.3. Site-level estimates (mean ± SE) by survey period of *Neoagarum fimbriatum* (a) foliar standing crop (g dry mass · m^{-2}), (b) specific growth rate (d^{-1}), (c) net rate of change (d^{-1}), and production rate (g dry mass · m^{-2} · d^{-1}). A missing bar indicates no data for that particular site and survey period except when noted by "(0)", in which case the data point was zero. Shaded panel indicates the months with the shortest photoperiod (October – March).

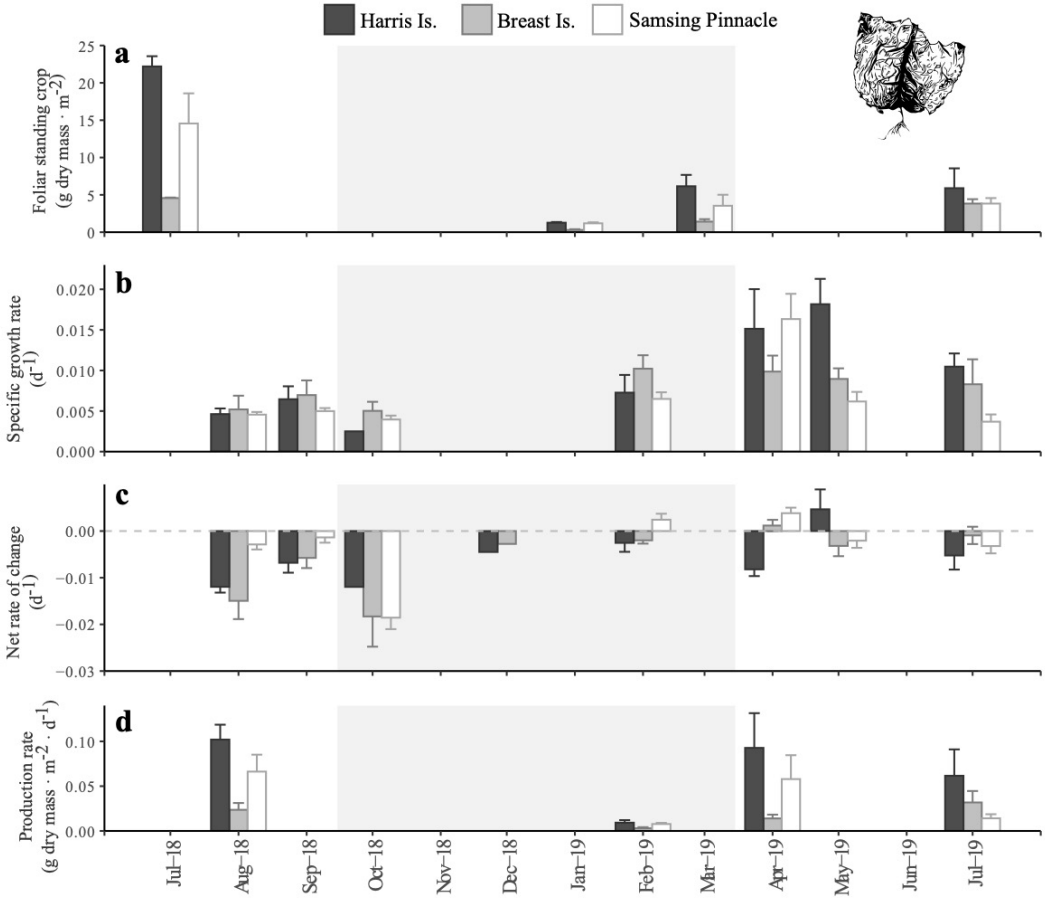

Figure 1.4. Annual variation in (a) seawater dissolved inorganic nitrogen as NO_x (µM) and in tissue (b) nitrogen and (c) carbon content of *M. pyrifera* surface canopy blades. Monthly from August 2018 to August 2019, kelp blades and water column seawater samples (0.5 m and 4.5 m depth) were collected on the same day at Breast Island. Outside of this time period, benthic seawater samples were collected opportunistically from kelp forest beds throughout Sitka Sound. Shaded panels indicate the months with the shortest photoperiod (October – March).

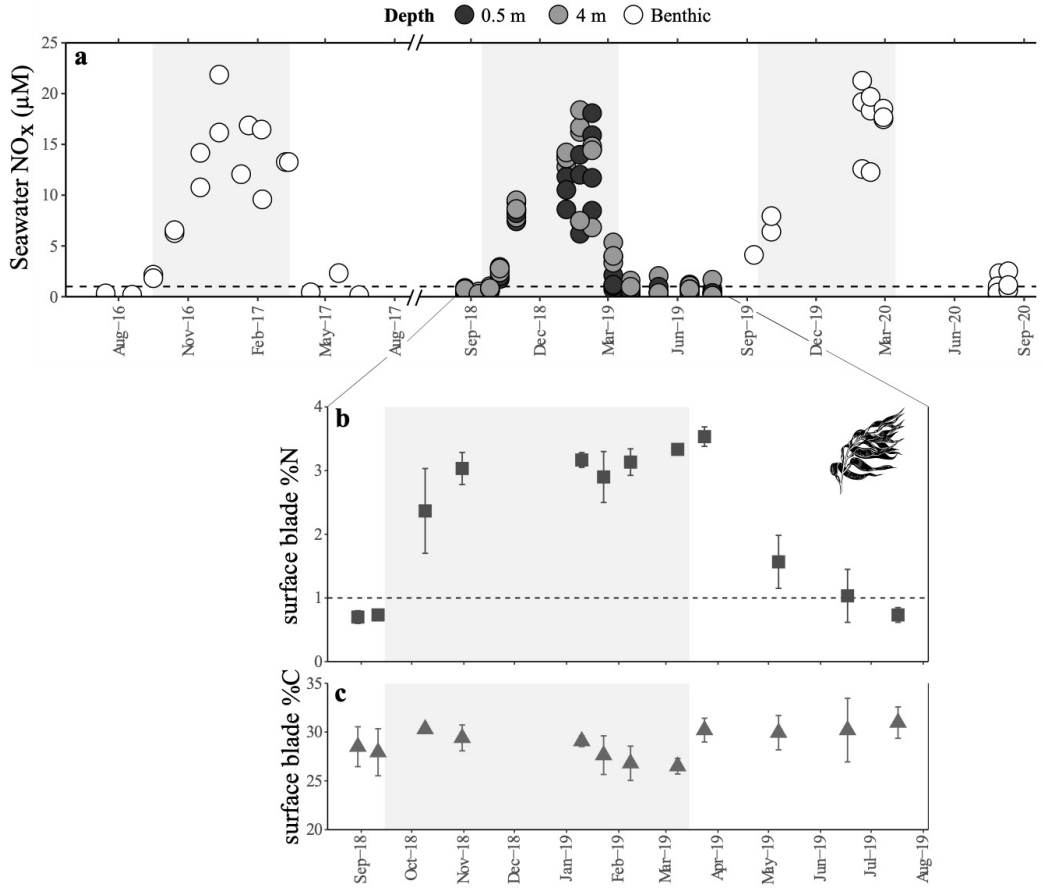

Figure 1.5. Seasonal production rates by canopy level for the giant kelp *M. pyrifera* and understory kelps *H. nigripes* and *N. fimbriatum* by (a) carbon mass (g C · m^{-2} · d^{-1}) and (b) nitrogen mass (g N · m^{-2} · d^{-1}) at Samsing Pinnacle.

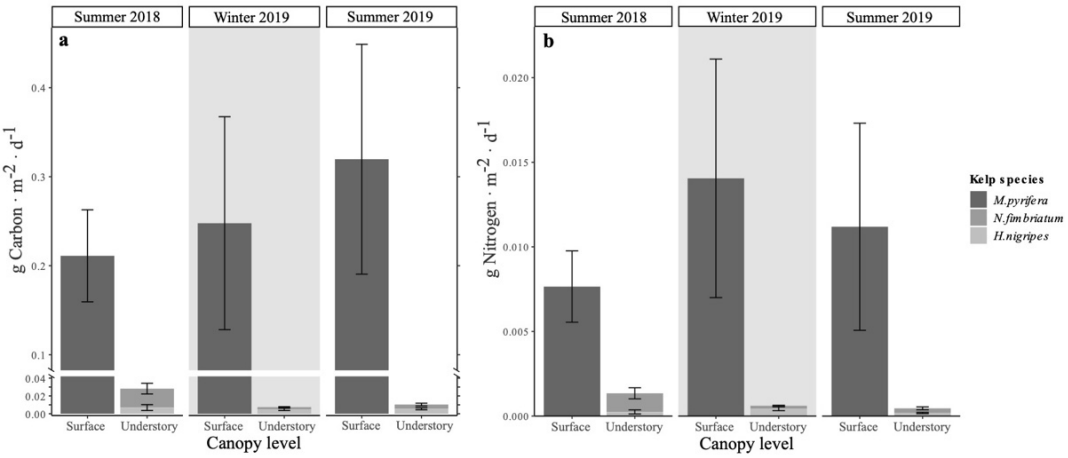

Chapter 2: Season influences interspecific responses of three canopy-forming kelps to future warming and acidification at high latitudes

Abstract

Variability in primary producers' responses to environmental change may buffer higher trophic levels against the negative impacts to basal resource composition. Then again, in instances where consumers rely on few species to meet their energetic requirements at specific times of the year, any alterations to the phenology of community production may significantly alter food web resilience. In high latitude kelp forests, a complementary annual phenology of seaweed production supports coastal marine consumers' metabolic needs across large seasonal variations in their environment. Yet, marine consumers in these systems may face significant metabolic stress in future winter environments, particularly if they lack the resources to support their increased energetic needs. In this study we investigate how the growth and nutritional value of three dominant, coexisting macroalgal species found in subpolar kelp forests will respond to ocean acidification and warming in future winter and summer seasons. We find that the three kelps *Macrocystis pyrifera*, *Hedophyllum nigripes*, and *Neoagarum fimbriatum* differ in their vulnerability to future environmental conditions, and that the seasonal environmental context of nutrient and light availability shapes these responses. Our results suggest that poleward fringe populations of *M. pyrifera* may be relatively resilient to anticipated ocean warming and acidification in this region. In contrast, ocean warming conditions caused a decrease in the biomass and nutritional quality of both understory kelps. Considering the unique production phenology of *H. nigripes*, we emphasize that negative impacts to this species in future winters may be of particular consequence to consumer

energetics in this system. This work highlights how interspecific variation in autotrophs' responses to global change can disrupt the diversity and phenological structure of energy supply available to higher trophic levels.

Introduction

Global environmental change is already affecting primary producers worldwide (Cavicchioli et al. 2019, Terrer et al. 2019, Walker et al. 2021). Anticipating how physiological effects on autotrophs scale up to affect higher trophic levels requires a robust understanding of how the quantity, quality, and identity of these basal resources will shift within different ecosystems (Ainsworth & Long 2004, Koch et al. 2013, Maschler et al. 2022). Species-specific variation in response to elevated CO_2 concentrations and temperatures may lead to a restructuring of primary producer community composition as well as disrupt the phenology of production in many systems (Cornwall et al. 2012, Franklin et al. 2016, Poorter 1988, Ullah et al. 2018). Further, effects of environmental change on the nutritional value or palatability of basal resources can significantly impact consumer energetics and food web structure (Campanyà-Llovet et al. 2017, Cebrian et al. 2009, Facey et al. 2014, Rosenblatt & Schmitz 2016). There is an urgent need to compare the responses of dominant, coexisting primary producers to global environmental change to assess whether interspecific variability can buffer the emergent, bottom-up effects in these ecosystems (e.g., Gilbert et al. 2020, Liu et al. 2018).

In marine ecosystems, macroalgae (seaweeds) constitute a major energy resource that supports biodiverse and complex coastal food webs (Graham 2004, Hurd et al. 2014). Similar to terrestrial plants, global environmental change is expected to have extensive impacts on macroalgal growth and biomass (Harley et al. 2012). Elevated

temperatures with ocean warming (OW) may enhance algal primary productivity within optimal temperature ranges, and negatively impact productivity once thermal optima are exceeded (Eggert 2012, Hurd et al. 2014, Kram et al. 2016). The effects of elevated seawater pCO_2 and reduced pH with ocean acidification (OA) on the photosynthesis of non-calcified seaweeds are expected to differ based on each species' carbon use strategy (Cornwall et al. 2012, Hepburn et al. 2011, Hurd et al. 2020, but see Paine et al. 2023). Further, elevated temperature and pCO_2 can interact with each other and other environmental variables such as light and nutrient availability to shape species' responses (Celis-Plá et al. 2015, Hollarsmith et al. 2020, King et al. 2017, 2020, Ladah & Zertuche-González 2022). Thus, effects on individual species will hinge on how environmental change layers onto the natural temporal and spatial variability of resources in a particular ecosystem (Kroeker et al. 2020).

In addition to the direct effects of global environmental change on macroalgal primary production and growth, OW and OA can alter their value to consumers. Increased temperatures will affect the rate of algal nutrient uptake (Raven & Geider 1988), and increased pCO_2 can increase thallus nitrogen content (Falkenberg et al. 2013, but see Olischläger et al. 2014). Increased nitrogen content can enhance a seaweed's palatability to herbivores that preferentially consume nitrogen-rich food sources (Duffy & Paul 1992, Hillebrand et al. 2000, Russell & Connell 2007). However, the presence of secondary metabolites that may deter grazing, such as

phenolic compounds, may be a stronger determinant of herbivores' consumption (Amsler et al. 2005, Demko et al. 2017, Granado & Caballero 2001, Steinberg 1985). Elevated pCO_2 and temperature can reduce, increase or have no effect on seaweed phenolic concentrations depending on the species (Arnold et al. 2012, Kumar et al. 2018, Phelps et al. 2017) and their relative access to light and nutrients (Celis-Plá et al. 2015). Future alterations to seaweeds' secondary metabolic processes have strong potential to change consumptive interactions and energy flow through the base of the coastal food web (Doubleday et al. 2019, Duarte et al. 2016, Jin et al. 2020).

Interspecific variation in macroalgal responses to environmental change will alter the composition of seaweed communities and disrupt the phenology of consumers' food supply (Harley et al. 2012). These effects will be particularly evident in seasonally dynamic environments. High latitude marine ecosystems are characterized by large annual variations in temperature, pCO_2, light, and nutrients that influence the seasonal dynamics of primary production and algal physiology (Bell & Kroeker 2022, Takahashi et al. 1993, Tian et al. 2001). Increases in temperature and pCO_2 will overlay the current abiotic resource variability in these systems, giving rise to novel environmental scenarios that will drive seasonally distinct effects on macroalgal physiology (Graiff et al. 2015, Gunderson et al. 2016, Harley et al. 2012, Kroeker et al. 2020). The energetic linkages among lower trophic levels in seasonally dynamic marine food webs are highly dependent on tight temporal alignment between food supply and consumer demand (Sydeman & Bograd 2009). Thus, shifts in the seasonal

phenology of macroalgal production and quality could lead to mismatches in the timing and strength of these consumptive interactions (Wahl et al. 2020). This may be particularly consequential at high latitudes if consumers experience heightened seasonal windows of metabolic stress under future environmental change (Kroeker et al. 2021).

The goal of this study was to quantify potential shifts in the quantity and quality of three dominant, coexisting seaweed species to ocean acidification and warming. Our study took place in Sitka Sound, Southeast Alaska, a high latitude region of the North Pacific where pronounced marine environmental change is anticipated in the next century (IPCC 2018, Mathis et al. 2015) We focus on three large, canopy forming kelp species that dominate macroalgal biomass within the giant kelp forests of this region: *Macrocystis pyrifera*, *Hedophyllum nigripes*, and *Neoagarum fimbriatum*. The annual growth regimes of these three species are distinct in Sitka Sound (Bell & Kroeker 2022), likely a reflection of their differing physiological optima and tolerances. *H. nigripes* is a cold-adapted understory kelp found primarily in Arctic and sub-Arctic waters (Dankworth et al. 2020, McDevit & Saunders 2010). This species' annual growth is controlled by a strong endogenous clock, with blade elongation initiating in January and curtailing abruptly in early summer (Bell & Kroeker 2022, Lüning 1993). In contrast, the more temperate kelps *M. pyrifera* and *N. fimbriatum* sustain relatively high growth rates through spring, summer and early fall (Bell & Kroeker 2022). Additionally, while *M. pyrifera* dominates the understory

kelps in absolute biomass and production rates, *H. nigripes* and *N. fimbriatum* are consistently more nitrogen dense per gram of tissue (Bell & Kroeker 2022). Thus, the co-occurrence of these kelps currently functions to provide a complementary energy supply to coastal consumers throughout the calendar year (Kroeker et al. 2021).

To isolate the seasonal effects of environmental change on these kelp species, we grew adult sporophyte blades of each macroalga within two, month-long experiments in winter (Feb-March) and summer (Aug-Sept). Experimental controls were designed to reflect current environmental conditions in Sitka Sound (this study, Bell et al. 2022, Bell & Kroeker 2022, Kroeker et al. 2021), and OA and OW treatments were based on projected end-of-century scenarios of ocean acidification and warming for this region (IPCC 2018, Mathis et al. 2015). At the end of the experiments, we assessed the seasonal impact of OW and OA on kelp growth rates, thallus nitrogen content, and carbon acquisition strategy based on thallus $\delta^{13}C$ values. Finally, to test whether kelp palatability was impacted by future warming and acidification, we used tissue of *H. nigripes* and *N. fimbriatum* grown during the experiments to perform feeding assays with a common kelp forest consumer. We hypothesized that the three kelp species would differ in their sensitivity to ocean warming and acidification. We also anticipated that impacts to the biomass and quality of *H. nigripes* in future winter conditions could be particularly consequential to kelp forest consumers, given the early season growth and nitrogen-rich resource that this species represents during a metabolically demanding season (Bell & Kroeker 2022, Kroeker et al. 2021).

In a prior study, we presented 3 years of environmental data from sensor packages deployed within high latitude kelp forests in Sitka Sound (Kroeker et al. 2021). While seasonal trends in seawater temperature, pH and dissolved oxygen data were generally consistent across the time series, there was some interannual variation in pH ranges and seasonal amplitudes of pH variability that compelled us to continue our sensor deployments. In this study, we report the next 3 years of sensor data from a new kelp forest site in the area as well as a site that underwent transition from a kelp forest to an urchin barren during this period (Bell & Kroeker 2022). These additional data provide a stronger picture of the natural seasonal environmental variability that coastal marine organisms can experience within high latitude kelp forests and rocky reef barrens. We use this information to better inform our interpretation of how these environments will change in the future, particularly in the context of our experimental results.

This research responds to the call for a more nuanced understanding of how global change will alter marine primary producer resources by integrating natural variation in environmental drivers (Campanyà-Llovet et al. 2017, Rosenblatt & Schmitz 2016, Wahl et al. 2020). We build from our close understanding of the natural environmental variability and kelp production dynamics in this system to isolate seasonally specific effects of OW and OA on three foundational seaweed species, and interpret the potential impact of these changes on community structure and interactions (Cebrian et al. 2009, Harley et al. 2017, Seibold et al. 2018). This work

will add significantly to our understanding of how asynchronous responses among co-occurring primary producers to global environmental change may shape the bottom-up effects on the ecosystems they support.

Methods

In situ environmental data

From January 2019 to January 2022, we used sensor packages to record environmental data at the benthos (~7 m MLLW) at two rocky reef sites in Sitka Sound, Alaska: Harris Is. (57.032 N, 135.277 W) and Samsing Pinnacle (56.988 N, 135.357 W). Both sensors were originally located at the lower depth limit of *Macrocystis pyrifera* kelp forests; however, during the course of this study, Harris Is. transitioned to urchin barrens (Bell & Kroeker 2022). We utilized two different SeapHOx sensor packages (Martz Lab, Scripps Institute of Oceanography and Sea-Bird Scientific) that measured temperature, pH, and dissolved oxygen (DO). During each deployment, sensors recorded data every 30 minutes. Data gaps occurred during data downloads, battery failures or sensor maintenance. In some cases, sensors were rotated among sites to maximize data continuity. Environmental data at Harris Is. from January 2016 to January 2019 has been reported previously (Kroeker et al. 2021).

We collected discrete water samples next to each sensor 1-2 times during each deployment for calibration of sensor pH. Water samples were collected without aeration and poisoned with saturated $HgCl_2$ (0.025%) in glass bottles within 20 minutes. Airtight samples were transported to the University of California Santa Cruz (UCSC) for analysis within 3.5 years of collection. We measured pH spectrophotometrically (Shimadzu, UV-1800) using *m*-cresol purple following best

practices (Dickson et al. 2007), with a mean standard error of 0.0012 pH units among sample triplicates. We measured total alkalinity (TA) using open cell titration (Metrohm, 905 Titrandro) and corrected against certified reference materials of CO_2 in seawater (Dickson laboratory, Scripps Institute of Oceanography). Mean standard error was 0.96 μmol kg^{-1} SW^{-1} among sample triplicates. To calculate in situ pH on the total hydrogen ion concentration scale (pH_T; mol kg^{-1} SW^{-1})(Dickson 1993), we used our laboratory measurements of spectrophotometric pH and TA, sensor measurements of in situ temperature and salinity recorded concurrently with discrete water sample collection, and stoichiometric dissociation constants (Dickson & Millero 1987, Mehrbach et al. 1973) as inputs to the program CO2SYS (Lewis & Wallace 1998, Pierrot et al. 2006). In cases where salinity was not recorded at the time of calibration, we used a densitometer (Mettler Toledo, DX45) to calculate salinity of the discrete water samples. We then used in situ pH_T values of discrete samples to calculate calibration coefficients at 25°C (E*25), which we used to correct sensor pH_T (Bresnahan et al. 2014). We estimated uncertainty in the sensors' pH_T time series by calculating the root-mean-square error (RMSE) from the relationship between pH_T values measured with discrete samples and pH_T calculated from the applied calibration coefficient models. We utilized the data cleaning Hampel filter in R (pracma::outlierMAD) to remove outliers from pH, temperature and DO data (Pearson 2011). We investigated the resemblance between diel pH variability and tidal action during spring 2019 by computing the cross-correlation between timeseries of the maximum diel difference in recorded pH_T values recorded at each site and the

maximum diel difference in observed tidal heights (m) verified at the Sitka, AK tidal station (NOAA station 9451600) from February 15 to May 20, 2019.

To compare in situ nutrient and light data with aquaria conditions during the experiment (see *Seasonal experiments for kelp species*, below), we collected environmental data at the experimental collection site: Talon Is. (57.073 N, 135.414 W), Sitka Sound. Benthic seawater was collected for determination of nutrient concentrations in February and August 2020 (N=3 samples^{-1} season^{-1}). Seawater for nutrient samples was immediately filtered through a 0.2 µm filter and frozen until analysis for dissolved inorganic nitrogen content as NO_x (NO_3 + NO_2) and ammonium (NH_4^+) on a Lachat QuikChem 8000 Flow Injection Analyzer at the University of California Santa Cruz Marine Analytical Laboratory (detection limits: < 0.28 µM NO_x, < 2.40 µM NH_4; average run measurement error < 0.1 µM NO_x < 0.8 µM NH_4). We used a Diving-PAM-II (Heinz Wlz GmbH) MINI-SPEC to haphazardly record the photosynthetic photon flux density (PPFD; μmol m^{-2} s^{-1}) reaching the benthos at more than 10 locations along the ~5 m depth contour on two clear days in winter (February 28) and summer (September 19).

Seasonal experiments for kelp species

To tease apart the effects of seasonal variation in light availability and nutrients on the response of high-latitude kelp species to pH and temperature, we conducted two separate laboratory studies: a 'winter' experiment from February 12 - March 18, 2020 (35 d), and a 'summer' experiment from August 15 - September 16, 2020 (32 d). In

our experimental design, analysis, and reporting, we endeavored to follow best practices for OA research with macroalgae (Cornwall et al. 2012, Cornwall & Hurd 2016). Both experiments took place at the Sitka Sound Science Center in a flow-through seawater system drawing source water from 20 m depth (MLLW) in Sitka Sound, Alaska. Incoming seawater was filtered to 20 μm and routed through a UV filter (Smart UV®, Pentair) before diverging into two temperature-controlled (TITAN® heat pump and Optima compact heaters, AquaLogic) recirculating tanks representing treatments for 'current' or control temperatures (7°C in winter; 14°C in summer) and 'future' OW projections (11°C in winter; 18°C in summer)(IPCC 2018) by season. From here, temperature regulated seawater was pumped into eight header tanks where pH was maintained at seasonal targets for 'current' or control levels (pH_T 7.6 in winter; pH_T 7.9 in summer) and 'future' OA projections (pH_T 7.2 in winter; pH_T 7.5 in summer) (Mathis et al. 2015) through a relay system ($N = 2$ header tanks per pH/temperature treatment). In both seasonal experiments, achievable pH_T setpoints for 'current' condition treatments were constrained by the ambient pH of incoming seawater and were therefore lower than in situ pH_T minima observed on local rocky reefs by ~0.1 - 0.2 pH units (Kroeker et al. 2021, and this study). A DuraFET sensor (Honeywell) in each header tank communicated real-time pH measurements to a controller (UDA 2152, Honeywell) that regulated injection of pre-equilibrated low pH seawater through solenoid valves into the headers to maintain pH at treatment set points. The low pH (~6) seawater was produced by bubbling pure CO_2 gas into two tanks of seawater flowing from each temperature-controlled tank.

Once in each header tank, the CO_2 and temperature-equilibrated seawater was continuously mixed before delivery to 24 experimental aquaria (N = 3 aquaria per header) at an average flow-through rate of 2-2.5 L min^{-1} $aquaria^{-1}$.

Seawater nutrient concentrations were not manipulated, and thus reflected what was delivered through source water inflow to the system during each experiment. Terrestrial outflow from heavy precipitation over Southeast Alaska's temperate rainforests and wind stress dynamics in the Gulf of Alaska control nutrient supply onto the Northeast Pacific shelves (Hermann et al. 2009, Hood & Scott 2008, Ladd & Cheng 2016, Stabeno et al. 2016). The complexities of how climate change may impact these drivers in tandem with altered phytoplankton productivity (Ji et al. 2010) means that there is little consensus on how seasonal nutrient supply into Sitka Sound may change. Therefore, we chose to assume that nutrient availability, like seasonal light availability, would not differ significantly in this region in the future. All aquaria were fitted with a full-spectrum light (Aqua Illumination) that provided seasonally relevant regimes of photosynthetically active radiation spectra and photoperiod within the aquaria based on prior measurements during overcast days in Sitka Sound (Bell et al. 2022). The entire experimental system was shielded from external light sources, and aquaria positions were randomized by treatment and location to minimize spatial variation among the random factors *aquaria* and *header*.

We monitored temperature, salinity, DO, and pH_{NBS} daily in each aquarium with a handheld meter (YSI). To capture diel variation in these parameters associated with

organismal photosynthesis and respiration, we also performed these measurements every three hours in each aquarium for 24 hrs, once during the winter experiment (March 4-5) and twice during the summer experiment (August 30-31, Sept 14-15). At the beginning, middle, and end of each experiment, we collected discrete water samples for determination of pH_T, TA, and nutrient concentrations in each aquarium and header tank. Discrete samples for pH_T, TA and nutrients were analyzed following the methods outlined in the *Environmental Data* section (above). Water chemistry samples from each tank had a mean standard error of 0.0013 pH units and 0.87 μmol kg^{-1} SW^{-1} among sample triplicates.

Kelp used in both winter and summer experiments came from 4.5-7.5 m depth at Talon Is., Sitka Sound. We collected these experimental 'individuals' as whole adult thalli (*Neoagarum fimbriatum* and *Hedophyllum nigripes),* or as single blades with their attached pneumatocysts that were cut from young sporophytes at approximately 1 m above their holdfasts (*Macrocystis pyrifera)*. During transport to the laboratory and prior to the start of the experiments (< 2 d), we held all algae continuously in ambient flow-through seawater (winter experiment: ~6°C, pH_T 7.8; summer experiment: ~13.5°C, pH_T 8.0). We removed individuals briefly only to clean off epiphytes and record initial morphometrics (maximum blade length, total wet mass) after trimming all blades to 10 cm total length. We also took pictures of each trimmed blade to estimate total surface area using ImageJ (NIH v1.8.0).

In both the winter and summer experiments, we randomly assigned 3 individuals of each kelp species to each experimental aquaria (N = 18 individuals species^{-1} treatment^{-1}). We affixed individuals upright in aquaria by placing their stipes or pneumatocysts through three-strand line suspended over the open ends of 5 cm tall PVC stands. After all seaweeds were processed for initial morphometrics, we gradually changed pH and temperature in treatment tanks stepwise over the course of 3 d to reach final setpoints. During the experiment, kelps were visually checked daily for necrosis and were lightly brushed biweekly during aquaria cleaning to remove diatoms.

At the end of each experiment, individuals were measured and photographed for final morphometrics. Due to the difficulty in capturing three-dimensional tissue growth and the error inherent in wet mass measurements, we estimated kelp growth rates using three different metrics: wet mass (g), maximum blade length (cm), and total blade surface area (cm^2). We used the initial ($G_{initial}$) and final (G_{final}) measurements of each metric to calculate three relative growth rates (RGR; d^{-1}) for each individual using the equation:

$$RGR_{(mass,length\ or\ surface\ area)} = \frac{log(\frac{G_{final}}{G_{initial}}) \cdot 100}{\Delta t}$$

where Δt (d) is the total days elapsed between the beginning and end of the experiment. Relative growth rates were used for subsequent statistical analyses of

experimental results. Absolute blade length extension rates were used to compare experimental growth to in situ kelp growth measurements (Bell & Kroeker 2022).

From each individual, we excised new blade tissue grown during the experiment adjacent to the intercalary meristem and pooled this tissue among species replicates in each aquarium. A portion of this tissue was frozen at -20°C for use in feeding assays (see *Algal palatability assays*, below). The other portion of this tissue was dried at 60°C for >24 hr and analyzed for nitrogen (N) content (% dry mass) and $\delta^{13}C$ values by the UCSC Stable Isotope Laboratory using a CE Instruments NC2500 elemental analyzer coupled to a Thermo Scientific DELTAplus XP isotope ratio mass spectrometer via a Thermo-Scientific Conflo III (routine measurement error ≤ 1.0 %C and ≤ 0.2 %N). We also analyzed blade tissue from non-experimental kelp individuals collected at Talon Is. in each season ('field controls'; N=6 species^{-1} season^{-1}) for elemental and isotopic analysis.

We quantified variability in relative growth rates, nitrogen content, and $\delta^{13}C$ values of each kelp species during each experiment using linear mixed-effects models (R; R Core Team 2022). We specified *pH*, *temperature* and the *interaction between pH and temperature* as fixed factors. In models of growth rate, we specified *aquaria* nested in *header* as random intercepts using restricted maximum likelihood. In models of kelp species' tissue nitrogen content and $\delta^{13}C$ values, in which samples were pooled by aquaria, we specified *header* as the random intercept using restricted maximum likelihood. We used Q-Q plots and Tukey-Anscombe plots to confirm that all models

satisfied assumptions of normality and homoscedasticity (Winter 2013). We used the Sattertwaithe's method for t-tests to determine p-values for the effects of fixed factors.

Algal palatability assays

We used tissue from *H. nigripes* and *N. fimbriatum* individuals grown in the laboratory (see *Seasonal experiments for kelp species*, above) to investigate whether future ocean conditions affect the palatability of these understory kelp species in either season. In April 2021, we modified methods used by Hay et al. (1994) to create 'gels' of homogenized kelp tissue suspended in agar and enmeshed in squares of window screen. Each 30 cm^2 gel was formed from 0.1547 ± 0.0004 g (mean ± SE) of freeze dried (FreeZone, Labconco) *H. nigripes* or *N. fimbriatum* tissue representing either current or future pH and temperature combinations. The total number of gels used for the feeding assays was limited by the available kelp tissue grown during each experiment, and was consequently lower for gels made from tissue grown in the winter experiment (*H. nigripes*: N = 11 gels $treatment^{-1}$, *N. fimbriatum*: N = 12 gels $treatment^{-1}$) versus the summer experiment (*H. nigripes*: N = 24 gels $treatment^{-1}$, *N. fimbriatum*: N = 23 gels $treatment^{-1}$). We ran palatability assays by feeding these seaweed gels to the common kelp forest grazer, *Strongylocentrotus droebachiensis* (green urchin). Urchins with a test diameter of 24 ± 3 mm were collected from the intertidal, starved for 48 hrs, and then placed in a flow-through chamber with a gel in ambient seawater conditions (~7 °C, ~8.0 pH) for 48 hrs. We photographed each gel

before and after the assay and determined relative consumption of seaweeds grown under different treatments using Image J (NIH v1.8.0). We assessed differences in relative consumption of *N. fimbriatum* or *H. nigripes* tissue using two-way Analysis of Variances (ANOVAs) with fixed factors of *treatment*, *season*, and the *interaction between treatment and season*. All data were checked for normality using QQ-plots and homoscedasticity was tested by visual inspection of the residuals. A Tukey's HSD post hoc comparison of means was used to determine significant pairwise differences among treatments.

Results

Environmental data

In line with environmental data reported previously from rocky reef sites in Sitka Sound (Kroeker et al. 2021), we observed that seawater pH_T at 7 m depth reaches a low of 7.8-7.9 in January and a high of 8.3-8.4 in May (Fig. 1.1a). Annual minima and maxima of pH_T values typically precede those of temperature by several months. Maximum diel pH_T differences in spring 2019 (up to 0.3 pH_T day^{-1}) exceeded 60% of the amplitude of annual pH_T variability at both sites. Cross-correlation between diel maximum differences in pH and tidal height during spring 2019 indicated a lag of 4 days between minimal tidal differences and maximal pH differences over this period at both sites (Fig. S1). The root mean square error (RSME) of the fit of calibration coefficients based on pH from discrete samples differed depending on the final quality of bottle samples available for calibration. For data from Samsing Pinnacle, RSME was 0.02 pH units for estimated in situ pH_T values for the period from January 2019 to January 2020, and 0.002 pH units from January 2020 to January 2021. For Harris Is. data, RSME was 0.008 pH units for the estimated pH_T values from January 2019 to 2020 and 0.02 pH units from January 2019 to January 2022.

Seawater temperatures swing from an annual low of ~7°C in March up to a high of ~15°C in August (Fig. 2.1b). DO concentrations range from ~9 mg/L in November to ~16 mg L^{-1} in May (Fig. 2.1c). Temporal variation in these environmental parameters at both Samsing Pinnacle and Harris Island were closely aligned. Seawater samples

collected at Talon Is. had average nutrient concentrations of 16.7 mg L^{-1} NO_x and 7.6 mg L^{-1} NH_4 in February and 1.4 mg L^{-1} NO_x and 2.8 mg L^{-1} NH_4 in August. PPFD measured at Talon Is. on clear days ranged from 50-90 μmol m^{-2} s^{-1} in February and 20-80 μmol m^{-2} s^{-1} in September.

Seasonal experiments for kelp species

Experimental conditions

Replicate experimental aquaria were successfully maintained at pH_T and temperature setpoints offset by -0.4 pH units and +4°C between current ("control") and future (OA and OW) treatments within each seasonal experiment (Table 1). Discrete water samples confirmed that pCO_2 also differed by treatment and experiment. Salinity, total alkalinity, and nutrient concentrations did not differ among treatment aquaria within each seasonal experiment. Dissolved oxygen concentrations were up to 1 mg/L higher in aquaria assigned a lower temperature treatment compared to aquaria with elevated temperatures within each experiment. Light regimes were maintained uninterrupted throughout each seasonal experiment at PPFD 10-25 μmol m^{-2} s^{-1}, 7.5 h d^{-1} (winter experiment) and PPFD 40-80 μmol m^{-2} s^{-1}, 11 h d^{-1} (summer experiment). Diel pH cycles within aquaria due to algal photosynthesis and respiration were up to 0.05 pH units during the winter and up to 0.1 pH units in the summer experiment, but did not differ among treatments. Due to analytical error, there were insufficient samples to assess the relative nutrient concentrations among

all treatments in either experiment. Experimental nutrient concentrations of NO_x and NH_4 are reported as mean values in each experiment (Table 1).

Kelp growth

Treatment effects on kelp growth rates were consistent regardless of growth metric. Hereafter, we report growth results in terms of relative change in individuals' wet mass (RGR_{mass}), which can best capture three-dimensional changes in individuals' stipe, pneumatocyst or blade morphologies.

The effects of OW and OA on kelp growth differed among species (Fig. 2.2). For one species (*H. nigripes*), growth was reduced in OW treatments, regardless of season (winter: $p < 0.001$, Table S2.1; summer: $p = 0.005$, Table S2.2). Another species' (*N. fimbriatum*) growth was not impacted under future winter OW (Table S2.3), but was reduced under elevated temperatures in the summer experiment ($p < 0.001$, Table S2.4). This is in contrast to growth of the kelp *M. pyrifera*, which was not affected by OW in either winter (Table S2.5) or summer (Table S2.6 experiments). There was no effect of pH or the interaction between temperature and pH on the growth of any species in the summer experiment. In the winter experiment, there was a marginally significant interaction between temperature and pH on *H. nigripes*' growth ($p = 0.057$). The combination of winter OW and OA conditions resulted in higher RGR_{mass} for *H. nigripes* than individuals grown under OW alone. There was no effect of pH or the interaction between temperature and pH on the growth of *N. fimbriatum* or *M. pyrifera* in the winter experiment.

In the winter experiment, blade length extension rates of *H. nigripes* grown in current pH and temperature treatments were lower than observed growth rates for this understory kelp in Sitka Sound in February and March (Fig. S2) (Bell & Kroeker 2022). Blade length extension rates of both *N. fimbriatum* and *H. nigripes* in current pH and temperature conditions of the summer experiment were comparable to observed length extension rates in August and September in Sitka Sound (Bell & Kroeker 2022). We do not have in situ blade extension data for *M. pyrifera* to enable comparison of experiment versus field growth rates.

Nitrogen content

Nitrogen content of all three kelp species (as % tissue dry mass) was reduced under certain OW conditions, with seasonal differences among the species (Fig. 2.3). Nitrogen content of *H. nigripes* was reduced under elevated temperatures ($p = 0.006$, Table S2.7) in the winter experiment, but not the summer experiment (Table S2.8). Meanwhile, elevated temperatures reduced the tissue nitrogen content of *N. fimbriatum* in both winter ($p = 0.030$, Table S2.9) and summer ($p = 0.012$, Table S2.10) experiments. There was no effect of either pH or the interaction of temperature and pH on %N of *H. nigripes* or *N. fimbriatum* in either season. Similar to *H. nigripes*, nitrogen content of *M. pyrifera* tissue in the winter experiment was decreased under elevated temperatures ($p = 0.004$, Table S2.11), but was not affected by OW in the summer experiment. However, OA conditions in the winter experiment caused an increase in *M. pyrifera* %N ($p = 0.032$). There was no interaction between

pH and temperature. In the summer experiment, *M. pyrifera* %N was not affected by temperature, pH, or the interaction between factors (Table S2.12).

$\delta^{13}C$ values

Ocean acidification treatments reduced $\delta^{13}C$ values in both seasons for *H. nigripes* (winter: $p < 0.001$, Table S2.13; summer: $p = 0.006$, Table S2.14) and *N. fimbriatum* (winter: $p = 0.002$, Table S2.15; summer: $p = 0.001$, Table S2.16). In contrast, tissue $\delta^{13}C$ values of *M. pyrifera* were not reduced under low pH conditions in the winter experiment (Table S2.17), but were reduced under OA in the summer experiment ($p = 0.009$, Table S2.18). In the summer experiment, *H. nigripes*' tissue $\delta^{13}C$ values were also reduced under elevated temperatures ($p = 0.006$). The most negative $\delta^{13}C$ values were observed in *H. nigripes* individuals grown under a combination of both OA and OW (Fig. 2.4), but we did not detect an interactive effect of pH and temperature on *H. nigripes*' tissue $\delta^{13}C$. Otherwise, there was no effect of OW or the interaction between OW and OA on the $\delta^{13}C$ values of the three kelp species in either experiment.

Algal palatability assays

We found that urchins consumed over 30% more of *H. nigripes'* tissue grown in future summer OW and OA than tissue grown under treatment controls in the summer experiment (Fig. 2.5; $p = 0.024$). We observed a marginally significant interaction between experimental treatment and season, as OW and OA conditions had no effect

on the palatability of *H. nigripes'* tissue grown in the winter experiment ($p = 0.969$; Table S2.19). There was no effect of pH and temperature treatment, season, or their interaction on the palatability of *N. fimbriatum* tissue (Fig S3; Table S2.20).

Discussion

Our study indicates that in high latitude coastal systems, future ocean warming will decrease the growth and nutritional content of certain kelps while ocean acidification will primarily drive changes in species' carbon use strategy. We also found that kelps' responses to future shifts in temperature and carbonate chemistry will depend on the seasonal environmental context, including the relative availability of light and nutrients in each season. Furthermore, these overlapping environmental drivers may indirectly affect higher order consumers via changes to seaweed palatability in certain seasons. Given the inherent differences in distributions, life histories and annual production dynamics among the subtidal kelps in this study (Bell & Kroeker 2022, Dankworth et al. 2020, Schiel & Foster 2015), we were unsurprised to find that seasonal scenarios of ocean warming and acidification elicited distinct responses in each macroalgal species. This research demonstrates that changing environmental conditions will shift the seasonal quality, quantity of basal resources in kelp ecosystems at high latitudes, likely reducing the functional biodiversity of these communities (Schlenger et al. 2021). Prior research in this system identified that future winter seasons may represent a period of vulnerability for calcified consumers, due to the overlap of enhanced physiological stress from low pH/high pCO_2 seawater at a time when macroalgal food supply is naturally at an annual minimum (Bell & Kroeker 2022, Kroeker et al. 2021). Our research expands this projection by revealing that consumers' stress in future winters may be compounded by pronounced

reductions in macroalgal biomass and nutritional content primarily due to warming in this season.

Of the three kelps we considered, *H. nigripes* was the only species to exhibit reduced growth under ocean warming scenarios in both winter and summer experiments. Optimal temperatures for growth and gametogenesis in this species have been shown to occur at ≤ 10℃ and decline above 15℃ (Druehl 1967, Franke et al. 2021, Longtin & Saunders 2016). Indeed, current in situ productivity of *H. nigripes* declines dramatically starting in August in Sitka Sound (Bell & Kroeker 2022), and our sensor data reveal this is just as seawater temperatures approach 15℃. Elevated temperatures in summer with ocean warming are likely to extend this seasonal period of reduced growth for *H. nigripes* in the future. Additionally, *H. nigripes*' low growth in the winter experiment under a future OW scenario of 11℃ suggests that other environmental variables such as relative light availability and nutrient supply may interact with temperature to define this species' seasonal thermal optima.

Distinct from *H. nigripes*, growth of the other two kelp species was not vulnerable to the elevated temperatures expected in future winters. The understory kelp *N. fimbriatum* displayed reduced growth only under summer OW conditions. In Sitka Sound, growth of *N. fimbriatum* thalli is observed year-round, although blade extension rates are generally higher in summer than winter (Bell & Kroeker 2022). While future summer OW conditions may challenge the thermal tolerance of this species during the warmest months of the year, its capacity for continuous production

in this system could buffer a reduction in its growth in this particular season. Growth of the giant kelp *M. pyrifera* was unaffected by OW scenarios in either seasonal experiment, suggesting that production of this species may be resilient to future warming during future winter and summers at high latitudes. Sitka Sound is situated at the poleward edge of *M. pyrifera*'s continuous range extent (Druehl 1970, 1981). Although intrapopulation variation in thermal tolerance has been observed in this species (Hollarsmith et al. 2020), these northern fringing *M. pyrifera* populations may possess enough phenotypic plasticity to afford a relative tolerance to anticipated OW conditions in this region (Becheler et al. 2022, King et al. 2020).

In contrast to the species-specific responses of growth rate to future environmental conditions, all three kelps in this study exhibited reduced tissue nitrogen content under winter scenarios of ocean warming. Currently in Sitka Sound, kelp nitrogen content increases in winter due to the ample seawater nutrient supply and low energetic requirements during this season of low light and low temperature (Bell & Kroeker 2022). The energetic expense of nutrient acquisition can be limited by low light levels (Hurd et al. 2014, Roleda & Hurd 2019). Yet some kelps, including *H. nigripes* and *M. pyrifera,* readily uptake nitrate at equal or higher rates in the dark compared to the light by mobilizing carbohydrate reserves (Harrison et al. 1986, Korb & Gerard 2000, Wheeler & Srivastava 1984). The additional metabolic demand for nutrients that can occur under elevated temperatures may undermine these kelps' ability to maintain nitrogen reserves in their tissues even when nutrients are replete,

as has been seen in temperate and Arctic populations of *Saccharina latissima* (Olischläger et al. 2014). Our results underscore the unexpected vulnerability of these high latitude kelps to nutritional depletion during a season associated with plentiful nutrient supply, even when projected future winter temperatures fall well within their current annual thermal range.

Seasonal differences in OW's impact on kelp nitrogen content likely arise from an interaction between environmental nutrient supply, temperature, and light on kelps' nitrogen uptake kinetics and usage (Endo et al. 2017, Mabin et al. 2019). As far as we are aware, there are few other studies that have considered the impact of OW on kelp nutritional content specifically under winter conditions of high nutrients combined with temperatures on the lower end of species' annual thermal range. More commonly, prior research has been set up similar to our summer experiment and reflect our results for *H. nigripes* and *M. pyrifera* in these conditions: OW treatments are chosen to exceed kelps' annual thermal maxima under low to moderate nitrogen concentrations (0.5-3 uM NOx), and these scenarios have no impact on kelp tissue nitrogen content (e.g., Brown et al. 2014, Mabin et al. 2019). Yet, we find it surprising that summer OW conditions had no effect on any of *M. pyrifera*'s measured physiological responses, given the documented vulnerability of this species to high temperature and low nutrient conditions in other studies (Schmid et al. 2020, Umanzor et al. 2021). We suspect that the results of our summer experiment may have been unintentionally influenced by a supplemental supply of nutrients to our

system. The intake for our experimental system drew seawater just offshore from a natural river mouth, which was distinguished by an accumulation of decomposing salmon carcasses during the second half of our summer experiment. We believe the concentrated outflow of nutrients from these fish in river water (authors' unpublished data) was picked up by our system's intake, leading to elevated ammonium concentrations in our aquaria compared to typical summer seawater nutrient concentrations in situ (Bell & Kroeker 2022). We also interpret that the higher mean tissue nitrogen content of the kelps grown in these aquaria compared to observed nitrogen content of kelps at this time of year in situ (Bell & Kroeker 2022) reflects how readily the macroalgae assimilated this supply of ammonium (Cedeno et al. 2021, Hurd et al. 2014). Therefore, the apparent resilience of kelps in our study to summer heat stress may have been due to the added heat tolerance conferred by having relatively high nitrogen reserves (Fernández et al. 2020, Gerard 1997, Schmid et al. 2020). We anticipate that under a more realistic simulation of seasonal environmental nutrient depletion, the negative effects of OW on kelp physiology may have been more pronounced in future summer scenarios.

Based on benthic irradiance data collected in the field on sunny days in winter and summer, we acknowledge that subtidal kelps can experience substantially higher light levels in the field in February than the static PPFD provided in our winter experiment. We hypothesize that this is the reason *H. nigripes*' growth rate under 'current' conditions in our winter experiment was lower than we have observed in the field at

the same time of year (Bell & Kroeker 2022). Many high latitude seaweeds' photosynthesis saturation points occur at much higher irradiances than are required for growth, enabling these species to capitalize on enhanced carbon assimilation under large fluctuations in light (Gómez et al. 2009, Scheschonk et al. 2019, Wiencke et al. 2009). It is also possible that a greater supply of light could have improved *H. nigripes*' resilience to elevated temperatures in the winter experiment (Andersen et al. 2013, Nejrup et al. 2013). However, the relatively low light within our winter experiment was not wholly inappropriate. The PPFD provided does reflect the lower range of irradiance levels observed at the benthos in Sitka Sound on overcast winter days (Bell et al. 2022). Additionally, precipitation is expected to increase in Southeast Alaska primarily in winter months (Cherry 2010, Markon et al. 2012, Shanley et al. 2015), which could result in greater cloud cover and reduced incident light at the benthos in the future. In view of the potential consequences that reduced *H. nigripes* biomass could represent for consumers in future winters, we advise further research into the interactive effects of light availability and OW on this species' production.

The clear response of all three kelp species' $\delta^{13}C$ values to OA conditions suggests that these kelps capitalize on enhanced CO_2 availability to optimize their carbon acquisition strategies. Presumably, the reduced $\delta^{13}C$ values indicate a downregulation of carbon concentrating activity with concomitant energetic savings (Cornwall et al. 2012, 2015b, Hepburn et al. 2011). However, this spare energy did not appear to be consistently invested into new growth, except perhaps by ameliorating the negative

impacts of OW on *H. nigripes* growth under winter conditions. In *M. pyrifera*, an increase in tissue nitrogen content under winter OA conditions indicates that this extra energy may have been mobilized to enhance nutrient uptake and assimilation. Intriguingly, this effect compensated for reduced nitrogen content under elevated winter temperatures when the two treatments were applied in tandem, suggesting a mitigating effect of OA on OW on *M. pyrifera*'s nitrogen utilization in future winters. Aside from these results, it is unclear whether the potential energetic benefits of OA conditions may lead to other ecologically consequential changes for these kelp species.

Our results also suggest that the combination of OW and OA may have biochemical effects on algal palatability beyond what we considered in our study. The increase in urchins' consumption of *H. nigripes* tissue grown in future summer ocean conditions could indicate a decrease in secondary metabolites, causing the algae to be more susceptible to grazing (Arnold et al. 2012, Hemmi & Jormalainen 2002, Swanson & Fox 2007). Increased grazing could also be due to a decrease in nutritional quality in the seaweed blade, causing compensatory feeding (Cruz-Rivera & Hay 2000, L. Falkenberg et al. 2014, Rodríguez et al. 2018). While we did not observe an effect of summer OA and OW on *H. nigripes*' nitrogen content, a nutritional decrease could be driven by a decrease in fatty acid, lipid, or mineral content (Britton et al. 2020, Galloway et al. in prep, Zhang et al. 2021). Our feeding assay results only begin to hint at the additional effects that OA and OW may have on macroalgal

physiochemical structure, and they reinforce the importance of testing the emergent effects of environmental change on food web interactions (Jin et al. 2020, Jin & Gao 2021).

Lastly, with this study we add to our previous environmental monitoring dataset within high latitude kelp forest habitats (Kroeker et al. 2021). Because one of our sensor deployment sites (Harris Is.) unexpectedly transitioned from a lush kelp forest to an urchin barren over the course of this deployment (Bell & Kroeker 2022), we have the opportunity to consider how this transition may have altered the seasonal environmental variability experienced by the rocky reef community at this site. Generally, we see no major changes to the annual patterns of temperature, pH, or DO at Harris Is. before (prior to 2019; see Kroeker et al. 2021), during (2018-2019), or after (2020-2022) the transition from kelp forest to urchin barren. The environmental data at Harris Is. after transition to an urchin barren closely mirror our sensor data collected concurrently within an intact kelp forest (Samsing Pinnacle). The pH_T of both benthic sensor time series also generally aligns with calculated pH_T of seawater collected over the same period at 1 m depth in the Sitka Channel (Whitehead et al. 2022). We interpret these findings to indicate that seawater biogeochemistry at the benthos of these high latitude kelp forests is driven primarily by seasonal phytoplankton production dynamics in the region and less influenced by local macroalgal production. The close correlation we find between diel tidal strength and diel pH_T variability at both sites supports our hypothesis that advection of water from

beyond each reef controls the benthic environment, regardless of macroalgal biomass. Koweek et al. (2017) concluded similar hydrographic controls on the benthic biogeochemistry within giant kelp forests in central California, but also found a significant effect of canopy production on the surface water carbonate chemistry. The degree to which photosynthesis within high latitude kelp canopies can impact water column biogeochemistry is an important question for future research, particularly considering the lower biomass and productivity of these fringe populations of giant kelp compared to those at the heart of this species' range (Bell & Kroeker 2022, Reed et al. 2009). In any case, it is unlikely that future changes to kelp primary production will influence the exposure of vulnerable benthic organisms to OA within high latitude giant kelp beds. Considering the pronounced short-term pH variability that these rocky reef communities are currently experiencing in this system during the spring, regional phytoplankton production and respiration dynamics will likely continue to drive the biogeochemical environment of these rocky reefs in the future (Hauri et al. 2020, Strom et al. 2016).

Altogether, our experimental results for these three common canopy-forming subtidal kelp species paint a picture of how the macroalgal energy supply in this system may shift in the future. Our finding that future warming had a greater impact than ocean acidification on the growth and nutritional quality of high latitude kelps is consistent with studies of macroalgae in other high latitude and subtropical habitats (Graba-Landry et al. 2018, Wahl et al. 2020). The vulnerability of the pan-Arctic understory

species *H. nigripes* is particularly noteworthy. In the winter, the reduction of both biomass and quality of this species could represent an energetically devastating loss for calcified rocky reef consumers facing additional metabolic stress associated with OA in the future (Kroeker et al. 2021). Meanwhile, high latitude populations of the more temperate kelp species *M. pyrifera* may be relatively resilient to the effects of OA and OW. Giant kelp may therefore continue to dominate total macroalgal production on reefs where it forms the surface canopy (Bell & Kroeker 2022). However, consumers cannot rely on this species alone to fulfill their nutritional needs (Kroeker et al. 2021). Thus, the combination of OA and OW threatens not only the functional biodiversity of the macroalgal community on these high latitude reefs, but also the resilience of the consumer community that depends on their production.

Acknowledgements

This work was supported by the National Science Foundation [OCE-1752600], the David and Lucile Packard Foundation, the North Pacific Research Board's Graduate Student Research Award (1748-02), the UCSC Physical and Biological Sciences 2019 Future Leaders in Coastal Science Award, the Seymour Marine Discovery Center's Student Research and Education Award, and the California State University Monterey Bay Undergraduate Research Opportunities Center. We thank B. Conaway, C. Gray, P. Sorenson, L. Wild, P. Cook, T. White, L. Strope, J. Gómez, M. Schouweiler, G. Houghton, and UCSC students in the 2020 Sitka field course for assistance in the field and laboratory. S. Lummis went above and beyond to help keep our experiments running and B. Walker generously analyzed many of our discrete samples. E. Donham, Y. Takeshita, and W. Evans provided invaluable advice and assistance in sensor troubleshooting, sample processing, and data analysis. We deeply appreciate everyone who supported this work.

Tables

Table 2.1. Seawater conditions (mean ± SE) in experimental aquaria by treatment and seasonal experiment. Temperature, salinity, and dissolved oxygen were measured daily in all experimental aquaria. pH_T, pCO_2, TA, and nutrient concentrations were determined from discrete water samples taken in each aquarium at the beginning, middle, and end of each experiment.

	WINTER EXPERIMENT				SUMMER EXPERIMENT			
Treatment	**Control**	**OA**	**OW**	**OA & OW**	**Control**	**OA**	**OW**	**OA & OW**
Dissolved Oxygen (mg/L)	9.5 ± 0.9	9.3 ± 1.2	8.5 ± 1.4	8.4 ± 1.5	8.5 ± 0.2	8.4 ± 0.2	7.9 ± 0.3	7.8 ± 0.2
Salinity (ppt)	31.3 ± 0.3	31.4 ± 0.3	31.3 ± 0.3	31.4 ± 0.3	31.0 ± 0.2	31.0 ± 0.2	31.1 ± 0.2	31.1 ± 0.2
Temperature (℃)	7.2 ± 0.1	7.3 ± 0.1	10.9 ± 0.7	10.9 ± 0.6	14.1 ± 0.1	14.2 ± 0.1	18.0 ± 0.9	18.0 ± 0.8
pH_T	7.65 ± 0.01	7.21 ± 0.01	7.66 ± 0.01	7.28 ± 0.01	7.88 ± 0.01	7.46 ± 0.02	7.84 ± 0.01	7.51 ± 0.02
pCO_2 (µatm)	1011 ± 22	2843 ± 87	1001 ± 23	2502 ± 50	592 ± 21	1667 ± 103	648 ± 14	1513 ± 67
TA (µmol/kg)	2120 ± 15	2122 ± 14	2121 ± 15	2125 ± 14	2116 ± 5	2116 ± 5	2116 ± 5	2115 ± 5
NO_3 concentration	16.3 ± 1.3				3.7 ± 0.4			
NH_4 concentration	4.8 ± 1.0				10.3 ± 1.4			

Figures

Figure 2.1. Time series of environmental data on two high latitude rocky reefs: one within an intact kelp forest (Samsing Pinnacle, green) and one within a kelp forest that transitioned to an urchin barren during this study (Harris Is., black). The overlapping time series show the close agreement in seasonal variability in seawater a) pH_T, b) temperature, and c) dissolved oxygen between the two sites.

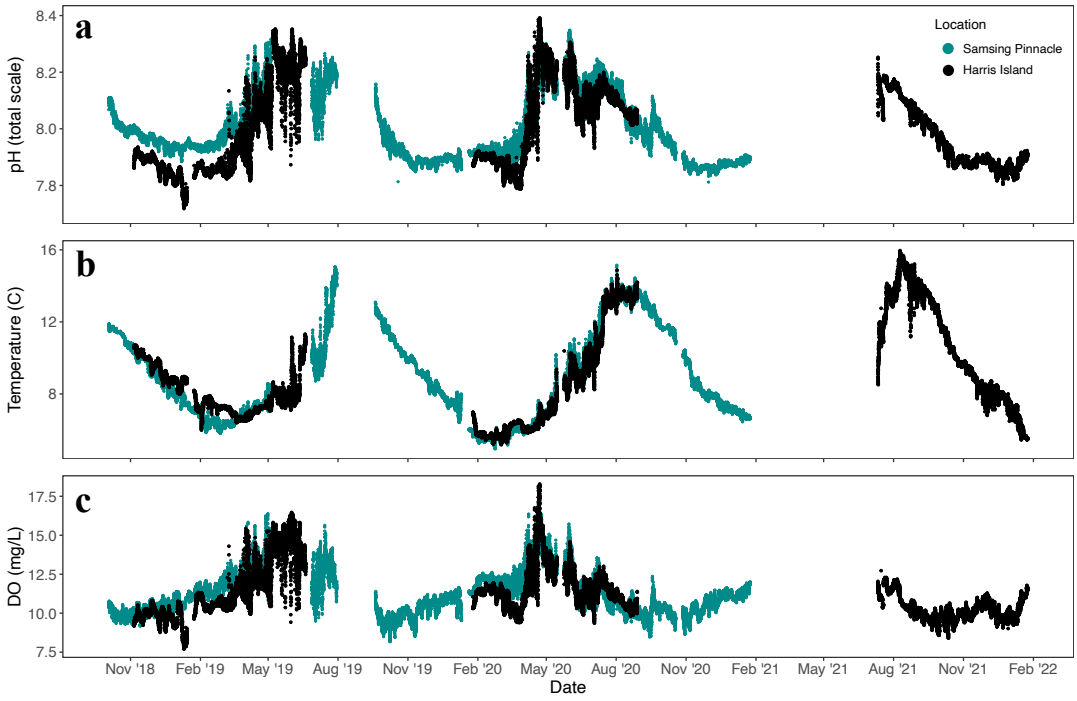

Figure 2.2. Relative growth rates (RGR_{mass}; mean ± SE) of three kelp species exposed to different treatment combinations of ocean acidification (OA) and warming (OW) within month-long laboratory experiments in winter and summer (N= 18 individuals $species^{-1}$ $treatment^{-1}$).

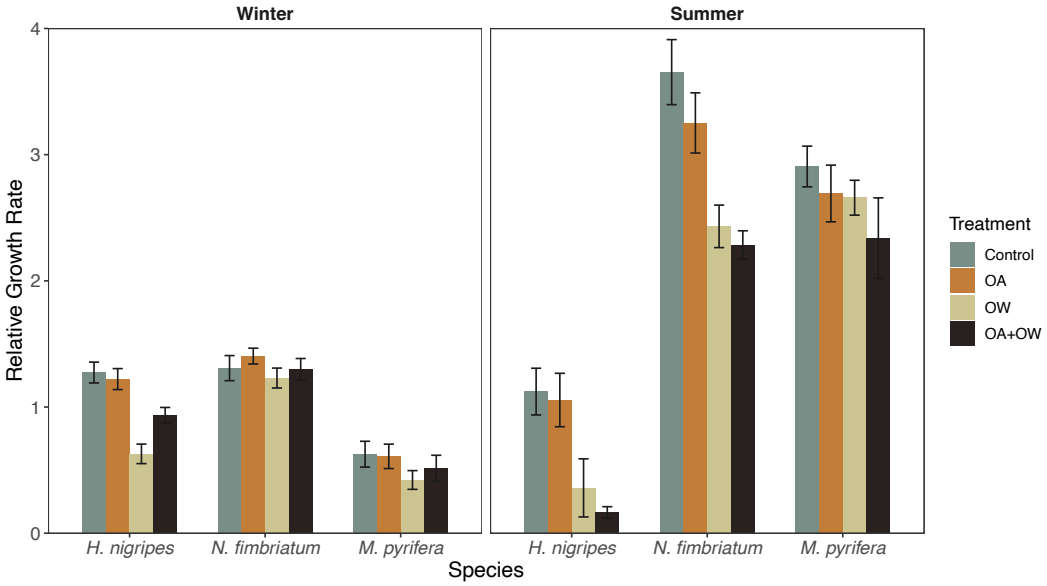

Figure 2.3. Tissue nitrogen content (%N; mean ± SE) of three kelp species exposed to different treatment combinations of ocean acidification (OA) and warming (OW) within month-long laboratory experiments in winter and summer (N= 18 individuals species^{-1} treatment^{-1}).

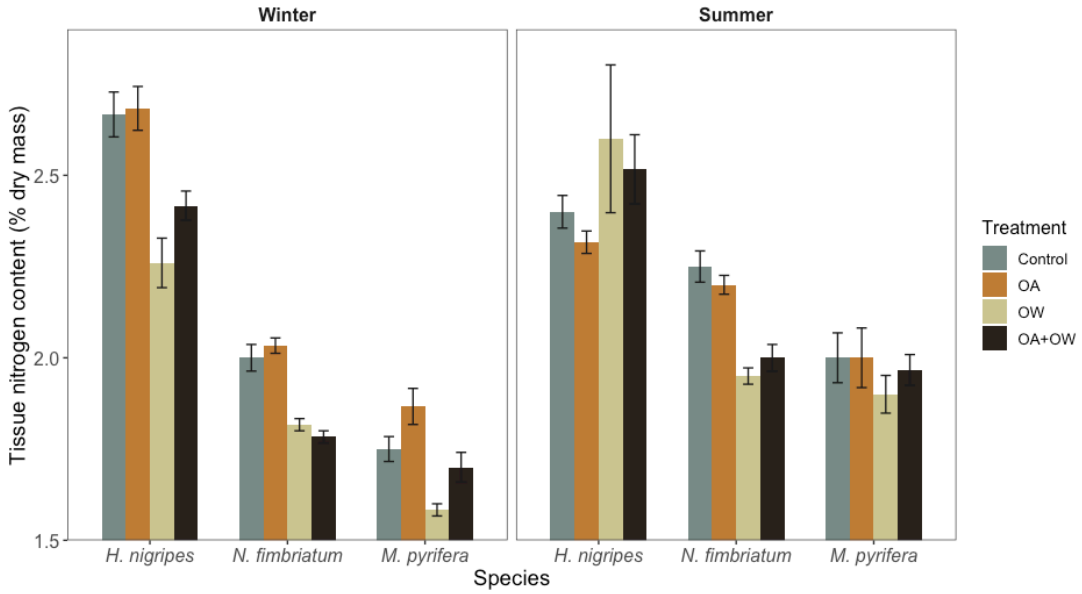

Figure 2.4. $\delta^{13}C$ values (mean ± SE) of three kelp species exposed to different treatment combinations of ocean acidification (OA) and warming (OW) within month-long laboratory experiments in winter and summer (N= 18 individuals species^{-1} treatment^{-1}). The dotted line at a $\delta^{13}C$ value of -30 is the putative threshold below which macroalgae exclusively rely on diffusive uptake of CO_2 and no longer invest energy in carbon concentrating mechanisms (Raven et al. 2002).

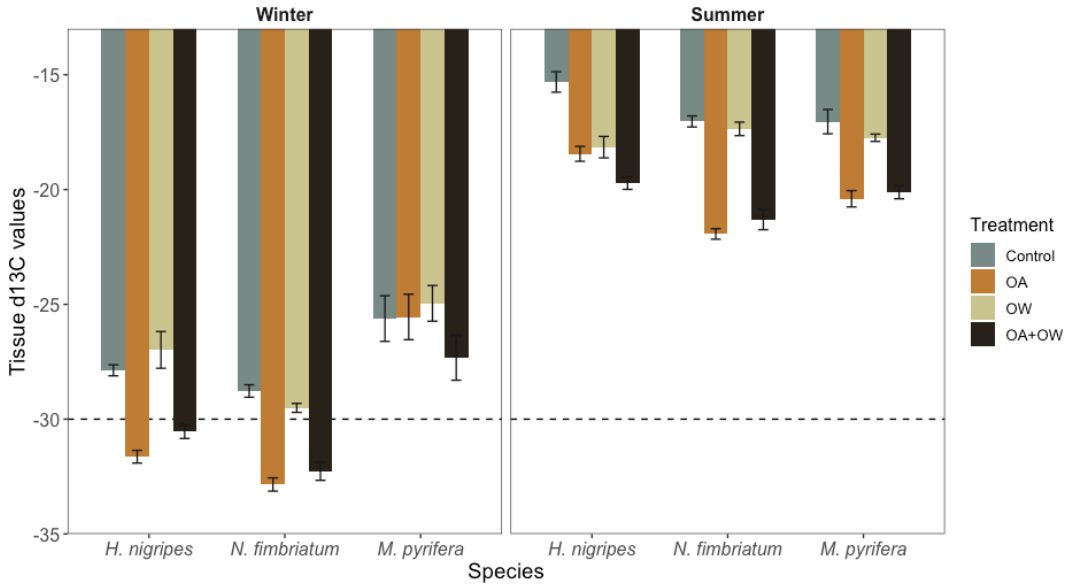

Figure 2.5. Relative consumption (mean ± SE) of experimentally grown *H. nigripes* tissue in feeding assays used to test the effects of seasonal pH and temperature treatment on the palatability of algal tissue to a common kelp forest grazer.

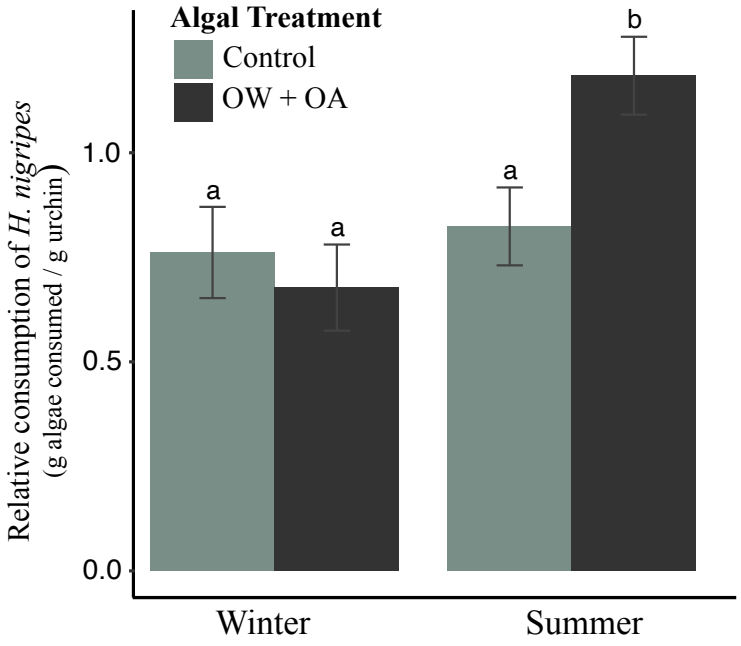

Chapter 3: High-latitude calcified coralline algae exhibit seasonal vulnerabiity to acidification despite physical proximity to a non-calcified alga

This chapter was originally published in a peer reviewed journal and is reproduced here for inclusion in this dissertation. The citation for the original publication is:

Bell, L. E., Gómez, J. B., Donham, E., Steller, D. L., Gabrielson, P. W., & Kroeker, K. J. (2022). High-latitude calcified coralline algae exhibit seasonal vulnerability to acidification despite physical proximity to a non-calcified alga. *Climate Change Ecology, 3*, 100049. https://doi.org/10.1016/j.ecochg.2022.100049

Abstract

The emergent responses of vulnerable species to global change can vary depending on the relative quality of resources available to support their productivity under increased stress, as well as the biotic interactions with other species that may alter their access to these resources. This research tested how seawater pCO_2 may interact with seasonal light availability to affect the photosynthesis and calcification of high-latitude coralline algae, and whether the responses of these calcified macroalgae are modified by physical association with a non-calcified seaweed. Through an in situ approach, our study first investigated how current seasonal environmental variation affects the growth of the understory coralline algae *Crusticorallina* spp. and *Bossiella orbigniana* in Southeast Alaska's kelp forests. We then experimentally manipulated pH to simulate end-of-century acidification scenarios, light regime to simulate seasonal light availability at the benthos, and pairings of coralline algal species with and without a fleshy red alga to examine the interactive effects of these variables on coralline productivity and calcification. Our results indicate that: 1) coralline species may face net dissolution under projected future winter pH and carbonate saturation state conditions, 2) differences in seasonal light availability in productive, high-latitude waters may not be distinct enough to modify coralline algal net calcification, and 3) association with a non-calcified red alga does not alter the response of these coralline algal species to ocean acidification scenarios. This research highlights the necessity of incorporating locally informed scenarios of environmental variability and community interactions when predicting species' vulnerability to global change.

Introduction

The emergent effects of global change on the ecology of individual species will ultimately depend on environment-ecosystem interactions. In particular, a given species' response will be shaped by the rate and magnitude of environmental change on the mean, variability, and extremes characteristic of their local environment. These regional attributes of an organism's environment are influenced both by large-scale physical forces, as well as smaller scale interactions with other species (e.g., Helmuth et al. 2002, Menge et al. 2003, Sanford et al. 2003, Suggitt et al. 2011, Chan et al. 2017). Furthermore, temporal variability in environmental conditions is often multivariate, such that variability in one abiotic driver often covaries with other drivers that can mediate species' responses to change. Understanding the emergent effects of global change therefore requires careful attention to the local characteristics of the environment experienced by organisms in nature.

Ocean acidification (OA) is a global process that threatens marine species worldwide (Doney et al. 2020). Most research considering marine species' responses to OA has been limited to short-term, static manipulations of carbonate chemistry in laboratory settings derived from mean environmental conditions. In nature, marine organisms experience pronounced temporal variability in carbonate chemistry, as well as other environmental factors that could mediate their response to OA (Hofmann et al. 2011, Kroeker et al. 2020). For example, high-latitude regions illustrate how temporal variability in carbonate chemistry, primarily seasonal in nature, aligns with seasonal variability in other ecologically important conditions. Specifically, seawater

pH and carbonate saturation states are lowest during winter months at high latitude (Feely et al. 1988, Siedlecki et al. 2017, Hauri et al. 2020, Kroeker et al. 2021), corresponding with the seasonal low in photoperiod. Marine macroalgae, which depend on carbon acquisition through photosynthesis, may be especially impacted by the potential interactions between OA and seasonal light availability characteristic of high latitudes (Russell et al. 2011, Celis-Plá et al. 2015, Britton et al. 2016, Briggs & Carpenter 2019). Furthermore, macrophyte species widely considered vulnerable to OA are generally embedded in diverse communities, where their interactions with other species can modify their relative OA exposure and available light (Clark et al. 2004, Burnell et al. 2014, Short et al. 2014, Cornwall et al. 2015a).

Calcium-carbonate containing coralline algae play an important ecological role in coastal marine ecosystems, often dominating benthic percent cover on tropical to temperate rocky reefs (Steneck et al. 2002, Shears & Babcock 2007, Morse & Morse 1996, Nelson 2009, Chenelot et al. 2011, Tebben et al. 2015). Coralline algae provide structural habitat, food, and chemical settlement cues for a wide diversity of invertebrate larvae . The high-magnesium calcite that these algae precipitate to form their thalli (Bilan & Usov 2001, Nash et al. 2019) is particularly vulnerable to dissolution under OA (Andersson et al. 2008, Ries 2011, Cornwall et al. 2021b). Reduced structural integrity, recruitment rate, and growth of coralline algae in high pCO_2 concentrations (Kuffner et al. 2008, Kroeker et al. 2013a, Hofmann & Bischof 2014, McCoy & Kamenos 2015) could affect their ability to compete for space with non-calcified algae (Hepburn et al. 2011, Porzio et al. 2011, Hofmann et al. 2012,

Kroeker et al. 2013b, Gomez-Lemos & Diaz-Pulido 2017). Given the foundational function of these reef-building calcifiers, future decreases in coralline algal abundance under OA may lead to myriad changes to coastal marine communities across the globe (Fabricius et al. 2017, Cornwall et al. 2021a).

The ability of calcifying coralline algae to compensate for increased dissolution as OA progresses is dependent on available light, as calcification is linked to photosynthesis-driven carbonate chemistry changes at the thallus surface (Pentecost 1978, Beer & Larkum 2001, Teichert & Freiwald 2014). Sub-saturating irradiances exacerbate the effects of OA by reducing the available energy needed to offset increased respiration costs (Briggs & Carpenter 2019, Wei et al. 2020). This dynamic is of particular interest at high latitudes, where seasonal variation in daylength and productivity already result in an overlapping winter window of decreased seawater pH and carbonate saturation state with reduced photoperiod that could be detrimental to marine calcifiers in the future (Kroeker et al. 2021). Indeed, many species of temperate coralline algae exhibit their highest growth rates during the summer season when day lengths are longer, and temperature, pH, and saturation state are higher (Lüning 1990, Roberts et al. 2002, Martin et al. 2006, Fietzke et al. 2015). However, there are species of calcified algae that demonstrate resilience to OA exposure by maintaining high pH at their surface (Cornwall et al. 2017, McNicholl et al. 2019), and some Arctic coralline algae can maintain high surface pH and growth even under limited light or dark conditions by decoupling carbon fixation and reducing respiratory release of CO_2 (Freiwald & Henrich 1994, Hofmann et al. 2018). While

these examples suggest that some coralline algae may be resilient to future OA, no generalizable pattern based on habitat or evolutionary history has yet emerged to enable accurate predictions of the response of unstudied species (Barner et al. 2018).

Coralline algal physiology can be intimately tied to their interaction with canopies of closely associated non-calcifying macroalgae. The physical presence of canopy-forming algae, including turf and foliose forms of red and brown algae, can substantially attenuate water flow within a seaweed bed, as well as metabolically alter the seawater chemistry experienced by underlying calcifiers (Gaylord et al. 2007, Short et al. 2014, 2015, Cornwall et al. 2015a). Macroalgae can modify carbonate chemistry in their associated boundary layers (Freiwald & Henrich 1994, Noisette & Hurd 2018) and in surrounding habitats, as seen within the surface waters surrounding a *Macrocystis pyrifera* kelp forest canopy (Koweek et al. 2017, Hirsh et al. 2020). Such slow-flow boundary-layer habitats could facilitate growth and calcification of coralline algae in relatively acidic or undersaturated conditions (Cornwall et al. 2013b, 2014, Hurd 2015, Krause-Jensen et al. 2016, Guy-Haim et al. 2020), although the effect of reduced water velocity may be highly specific to species and habitat (Comeau et al. 2019). On the other hand, daytime benefits to coralline algae of increased pH and saturation state in the presence of a non-calcifying algal canopy can be offset by the relatively more acidic and less saturated environment experienced during nighttime respiration (Cornwall et al. 2015a). Enhanced diurnal pH fluctuations have been demonstrated to reduce growth rates and calcification of both juvenile and adult coralline algae, particularly in OA conditions (Cornwall et al.

2013a, Roleda et al. 2015, Johnson et al. 2019). Additionally, shading caused by neighboring algal canopies can directly impact photosynthesis, and the combination of low light and slower flow has been linked to reduced calcification for some coralline species (Comeau et al. 2019, Bulleri 2006). In systems where coralline species are sensitive to changes in seawater carbonate chemistry, the specific interactions between macroalgal calcifiers and non-calcifiers may influence the direction of the aggregate response of coralline species to future OA.

The seaweed communities found along the outer coast of Southeast Alaska include the northernmost continuous band of *Macrocystis* kelp forests in the world, which also demarcate the northern and southern range limits of a suite of associated nearshore algal and invertebrate species (Schiel & Foster 2015). Although this high-latitude crossover region of relatively high marine biodiversity is considered 'sub-polar', biological processes within the Gulf of Alaska are still governed by significant environmental seasonality, similar to that seen in higher Arctic waters. Heavy coastal precipitation in the fall and winter months combines with cold temperatures, short daylight hours, and reduced water column productivity to influence the carbonate chemistry of this system (Siedlecki et al. 2017, Hauri et al. 2020, Evans et al. 2015), leading to an annual pH minimum in late winter (Jan-Feb) (Kroeker et al. 2021). This region is also susceptible to the rapid climatic changes already being observed at higher latitudes, where persistent undersaturation of marine surface waters is anticipated within the next 40 years (Feely et al. 2004, Steinacher et al. 2009). The combination of biodiversity, seasonality and vulnerability to global change that

characterizes the coastal seaweed communities of this area highlights their potential as bellwethers for how future increases in seawater pCO_2 may alter the responses and interactions among algal species in other, lower-latitude systems (Fabry et al. 2009).

In this study, we explore how variation in carbonate chemistry and light availability impact the growth of high latitude coralline algae, and how their naturally close proximity to a non-calcified algal species may modulate these responses under future OA scenarios. To accomplish this, we incorporated both field monitoring and laboratory manipulation of species representing the two dominant coralline algal morphotypes in Southeast Alaska: erect, branched geniculate and crustose non-geniculate. Given the limited prior research on calcified coralline algae in this region and the necessity of using DNA sequencing to accurately distinguish morphologically ambiguous coralline algal species (Twist et al. 2019, 2020), we employed molecular methods to identify whether our findings applied to a species-specific or genus-specific level. By considering algal responses to OA in the context of their natural environmental variation as well as interactions with other species, this research answers a call to embrace ecological complexity to better understand community-level effects of global change (Kroeker et al. 2020, Gaylord et al. 2015, Kroeker et al. 2017).

Methods

Subtidal light availability

Year-round variation in relative light intensity reaching the benthos on coralline reefs in Sitka Sound, AK was measured using submersible pendant light loggers (Onset HOBO). From 2017-2020, we intermittently deployed two light loggers at ~7m depth (MLLW) at each of four rocky reef sites with high coralline algal cover and varied *Macrocystis pyrifera* kelp canopy cover (Harris Is.: 57.032N, 135.277W; Breast Is.: 57.039N, 135.333W; Samsing Pinnacle: 56.988N, 135.357W; Sandy Cove: 56.986N, 135.321W; Fig. S3.1). At each site, both loggers were placed within 1m of each other, oriented to face the water surface, and programmed to record light intensity (lux; lumen m^{-2}) every 30 min. We used two loggers at each site in order to correct for differences in orientation or macroalgal canopy cover immediately above the two loggers. The light loggers were cleaned every 1-3mo, although overall fouling was low. To compare relative light availability at the benthos throughout the year, we transformed our data to integrate both daily variation in light intensity and seasonal variation in day length. For every day with a complete set of deployment data (both loggers recording for 24h), we calculated the average total luminous exposure (lumen-hr m^{-2}) experienced at the benthos for each hour of the day and then summed these values to get an estimate of average luminous exposure at the benthos each calendar day of the year (lumens d^{-1} m^{-2}).

Because measurements of illumination (lux) do not necessarily correlate with the photosynthetic photon flux density (PPFD; μmol m^{-2} s^{-1}), which is more physiologically relevant to macroalgae, we also haphazardly recorded hundreds of instantaneous measurements of PPFD at the benthos in winter and summer seasons at each site using a Diving-PAM-II (Heinz Walz GmbH) MINI-SPEC. With these values, we generated average ranges of PPFD reaching the benthos, which were used to inform PPFD levels for the seasonal light regime treatments in the laboratory experiment (section 2.4).

Coralline algae collection and species verification

We used DNA sequencing to identify the species represented by two spatially dominant morphotypes of crustose and geniculate coralline algae found subtidally in Sitka Sound. Individuals of each morphotype were collected from a subtidal rocky reef on Marshall Is., Sitka Sound, AK (57.032N, 135.273W) in Aug 2017. Crustose individuals targeted for collection were those that had a morphology that could easily be separated from the rocky substrate, often disc-shaped with distinct white growing edges. Geniculate individuals were collected to include the basal holdfast. The two morphotypes, which we initially grouped using morpho-anatomical cues, were the focus of our field and laboratory experiments. A subset of individuals of each morphotype that were used in the laboratory experiment (crustose: n=16; geniculate: n=13) were vouchered and desiccated in precipitated silica gel. Specimens were

extracted following the protocol by Hughey et al. (2001), as modified by Gabrielson et al. (Gabrielson et al. 2011) for coralline algae. The primer pair F753/RrbcS (Freshwater & Rueness 1994) was used to amplify 694bp of *rbc*L 3' following Hughey et al. (2001). Contigs were assembled using Sequencher 5.2.4 (Gene Codes Corp., Ann Arbor, MI, USA), aligned in Geneious Prime (2020.2.4 Biomatters Ltd.) and subjected to BLAST analyses in GenBank.

The term *Crusticorallina* spp. was applied to the group of crustose individuals collected in the field and used in all experiments. Genetic analyses identified the group to contain 3 distinct species: *Crusticorallina painei, C. adhaerens, and C. muricata.* The physiological results apply to the group. The geniculate coralline species was verified as *Bossiella orbigniana*. All sequences were 100% matches to sequences of each of the taxa in GenBank, all of which have had their type specimens sequenced. Vouchers are deposited in NCU (Table S3.1; herbarium acronym follows Index Herbariorum online (Thiers 2021)).

Seasonal growth rate of coralline algae

To assess *in-situ* seasonal changes in coralline algal growth rates, we collected specimens of *Crusticorallina* spp. and *B. orbigniana* in Dec 2017, July 2018, and Jan 2019 at Marshall Is., Sitka Sound. Individuals of each morphotype were cleaned by removing epiphytic algae and invertebrates with tweezers, and then placed in an aquarium of recirculating seawater with 100mg L^{-1} concentration of the membrane-

permeable live-cell labeling fluorescent dye Calcein for 6h. This dye is absorbed by metabolically active meristematic tissue of the alga at the time of the stain (Lewis & Diaz-Pulido 2017), thus providing a growth benchmark for subsequently added tissue. After staining, each coralline individual (*Crusticorallina* spp.: a 'disc' with at least a 50% intact growing edge; *B. orbigniana*: a 'floret' containing 4-10 apical fronds) was attached to a small PVC stand by using z-spar epoxy putty to affix the older, non-meristematic tissue. Individuals on stands were then outplanted into the field on plates (2 crustose and 2 geniculate indiv. plate^{-1}) and bolted onto rocky reef substrate at 10m depth MLLW at the edge of a giant kelp forest at Harris Is. Coralline algae were retrieved after 2-3mo, for total outplant durations of 67d (winter 2018), 66d (summer 2018), and 103d (winter 2019). Seawater pH and temperature during deployment periods were monitored with a SeapHOx sensor (Sea-Bird Scientific) (Kroeker et al. 2021) deployed within 10m of the coralline outplant locations (mean ± SD: winter 2018: pH_T=7.89±0.04, temp=7.2±0.5°C; summer 2018: pH_T=8.11±0.09, temp=11.6±2.1°C; winter 2019: pH_T=n.a., temp=7.2±0.4°C).

To measure linear growth, the coralline algae were imaged using a fluorescent lamp channel on a Ziess AxioZoom microscope at the UCSC Microscopy Center. Average growth extension from the original fluorescent stain was calculated for each individual using ImageJ (NIH v1.8.0) by analyzing measurements from up to 13 randomly selected points along the growing edge of the disc (*Crusticorallina* spp.) or from up to 17 randomly selected apical fronds in the floret (*B. orbigniana*). Growth data from the two winter season deployments were not significantly different for

either coralline morphotype, and thus were pooled for analysis for each morphotype. Length extension (mm d^{-1}) was compared between seasons for each morphotype and between morphotypes using one-way Welch's ANOVAs (package "stats" in R (R Core Team 2022)) due to inequality of variance and unbalanced design - a result of high variation in final sample size among deployments following random losses in the field as well as inconsistent fluorescent stain uptake (*B. orbigniana* summer, n=13; *B. orbigniana* winter, n=34; *Crusticorallina* spp. summer, n=7; *Crusticorallina* spp. winter, n=25). Adjusted p-values for these analyses were calculated using Bonferroni corrections for multiple comparisons.

Ocean acidification laboratory experiment

To test the response of the *Crusticorallina* spp. and *Bossiella orbigniana* to future OA scenarios, we used an 18-aquaria indoor experimental system with flow-through seawater at the Sitka Sound Science Center to simulate three static pH_T levels (current summer = 8.0, future summer/current winter = 7.7, future winter = 7.4) under two seasonal light regimes simulated with full-spectrum aquarium lights (AI Prime HD) (summer = PPFD 55µmol m^{-2} s^{-1}, 13h d^{-1}, winter = PPFD 40µmol m^{-2} s^{-1}, 6h d^{-1}). We had a total of 3 aquaria for each of the 6 treatment combinations (Fig. S3.2). Experimental pH levels were chosen to reflect current seasonal minimums of coastal pH measured at Harris Is. from 2016-2017 (Kroeker et al. 2021), as well as end-of-century projections for Gulf of Alaska pH levels based on RCP 8.5 (-0.3 pH_T from

current levels (Mathis et al. 2015)). Experimental light regimes were defined using seasonal averages for day length and measured irradiance level at 10m depth at Harris Is. (described in section 2.1). Our experimental system was not designed to control for temperature; seawater in all aquaria followed natural temperature variation in the system's seawater source throughout the experiment. A full description of the pH control for this system can be found in Kroeker et al. (2021), but in short: pH was regulated using a relay system that controlled mixing of pre-equilibrated low-pH seawater (formed by bubbling pure CO_2 gas into seawater: pH≅6.0) and ambient pH seawater into 9 header buckets (n=3 headers per pH treatment) that then flowed into the experimental aquaria. Each header bucket was equipped with a pH sensor (DuraFET, Honeywell) communicating with a controller (UDA 2152, Honeywell) to regulate flow of the low pH water through solenoid valves to maintain pre-programmed pH setpoints. The layout of our experiment was designed to minimize spatial variance among the random factors, aquaria and headers, by randomizing treatment assignments and relative locations throughout the system.

Within each pH level and light treatment combination, half of the individual *Crusticorallina* spp. and *B. orbigniana* were randomly assigned to be paired in close proximity with *Cryptopleura ruprechtiana* (n=6 species treatment^{-1}), a dominant subcanopy-forming fleshy red alga in Sitka Sound frequently found growing in association with coralline algae. All algal individuals were collected on Aug 5, 2017 at Marshall Is., Sitka Sound, and cleaned using the same methods as described in section 2.3. Algal individuals were then elevated off the bottom of experimental

aquaria using PVC stands topped with plastic mesh (see Fig. S3.2B). Total experimental duration was 45d (Aug 7-Sept 21, 2017). To monitor treatment conditions, we used a handheld meter (YSI) to take daily temperature readings in the replicate aquaria and measure salinity of incoming seawater daily just upstream of our experimental system. Additionally, discrete water samples were collected from replicate aquaria at four timepoints (Aug 18, 22, 25, and Sept 15) for determination of pH (total scale) and total alkalinity (TA). Discrete samples were collected without aeration in amber glass bottles, immediately poisoned with saturated $HgCl_2$ (0.025% volume^{-1}), and capped to prevent air exchange.

Discrete water samples for laboratory measurements of pH and/or TA were transported to UCSC for analysis within 8 months of collection. We measured pH spectrophotometrically (Shimadzu, UV-1800) using m-cresol purple dye following best practices (Dickson et al. 2007), with an average standard error of ±0.0013 pH units among sample triplicates. TA measurements were performed using open cell titration (Metrohm, 905 Titrandro) and corrected against certified reference materials of CO_2 in seawater (Dickson laboratory, Scripps Institution of Oceanography), with an average standard error of ±0.933μmol kg^{-1} SW^{-1} among sample triplicates. To calculate pH_T in the replicate aquaria at the time of water sampling, we used our measurements of spectrophotometric pH, TA, temperature, and salinity, as well as the dissociation constants (Mehrbach et al. 1973, Dickson & Millero 1987) as inputs to the program CO2SYS (Lewis & Wallace 1998).

Algal net calcification and growth

The effects of each experimental pH and light treatment combination and fleshy red algal association on coralline net calcification rate were assessed using the buoyant weight technique (Jokiel et al. 1978), as well as the alkalinity anomaly technique. To determine total relative change in calcified mass over the experimental period, each coralline thalli's buoyant weight was measured to the nearest 0.0001g at the beginning and end of the experiment on a balanced platform suspended below a microbalance in a temperature-monitored seawater bath. All fouling organisms were removed prior to taking measurements. To ensure precision, buoyant weights were repeated for each individual until measurements differed by less than ±0.005g, and then an average was taken of the measurements falling in this range of precision. Initial and final buoyant weights (BW; g) were used to calculate relative net calcification rate (RCR_{net}; g g^{-1} d^{-1}) of each individual alga using the equation:

$$RCR_{net} = \frac{log(\frac{BW_{final}}{BW_{initial}}) \cdot 100}{\Delta t}$$

where Δt (d) is the total days elapsed between the beginning and end of the experiment.

Total alkalinity (TA) incubations were run in the last week of the experiment on a subset of coralline algae from each treatment (n=3 individuals $treatment^{-1}$ $species^{-1}$) by isolating individuals in 245mL glass chambers filled with seawater from their associated aquaria and sealed airtight. Paired *C. ruprechtiana* were not included

in incubation chambers, in order to isolate the physiological responses of the coralline algae. Chambers were placed on a magnetic stir plate in a water bath at consistent temperature (13℃), with stir bars able to spin freely underneath coralline algae separated by a mesh screen. All incubations were run under a mean PPFD of 80μmol m^{-2} s^{-1} for 3h. At the end of the incubation period, seawater from each chamber was collected to measure endpoint TA. Seawater for TA incubation chamber controls was collected from corresponding aquaria at the beginning of each incubation round and used to measure any background TA variation in empty chambers during the incubation period. All discrete water samples for TA were poisoned and processed as outlined in section 2.4.

TA measurements from coralline algal incubations were used to calculate short-term net calcification (G_{net}; μmol g^{-1} DW h^{-1}) using the equation:

$$G_{net}(CaCO_3) = \frac{\Delta TA \cdot \nu}{2 \cdot DW \cdot \Delta t}$$

where ΔTA (μmol $kgSW^{-1}$) is the change in total alkalinity from the beginning to end of the incubation period corrected to chamber controls, ν (L) is the chamber volume, DW (g) is the dry weight of the alga, and Δt (h) is the total incubation time (Smith & Key 1975, Martin et al. 2006). Dry weights (DW; g) for the living coralline thalli used in TA incubations were estimated from buoyant weight (BW; g) measurements using the equation (Jokiel et al. 1978):

$$DW = \frac{BW}{1 - (\frac{\rho_{SW}}{\rho_{calcite}})}$$

where we used a seawater density (ρ_{SW}) of 1.02g cm^{-3} (from average temperature and salinity data at the time of BW) and a calcite density ($\rho_{calcite}$) of 2.71g cm^{-3}.

Growth rates of *C. ruprechtiana* reared in association with coralline algae in the different treatment conditions were quantified by measuring tissue wet weights (WW; g) at the beginning and end of the experiment. Thalli were removed from seawater, patted uniformly dry, and immediately weighed on a standard microbalance to the nearest 0.0001g. Relative growth rate (RGR_{net}; g g^{-1} d^{-1}) of each individual alga was calculated using the equation:

$$RGR_{net} = \frac{log(\frac{WW_{final}}{WW_{initial}}) \cdot 100}{\Delta t}$$

where Δt (d) is the total days elapsed between the beginning and end of the experiment.

We quantified variability in experiment-integrated relative net calcification rate and short-term net calcification rate of each coralline morphotype using linear mixed-effects models (package "lme4" in R) with *pH*, *light regime, association with C. ruprechtiana, and all of the interactions between these factors* as fixed factors and *experimental aquaria* nested in *header* as random intercepts using restricted maximum likelihood. Variability in the relative growth rate of *C. ruprechtiana* was analyzed using a similar model, except fixed factors were only *pH*, *light regime, and pH*light regime*. All models satisfied assumptions of normality and homoscedasticity. We determined p-values for the effects of fixed factors and their

interactions using the Sattertwaithe's method for t-tests (package "lme4" in R). Post-hoc tests of pairwise differences among means of significant factors were performed using the Tukey method of multiple comparisons (package "multcomp" in R).

Experimental photophysiology

In vivo photophysiology was characterized for all red algal species at the end of the experiment by measuring the rate of oxygen evolution produced by algal thalli at seven irradiance levels. Following the final buoyant mass measurement, a small piece of thallus (mean ± SE: *B. orbigniana*: 0.17±0.02g; *Crusticorallina* spp.: 0.53±0.03g; *C. ruprechtiana*: 0.07±0.003g) was taken from haphazardly selected individuals (n=3 treatment^{-1} species^{-1}) and placed in a 69mL incubation chamber filled with seawater from the associated aquaria and equipped with a stir bar and an oxygen sensor spot (PreSens SP-PSt4-SA). Sensor spots were calibrated daily using a two-point correction of 100% (air-saturated water) and 0% (1% Na_2SO_3 and 0.05% $Co(NO_3)_2$ standard solution) saturation. Incubation chambers were sealed airtight using clear plexiglass lids affixed with vacuum grease and submerged onto a magnetic stir plate in a temperature-controlled water bath. Full-spectrum aquarium lights (AI Hydra HD) were used to expose thalli in chambers to seven consecutively increasing irradiance levels (~PPFD 0, 20, 70, 140, 320, 425, 720µmol m^{-2} s^{-1}). A fiber optic O_2 sensor (Fibox IV, Presens) was used to record the dissolved oxygen concentration in each chamber at 30, 45 and 60min after each irradiance level was

reached. Chamber seawater was refreshed after the fourth irradiance step to avoid nutrient depletion and oxygen supersaturation. Dissolved oxygen evolution rate (mg O_2 min^{-1}) at each irradiance level was calculated using linear regression, corrected against paired chamber controls (no algae), and normalized to chamber volume and thalli wet mass.

We used nonlinear regression models (package "nlstools" in R) to mathematically fit our calculations of algal oxygen evolution rate by irradiance level to photosynthesis-irradiance (P-E) curves using the double exponential decay function:

$$NP = P_{max} \cdot (1 - \frac{-\alpha \cdot I}{e^{Pmax}}) \cdot \frac{-\beta \cdot I}{e^{Pmax}})$$

where NP = net production (mg O_2 g^{-1} min^{-1} L^{-1}), P_{max} = maximum photosynthetic rate that could be sustained with no photoinhibition (β=0), α = photosynthetic efficiency parameter (initial slope), β = photoinhibition parameter, I = irradiance level (μmol m^{-2} s^{-1}) (Platt et al. 1980). Nonlinear least squares estimates for parameters P_{max}, α, and β were calculated for each coralline morphotype by treatment combination by fitting the above model to pooled photophysiology data from treatment replicates and performing an iterative estimation procedure assuming normal distributions. Validity of model fit was visualized by superimposing the fitted curves over the raw data and assessing estimated standard errors and *t*-test statistics for the estimated parameters. The effect of pH on individual parameters was determined by testing whether the addition of a binary parameter differentiating pH

treatment to the model significantly altered any of the estimates for P_{max}, α, and β. Where pH was found to have a significant impact on optimal model parameters, accuracy of this estimated effect was assessed by visually comparing 'goodness of fit' of the predicted model containing the pH parameter to the original model fitted to the empirical data.

Results

Subtidal Light Availability

Average daily luminous exposure (lumens d^{-1} m^{-2}) reaching the benthos at all four monitoring sites between 2017 and 2020 (Fig. 3.1) was lowest in late fall and early winter (Oct - Jan). At three of the four sites, site-specific monthly averages of luminous exposure at the benthos in the late winter (Feb-Apr) were similar or higher than averages of luminous exposure recorded in the summer months (May-Aug). At all sites, average ranges of PPFD measured at the benthos during moderately overcast days typical of Southeast Alaska were very similar between winter (10-40µmol m^{-2} s^{-1}) and summer (10-60µmol m^{-2} s^{-1}) months.

Seasonal growth rate of coralline algae

Our results indicate that the average length extension rate of *B. orbigniana* was marginally faster in the summer (0.06±0.03mm d^{-1}) than in the winter (0.04±0.01mm d^{-1})($p=0.054$; Fig. 3.2,Table S3.2). We did not detect a seasonal difference in average length extension rate for *Crusticorallina* spp. ($p=1.000$). Annual average length extension rates of *B. orbigniana* (0.04±0.02mm d^{-1}) were significantly faster than annual growth rates of *Crusticorallina* spp. (0.02±0.01mm d^{-1}; $p<0.001$).

Ocean acidification laboratory experiment

Treatments were maintained at setpoint targets for pH_T under our assigned winter or summer light regime for the duration of the experiment, and discrete water samples taken from experimental aquaria confirmed that seawater pCO_2 and calcite saturation state also differed by treatment (Table 1). Temperature, salinity and total alkalinity remained stable in all treatments. Temperatures during the experiment (13.6±0.7°C) are representative of typical late summer (Aug-Sept) temperatures observed at Harris Is. reef in Sitka Sound (~14°C) (Kroeker et al. 2021).

Algal net calcification and growth

RCR_{net} differed by pH treatment in both *B. orbigniana* ($p<0.001$;Table S3.3) and *Crusticorallina* spp. ($p<0.001$;Table S3.4) (Fig. 3.3). Coralline algae grown under pH 7.4 (future winter scenario) experienced net dissolution (i.e., $RCR_{net} < 0 g g^{-1} d^{-1}$), regardless of light regime or close association with *C. ruprechtiana*. For both coralline algal morphotypes, only this lowest pH treatment (7.4) resulted in a significant decrease in RCR_{net} compared to a current summer scenario of pH 8.0 ($p<0.001$). RCR_{net} of *Crusticorallina* spp. under a future winter scenario of pH 7.4 was also lower than in the current winter scenario of pH 7.7 ($p<0.001$). For *Crusticorallina* species, there was an interaction between light regime and association with *C. ruprechtiana* on RCR_{net} ($p=0.024$). Pairwise comparisons indicated that *Crusticorallina* spp. individuals raised under a summer light regime had lower RCR_{net} when paired with *C. ruprectiana* than when reared independently ($p=0.05$), and that

RCR_{net} of *Crusticorallina* spp. not paired with *C. ruprectiana* was marginally lower when individuals were raised under winter light compared to summer light, although this latter comparison was not statistically significant (p=0.077).

Short-term net calcification (G_{net}) of *B. orbigniana* (Fig. 3.4A) was reduced with pH (p=0.004;Table S3.5). G_{net} was lower in *B. orbigniana* thalli grown at pH 7.4 compared to thalli grown at pH 7.7 (p=0.003). However, no difference was observed between G_{net} of thalli maintained at pH 8.0 compared to other treatments. *B. orbigniana* paired with *C. ruprechtiana* in experimental aquaria had higher G_{net} during incubations (p=0.024), but there was no interaction between algal association and pH treatment. We did not detect an effect of pH or association with *C. ruprechtiana* on the G_{net} of *Crusticorallina* spp., and light regime had a marginal but not statistically significant effect on the crustose species' G_{net} (p=0.074;Table S3.6)(Fig. 3.4B). In contrast to RCR_{net} (buoyant weight technique), G_{net} (alkalinity technique) remained net positive regardless of pH treatment for all coralline algal species.

RGR_{net} of *C. ruprechtiana* over the duration of the experiment was lower under winter light regime in all pH treatments (p=0.039;Table S3.7), with no interaction between pH and light regime (Fig. S3.3).

Experimental photophysiology

We did not detect any effect of pH treatment, light regime, or association with *C. ruprechtiana* on the photosynthetic parameters of the coralline algal species' P-E curves ($p > 0.05$). Photophysiology data for the coralline algal species were pooled across treatments to generate parameter estimates for average P-E curves for the two morphotypes (Fig. 3.5;Table S3.8). We did detect a highly significant effect of pH on *C. ruprechtiana* P_{max} ($p<0.001$; Tables A.9 and A.10), with individuals exhibiting more than a 50% increase in this photosynthetic parameter at pH 7.4 compared to pH 8.0, regardless of light regime.

Discussion

Our results indicate that in the absence of evolutionary adaptation (Cornwall et al. 2020, Moore et al. 2021), the end-of-century projection for winter seawater pH and calcite saturation state in the Gulf of Alaska could lead to net dissolution of the encrusting *Crusticorallina* species and of the geniculate species *Bossiella orbigniana*. Understanding how concurrent changes in temperature will influence this outcome is a critical next step. Compared to the effects of seasonal variation in light availability and association with a non-calcified macroalgal species, pH and saturation state had a more pronounced impact on coralline algal calcification and thus may be more important in mediating the physiological response of these calcified algae in the future (Cornwall et al. 2021b). Although many species of fleshy macroalgae found in close association with coralline algae - such as the red alga *Cryptopleura ruprechtiana* considered in this study - exhibit enhanced photosynthetic rates under future ocean pCO_2 levels (Kübler et al. 1999, Hepburn et al. 2011), increased production for one macrophyte does not necessarily confer benefits or refuge to another (e.g., Bulleri 2006, Cornwall et al. 2015a, Comeau et al. 2019). Future dissolution of these foundational coralline algal species could have profound consequences for the productivity, biodiversity, and community structure of temperate rocky reefs by altering their competitive interactions with other macroalgae and reducing settlement cues and refuge habitat for invertebrate larvae and adults. At a broader level, this research highlights the importance of testing whether local

variability and interactions of abiotic and biotic factors in functioning ecosystems will impact the vulnerability of specific species to global change drivers such as OA.

Although we recorded positive growth via linear tissue extension during field outplants in both summer and winter seasons, month-long laboratory simulations suggested that net calcification of coralline algal species grown in current winter pH conditions, albeit at higher temperatures than experienced in the field, may already hover near zero (Fig. 3.3). As noted, discrepancies between our *in-situ* versus experimental growth rates may have arisen due to differences in temperature and pH conditions during field deployments compared to conditions in experimental aquaria, and because of logistical constraints preventing our use of directly comparable methods. For example, the average temperature used in the lab simulations was 6.4°C higher than the average temperature measured during the winter field outplant experiment, which may have altered the effects of low pH on coralline algal physiology (Cornwall et al. 2021b). Additionally, our technique for measuring growth via linear extension may not necessarily correlate with net calcification, as coralline algae can alternate their energetic investment in cellular size versus calcification (McCoy 2013, Ragazzola et al. 2013, 2016, McCoy & Ragazzola 2014), particularly in regions with high seasonality (Freiwald & Henrich 1994). Our data suggest there is an overall decreasing trend in coralline algal net calcification with decreasing pH that may not have been detectable among all pH treatments given our sample size. Considering the net dissolution observed in both coralline algal morphotypes under

simulated future winter pH conditions, future summer pH conditions will need to be consistently favorable to calcification and growth for these coralline algal species to achieve positive net calcification over the course of the year. Our laboratory results indicate that the anticipated shift in carbonate chemistry with OA that will decrease saturation state and bring future summer pH to the level of current winter pH (7.7) is likely to jeopardize this favorable seasonal window for calcification.

Short-term net calcification of experimental coralline algae during incubations revealed slightly different patterns than were seen in net calcification over the full experiment duration. Although all of the coralline species assigned to the lowest pH treatment (7.4) exhibited the lowest short-term net calcification, average calcification remained net positive in all treatments during the incubations. This is in contrast to the net dissolution observed over the month-long experiment in coralline algae assigned to the same pH 7.4 treatment. Unlike the net calcification rates integrated over experiment-long conditions, which exposed coralline algae to diel cycles of light and dark, these short-term incubations were run continuously in the light - effectively isolating the ability of these coralline algae to maintain net calcification during photosynthesis. Thus, the combined results from experiment-integrated and short-term net calcification calculations suggest that the detrimental effects of pH 7.4 conditions on coralline algal calcification are driven by dissolution under nighttime respiration, which effectively overwhelm the reduced levels of daytime calcification at low pH (McNicholl et al. 2019, Kwiatkowski et al. 2016). Our results also indicate that these coralline species will not be able to leverage any enhanced photosynthesis

under increased pCO_2 conditions to aid in daytime calcification in the future. The absence of a low pH or high pCO_2 effect on coralline photophysiology parameters in this study is consistent with observations in other coralline algal species that are confirmed to use carbon-concentrating mechanisms, such that they are not carbon-limited under current seawater conditions (Comeau et al. 2013, Hofmann & Heesch 2018, Bergstrom et al. 2020).

We did not detect an effect of seasonal light regime on the calcification of *B. orbigniana*, nor on the photophysiology of either morphotype, although numerous studies have shown light availability to be a major driver of coralline response to OA in other systems (Russell et al. 2011, Comeau et al. 2014, Celis-Plá et al. 2015, Briggs & Carpenter 2019). In contrast, net calcification of *Crusticorallina* spp. raised under a summer light regime decreased when these individuals were paired with (and potentially shaded by) a *C. ruprectiana* alga, which may reflect an effect of light on the growth of these crustose coralline algae. Additionally, low light acclimation may be responsible for the increase in short-term net calcification rate of *B. orbigniana* individuals shaded by *C. ruprechtiana* in experimental tanks, as well as a possible (but not statistically significant) increase in short-term calcification rate of winter light-acclimated crustose coralline algae. In these instances, we suspect that reduced light transmission through the incubation chambers may have favored low-light acclimated individuals. Increased replication within our treatment groups would have enabled a more statistically robust consideration of the effect of light. It is also important to note that while our light regime treatments differed considerably in

simulated photoperiod (summer: 13h d^{-1}, winter: 6h d^{-1}), maximum irradiance levels as measured by photosynthetic photon flux density (PPFD) did not differ markedly between the treatments (summer: 55μmol m^{-2} s^{-1}; winter: 40μmol m^{-2} s^{-1}). Considering the similarity in modeled oxygen evolution rate at these irradiances in the P-E curves generated for each coralline species-group (Fig. 3.5), the two seasonal light regime treatments may simply not have been distinct enough to promote detectable differences in coralline photosynthetic response within our experimental design.

The varied effects of simulated seasonal light regimes on coralline algal net calcification in the lab raises the question of whether seasonal differences in light availability reaching the benthos in the field truly differ enough to modulate coralline algal response to future OA. Benthic irradiance data indicate that 24h totals of luminous exposure (Fig. 3.1) and PPFD reaching the seafloor may not be as seasonally distinct as previously assumed, or at the very least, are inconsistent among sites. The high seasonal productivity in this system may influence this pattern: although total day lengths are shorter in the winter months, water column productivity and macroalgal canopy biomass over rocky reefs are relatively low (Kroeker et al. 2021), resulting in clearer waters and reduced canopy shading that could facilitate higher transmission of light to the benthos. In contrast, summer months are characterized by high planktonic productivity and lush canopies of fast-growing non-calcified algae, such as the subcanopy-forming fleshy red alga *C. ruprechtiana* that demonstrated enhanced growth under a summer light regime (Fig A.3). In terms of

the total PPFD reaching an alga's thallus over the course of a day, the reduced light transmission to the seafloor in the summer may offset the greater number of total daylight hours in this season. This could lead to similar if not higher levels of average relative light intensity over a 24h period in the winter season - particularly at sites with canopy-forming kelps. We observed such a pattern in our field irradiance data, where the site with the highest density of canopy-forming kelps (Samsing Pinnacle) experiences monthly maximums in luminous exposure in February and March, whereas the site with the lowest kelp densities (Harris Is.) experiences maximum luminous exposure values from May to July.

Although research on global change impacts to marine macrophytes has been limited in this region, the net productivity of non-calcified seaweeds is generally anticipated to either increase or show no change under future warming and OA (Harley et al. 2012, Kroeker et al. 2013a). Thus, the extent of seasonal shading caused by canopy-forming species may remain similar or intensify in the future. While the maximum photosynthetic rate of the red alga *C. ruprechtiana* increased under the future winter pH conditions, this did not translate to a detectable change in thallus wet weight; instead, this species may have allocated its enhanced carbon reserves under low pH conditions to other biological activities, such as the accumulation of sugars, polysaccharides and amino acids (Kumar et al. 2018, 2020). The absence of a consistent effect of fleshy red algal association on coralline algal calcification was possibly due to inconsistencies in the amount of shading among each coralline-*Cryptopleura* pairing (see Fig. S3.2B), rather than an indication that shading by other

canopy-forming macroalgal species is not relevant to coralline algal physiology. According to the P-E curves generated for the coralline algae, current average irradiance levels in the field fall below the light intensity at which these species exhibit maximum photosynthetic rates. Consequently, any decrease in light availability reaching the benthos resulting from enhanced productivity of canopy-forming macroalgae under future OA and warming (Reed & Foster 1984, Harley et al. 2012) will theoretically lead to a reduction in coralline algal photosynthetic capacity. Additionally, our results suggest that even in close association with a non-calcified alga experiencing enhanced photosynthetic rates under OA conditions, coralline algae do not benefit from this localized draw-down of CO_2 nor from any canopy-related flow attenuation that could have altered calcification dynamics across their diffusion boundary layers (Guy-Haim et al. 2020). It is possible that the effect of fleshy red algae on coralline algal calcification could differ based on variation in benthic flow. Unfortunately, we did not account for this variable in our study design. While standard flow rates in this experimental system are 2-3L/min, we did not measure within-aquaria flow during this study, and we have not measured in situ flow rates on subtidal rocky reefs of this region. Yet, our results are consistent with studies demonstrating variable or negligible benefits of canopy-forming algae on benthic organism calcification (Short et al. 2014, Koweek et al. 2017). We anticipate that the resilience of these coralline algal species to OA in this high-latitude, light-limited benthic environment will not be radically improved via their physical associations with other, non-calcified macroalgae.

Our laboratory study successfully simulated ecologically-relevant combinations of current and projected pCO_2 and light regime in Sitka Sound, yet it is important to note that we were unable to manipulate another critical environmental variable that will shift with global climate change: temperature (Gattuso et al. 2015). Ocean warming is anticipated to adversely affect the photophysiology and calcification of some coralline algae, and the effect of future temperature increases may exacerbate the effects of increasing pCO_2 on coralline dissolution (Martin & Gattuso 2009, Vásquez-Elizondo & Enríquez 2016, Cornwall et al. 2019). While the temperature range observed in all aquaria over the course of the experiment reflects conditions that these coralline algae naturally experience in late summer (Aug-Sept) in Sitka Sound (Kroeker et al. 2021), such temperatures exceed what would be expected within the scenarios simulated with our study's pCO_2 and light regime treatments. Because seasonal variation in temperature and pH in this system are not synchronous (Kroeker et al. 2021), this seasonal maximum in temperature does not align temporally with the annual pCO_2 extremes that this study's treatments were based upon. As a consequence, our results may overestimate the effects of pCO_2 and light regime on coralline physiology and calcification for each scenario (Cornwall et al. 2019). Then again, in a recent synthesis of coralline algal research that considered the interactive effects of OA and increased temperatures, the majority of included studies found that OA was the more dominant driver of coralline algal response and that the addition of temperature did not change the effect of OA on coralline algal physiology (Cornwall et al. 2021b). Future research will need to address the impact of

temperature on the physiology of these high-latitude coralline algal species in order to assess the contribution of this driver and its interaction with other global change stressors.

Crustose and geniculate coralline algae found within the same coastal systems often differ in overall rates of production and calcification (McCoy & Kamenos 2015, Vásquez-Elizondo & Enríquez 2016, Noisette et al. 2013), which may reveal disparate vulnerabilities to future OA between these two morphological forms. Comparing the two morphotypes considered in this study, the geniculate form (*B. orbigniana*) exhibited higher photosynthetic capacity, field length extension rates, and net calcification rates than the crustose form (*Crusticorallina* spp.). These differences between the two morphotypes, combined with the overall lower light adaptation of the crustose individuals, may lead to higher susceptibility of crustose coralline algae to corrosion under OA and a higher potential for thallus breakage under stress in this system (Ragazzola et al. 2012). Combined with decreased growth rate as OA progresses, this may rapidly affect crustose species' ability to compete for space at the benthos with geniculate coralline algae and could lead to shifts in the structure and biodiversity of coralline algal assemblages (McCoy & Pfister 2014, Cornwall et al. 2021b).

Ultimately, if coralline algal dissolution outpaces calcification throughout the year at high latitudes under future global change scenarios, both encrusting and geniculate species considered in this study will be vulnerable to increased

competition for space by non-calcified macroalgae (Kuffner et al. 2008, Kroeker et al. 2013b, Schoenrock et al. 2016, Gomez-Lemos & Diaz-Pulido 2017, Cornwall et al. 2021b). The diverse and essential roles that coralline algae play in temperate rocky reef systems - as foundational reef structure, year-round primary producers and carbon reservoirs, and settlement habitat for associated invertebrates (McCoy & Kamenos 2015) - will shift with changes in their relative biomass. Ecological research considering the long-term community-level consequences of a reduction or absence of macrophyte calcifiers across a diversity of marine systems should continue to be prioritized if we seek to effectively anticipate the bottom-up effects on coastal ecosystem function across the world.

This study confirms the vulnerability of two spatially dominant, yet previously unstudied morphotypes of calcium carbonate containing algae in the northern Pacific to end-of-century projections of OA in this region. While high-latitude coralline algae already experience annual swings in seawater carbonate chemistry of over 0.4 pH units between winter and summer seasons (Kroeker et al. 2021), we have confirmed that the geniculate alga *Bossiella orbigniana* and individuals from the crustose alga genus *Crusticorallina* are still able to add calcified tissue via linear extension from their meristems through both seasons in the field. In contrast, under laboratory-simulated pH conditions expected in the winter months by year 2100, both coralline morphotypes exhibited net dissolution and no change in photosynthetic performance.

Although the long daylight hours that characterize high-latitude summers might be expected to benefit coralline algal photosynthesis and calcification capacity, our results suggest that the actual difference in seasonal light availability reaching the benthos in this temperate subtidal system may not be sufficient to significantly modulate coralline algal productivity. In fact, increasing productivity and canopy-coverage by non-calcified macroalgae under future OA and warming may further reduce irradiance levels at the benthos during the summer (Harley et al. 2012). Given that the relatively higher pH summer season may represent the only annual opportunity for coralline algae to achieve positive net calcification under future OA scenarios in this region, increased shading by closely associated algae - particularly in the absence of any ameliorating effect on local carbonate chemistry - may ultimately limit coralline algal resilience to dissolution.

Anthropogenic emissions of CO_2 and the concomitant decrease in oceanic pH and carbonate saturation state will overlay onto spatially and temporally variable, ecologically complex marine systems. This research responds to a call to incorporate seasonally dependent abiotic and biotic interactions in our consideration of vulnerable species' response to global change drivers, a challenging yet necessary approach in the coming era of climate change science that can be used to identify where and when future conditions of enhanced stress are most likely to occur. We strongly recommend that future research investigating the emergent effects of global change in marine macroalgal communities continues to consider how seasonality and other natural

variability interacts with global change drivers to shape the responses of a wide diversity of co-occurring and interacting seaweed species.

Acknowledgements

This work was supported by the National Science Foundation [OCE-1752600], the David and Lucile Packard Foundation, the Koret Foundation, and the UCSC Maximizing Access to Research Careers (MARC) U*STAR program (NIH 2T34GM007910-38). DNA sequencing supported by a family trust to PWG.

We thank C. Powell and E. O'Brien (UCSC) and J. Klejka for their invaluable assistance in the field and laboratory, T. Vision (UNC, Chapel Hill) for lab space and equipment, and D. Wilson Freshwater (DNA Analysis Core Facility, Center for Marine Sciences, UNC, Wilmington) for final sequencing. We also thank P. Raimondi (UCSC) for his assistance with our linear mixed model analyses, M. Kilpatrick (UCSC) for his guidance with our photophysiology data analysis, B. Abrams (UCSC Life Sciences Microscopy Center) for his support with fluorescent imaging analysis, and the Sitka Sound Science Center staff for their diving and facilities support in Sitka.

Tables

Table 3.1. Seawater carbonate chemistry data (mean ± SD) by treatment over the duration of the 2017 laboratory experiment. Temperature and salinity were measured daily using a handheld meter (YSI) in all experimental aquaria (temperature) or just upstream of inflow to the experimental system (salinity). Discrete water samples were collected within each aquaria at the beginning and end of the experiment plus at least one mid-point (n=3-4 aquaria^{-1}) for measurement of pH_T and total alkalinity (TA), and pCO_2 and saturation state (Ω) of calcite were calculated from measured parameters.

Treatment	Current summer pH	Current winter pH	Future winter pH
Temperature (°C)	13.6 ± 0.7	13.6 ± 0.7	13.6 ± 0.7
Salinity (ppt)	29.5 ± 1.7		
pH_T	7.99 ± 0.06	7.70 ± 0.05	7.40 ± 0.03
pCO_2 (µatm)	437 ± 76	919 ± 125	1904 ± 172
TA (µmol kg^{-1})	2105 ± 14	2100 ± 11	2100 ± 17
Ω calcite	2.81 ± 0.36	1.51 ± 0.21	0.79 ± 0.06

Figures

Figure 3.1. Average daily luminous exposure at the benthos (~7m MLLW) at four rocky reef monitoring sites in Sitka Sound, Alaska. Boxplots represent data averaged by calendar day across 4 years (2017-2020), summarized by month.

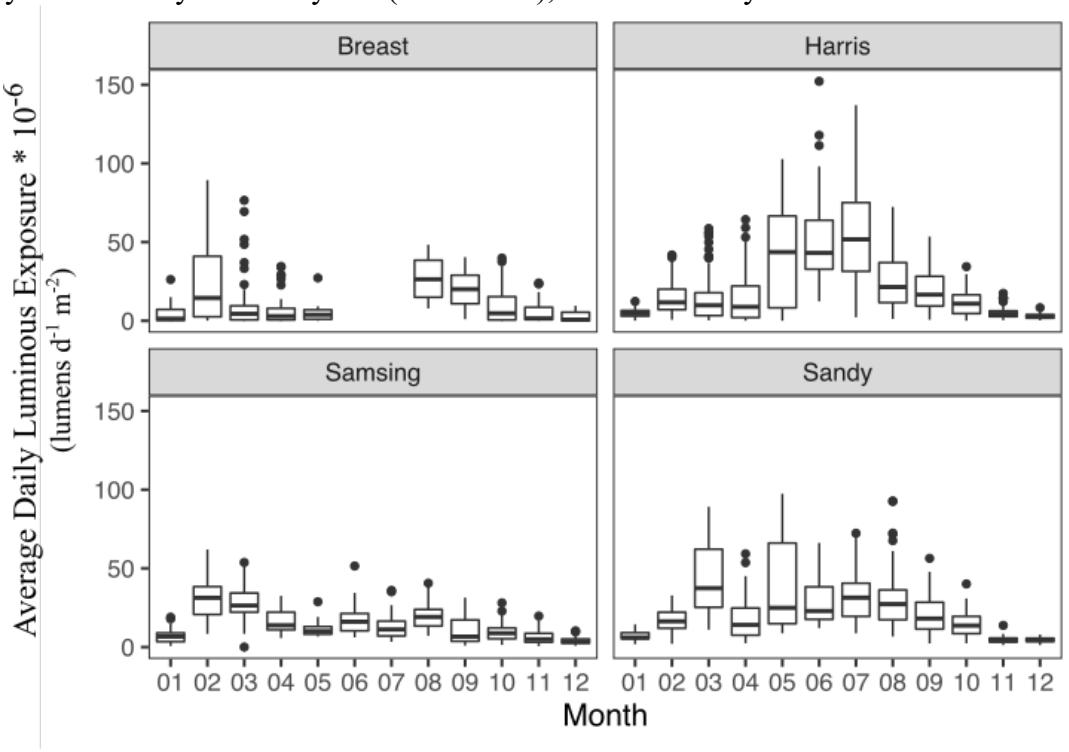

Figure 3.2. Mean field growth as the rate of seasonal linear length extension for common species of coralline algae on a rocky reef (Harris Is.) in Sitka Sound, Alaska. Italicized numbers in brackets indicate sample size per group, and lowercase letters denote statistically significant differences among season and species.

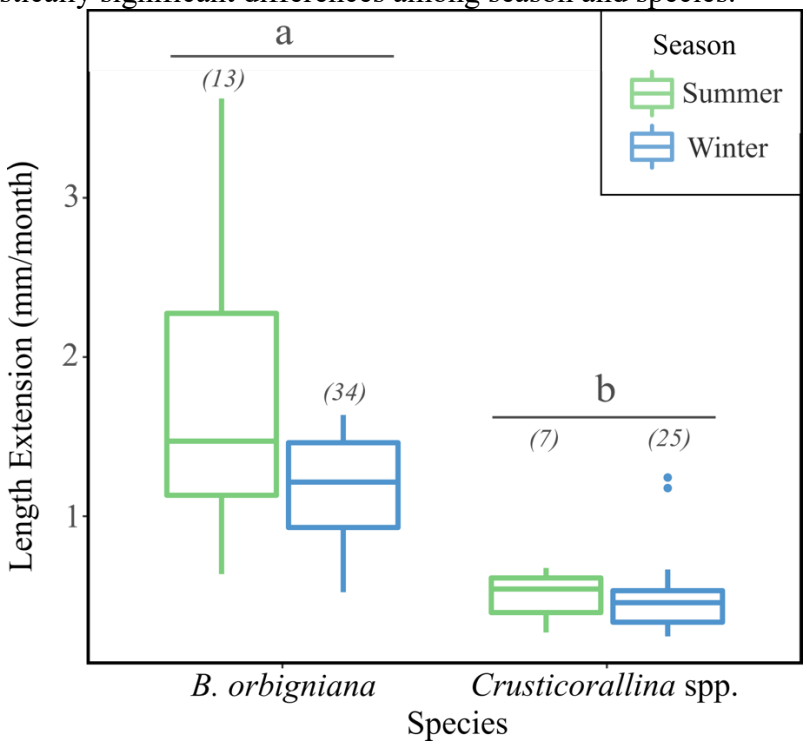

Figure 3.3. Relative net calcification rates (RCR_{net}) of *B. orbigniana* (A) and *Crusticorallina* spp. (B) exposed to different treatment combinations of pH, seasonal light regime, and association with a non-calcified alga (*C. ruprechtiana*) during a month-long laboratory experiment (n=6 individuals treatment^{-1}). Lower case letters denote significant pairwise differences among pH treatment levels.

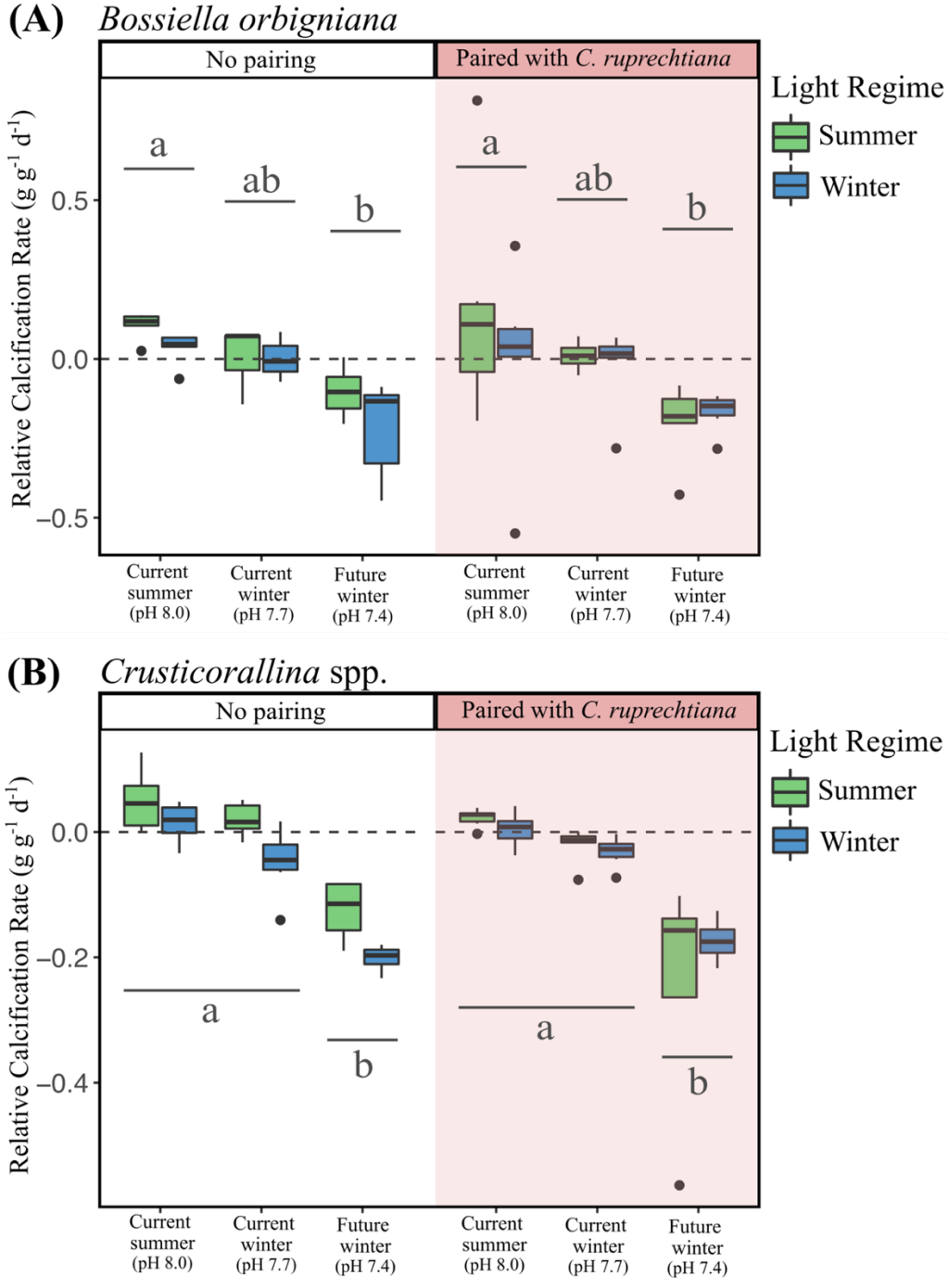

Figure 3.4. Short-term net calcification rates (G_{net}) of both *B. orbigniana* (A) and *Crusticorallina* spp. (B) during 3hr total alkalinity (TA) incubations under continuous light. Data are summarized based on the assigned treatment conditions of pH, light regime, and association with a non-calcified alga (*C. ruprechtiana*) that each coralline was exposed to prior to TA incubations (n=3 individuals treatment^{-1}). Lower case letters denote significant pairwise differences among pH treatment levels, while upper case letters denote differences between association treatments.

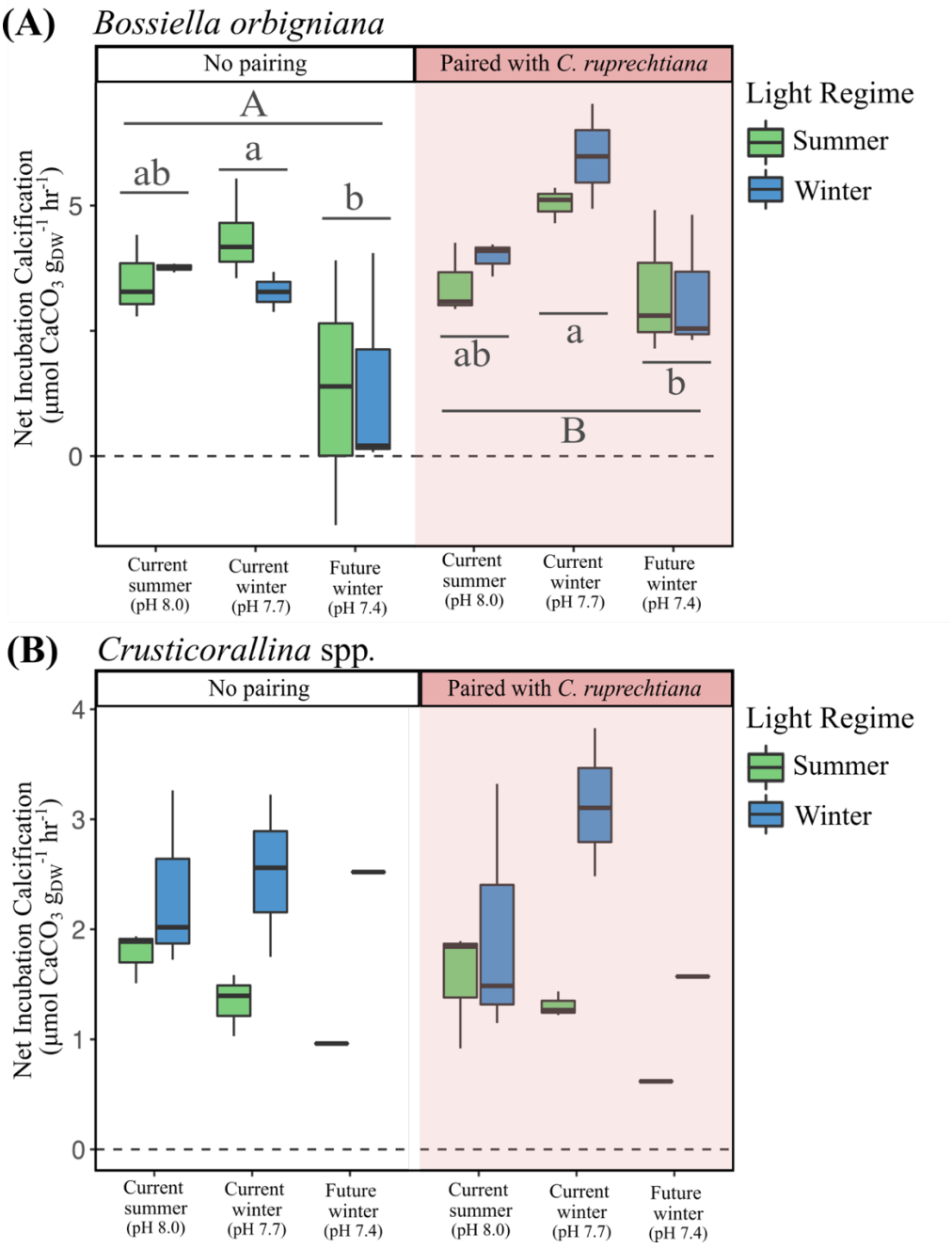

Figure 3.5. Mean photosynthesis-irradiance (P-E) curves (lines) generated from repeated oxygen evolution rate measurements (circles) at multiple irradiance levels for three red algal species-groups (n=36 individuals species^{-1}). P-E curves for coralline algal species *B. orbigniana* and *Crusticorallina* spp. are shown pooled across all experimental treatments, whereas photophysiology data for the non-calcified alga *C. ruprechtiana* are indicated separately by pH treatment.

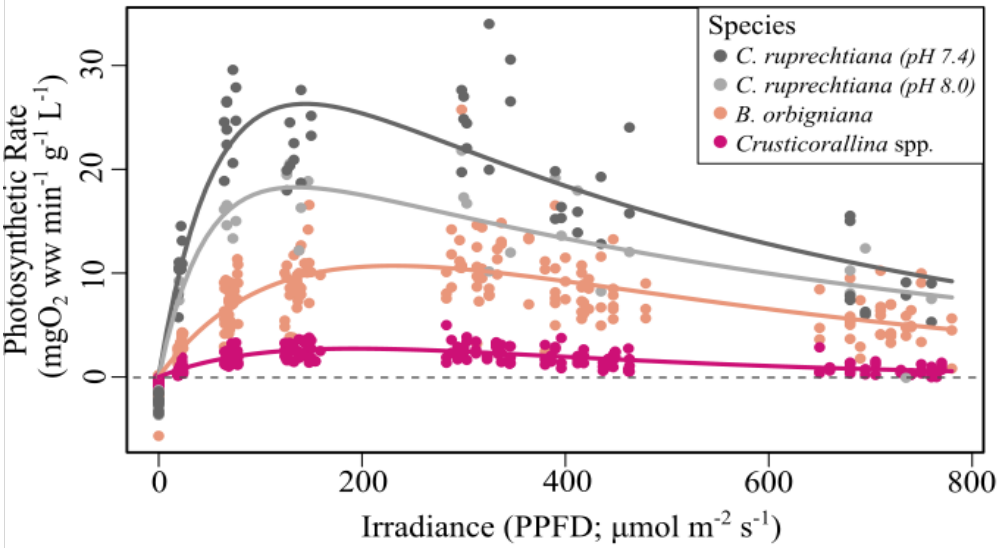

CONCLUSION

This body of work represents a comprehensive assessment of how global change will impact macroalgal producers in environmentally dynamic, temperate coastal oceans. My field studies reveal the current production regimes of calcified and non-calcified seaweeds under seasonal variations in light, nutrients, pCO_2 and temperature. My experimental results indicate how environmental change may affect the phenology, quantity, and quality of basal energy supply, and may even alter the structural foundation of rocky reef habitats. Taken together, this dissertation describes the ecology of change within a productive, interconnected ecosystem, with broad implications regarding the emergent effects of climate change within marine and terrestrial systems worldwide.

In **Chapter 1**, I first investigate the annual production dynamics of three dominant, canopy-forming kelp species in situ and characterize the natural abiotic variability of their environment. I find that *Macrocystis pyrifera*, *Neoagarum fimbriatum*, and *Hedophyllum nigripes* differ in their phenology and magnitude of carbon and nitrogen production, resulting in a complementary supply of energy for macroalgal consumers through the year. I also provide the first robust, year-round estimation of *M. pyrifera* carbon production and turnover at the poleward fringe of its range. I then use my localized understanding of kelp ecology alongside a rich dataset of in situ environmental conditions to design realistic, seasonal scenarios of ocean warming and acidification, and test their effect on kelp production in **Chapter 2**. These

experiments reveal that macroalgal growth, nitrogen content, and palatability to consumers under future environmental conditions differs by species and season. I find that the giant kelp *M. pyrifera* is relatively resilient to ocean warming and acidification in future winter and summer seasons, whereas the understory kelps experience negative impacts to both their growth and nutritional content. The high latitude endemic species *H. nigripes* appears especially vulnerable to ocean warming, and I suggest that negative effects on this species will undermine a critical supply of energy for consumers in future winters. Finally, in **Chapter 3**, I shift my focus to the calcifying coralline algae that provide structural habitat, food, and settlement cues for invertebrate larvae on these temperate rocky reefs. My field studies of in situ growth rates indicate the slow and steady, year-round production of the dominant encrusting and geniculate coralline species in this system, *Bossiella orbigniana* and *Crusticorallina* spp. I then use a multi-factor experimental design to test the seasonal effects of acidification on these calcifying species in the context of their typical proximity to a non-calcified alga. I find marked negative effects of ocean acidification on the coralline species' growth in future winter conditions, regardless of light availability. I also find that the enhanced photosynthesis of a physically adjacent, non-calcified alga does not mitigate the corrosivity of ocean acidification to the calcified algae. I conclude that negative impacts of ocean acidification on coralline algae will undermine the structure and biodiversity of high latitude rocky reef communities, with subsequent effects for higher trophic levels that depend on these habitats for food and refuge.

This research arrives at a critical moment. Macroalgal communities worldwide are shifting in response to climate change (Poloczanska et al. 2013, Krumhansl et al. 2016, Smale 2020), with the overall production and standing biomass of seaweeds expected to increase in high latitude regions (Krause-Jensen & Duarte 2014, Krause-Jensen et al. 2020). Meanwhile, the last few years have brought an accelerating interest in the idea of harnessing macroalgal production for carbon dioxide removal as a climate change solution (e.g., Krause-Jensen & Duarte 2016, Laurens et al. 2020, Ross et al. 2022, Yong et al. 2022). Concurrently, the global seaweed mariculture industry has been growing exponentially (Buschmann et al. 2017, Cai et al. 2021), and there are lofty expectations for the success of this burgeoning industry in subpolar regions like the Gulf of Alaska (AMTF 2018, Stekoll 2019). Yet, despite the heightened interest in the production potential of macroalgae at high latitudes, there is a scarcity of in situ data on year-round kelp production dynamics in polar and subpolar environments (Pessarrodona et al. 2022). My dissertation research addresses this critical knowledge gap by highlighting the environmental drivers and limitations of macroalgal productivity in seasonal, cold temperate environments. These findings can be used by seaweed researchers, policymakers, and industry professionals to inform and calibrate expectations of future macroalgal production in these regions. Finally, as commercially and culturally important high latitude fisheries face considerable risk from ocean warming and acidification (IPCC 2018, Mathis et al. 2015, Hollowed et al. 2022), it is critical for resource managers to consider the indirect, bottom-up effects of global change within these productive marine food

webs. My dissertation provides examples of the many ways in which these foundational coastal habitats and basal energy sources are likely to shift in the future. It is now our collective responsibility to respect the imminence of these changes, and commit to adapting our relationship with these valuable marine ecosystems to ensure their conservation.

APPENDICES

Appendix 1: Supplementary Material for Chapter 1

Figure S1.1. Per-plant proportions of *Macrocystis pyrifera* fronds grown or fronds lost compared to starting frond density (mean ± SE; top panel) and the site-level plant loss rate (bottom panel) during each survey period at (a) Breast Is., (b) Harris Is. and (c) Samsing Pinnacle. A missing bar indicates no data for that particular site and survey period except where noted by "(0)", in which case the data point was zero. Shaded panels indicate the months with the shortest photoperiod (October – March).

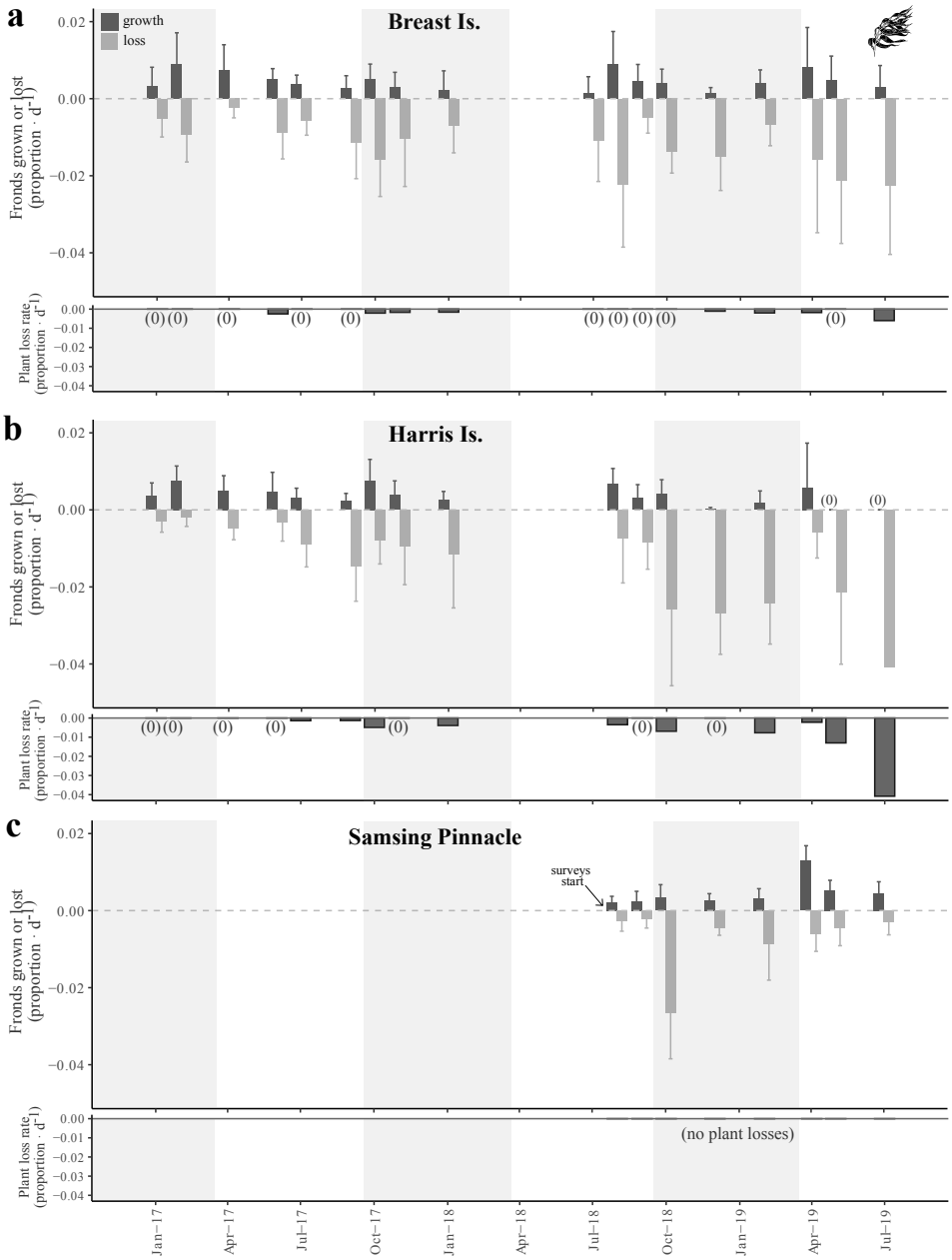

Figure S1.2. Linear growth and erosion rates (cm · d^{-1}) of *Hedophyllum nigripes* blades (mean ± SE; top panel) and the site-level plant loss rate (bottom panel) during each survey period at (a) Breast Is., (b) Harris Is. and (c) Samsing Pinnacle. A missing bar indicates no data for that particular site and survey period except where noted by "(0)", in which case the data point was zero. Shaded panel indicates the months with the shortest photoperiod (October – March).

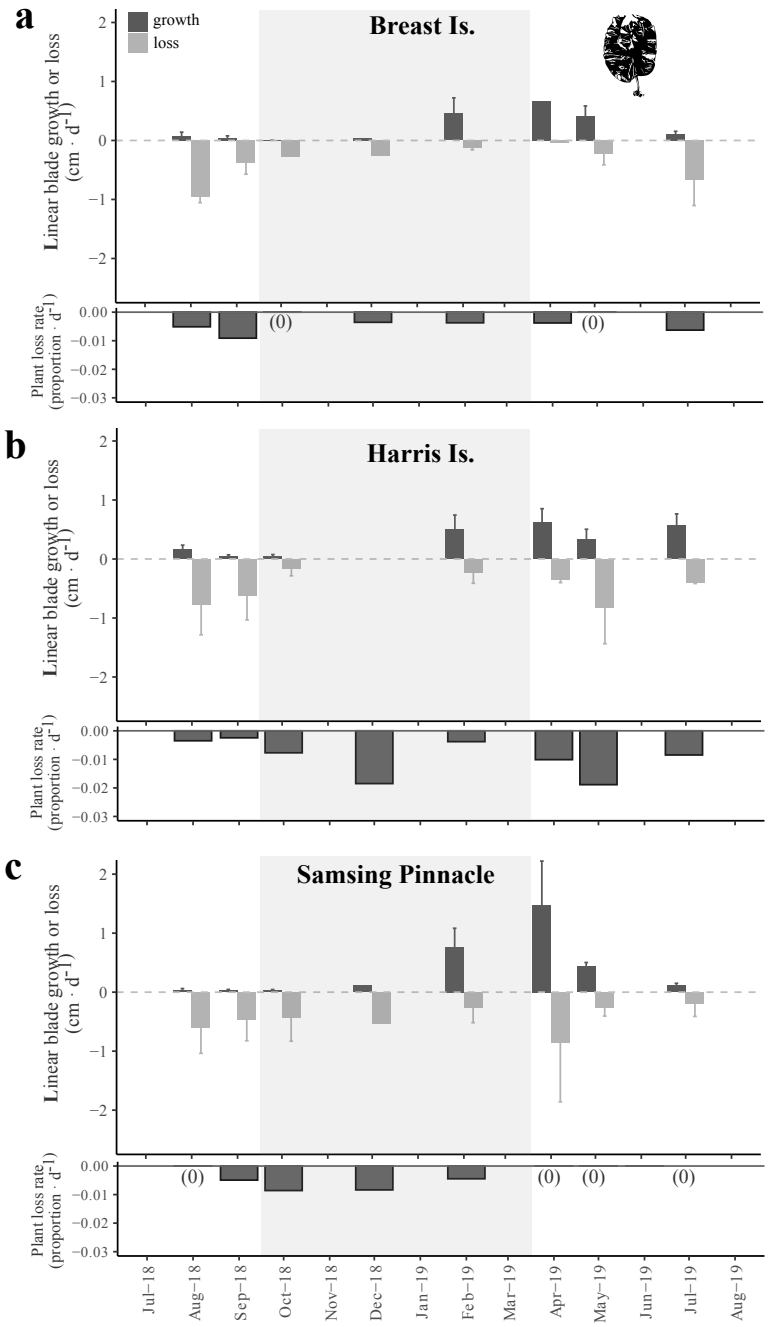

Figure S1.3. Linear growth and erosion rates (cm · d^{-1}) of *Neoagarum fimbriatum* blades (mean ± SE; top panel) and the site-level plant loss rate (bottom panel) during each survey period at (a) Breast Is., (b) Harris Is. and (c) Samsing Pinnacle. A missing bar indicates no data for that particular site and survey period except where noted by "(0)", in which case the data point was zero. Shaded panel indicates the months with the shortest photoperiod (October – March).

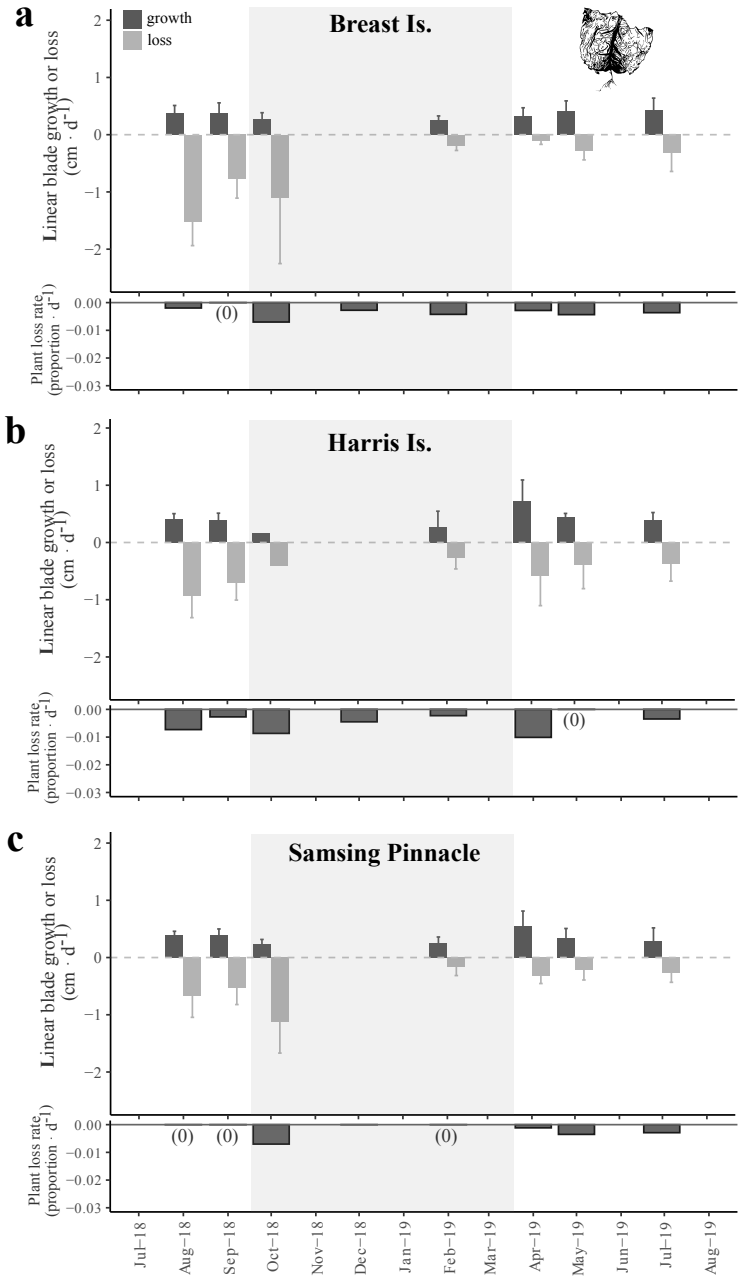

Figure S1.4. Spearman rank correlation scatter plot for log-transformed seawater NOx concentrations (μM) from 4.5 m depth versus nitrogen content (as % dry mass) of *M. pyrifera* surface blades at Breast Is (mean ± SE). Linear regression and 95% confidence interval are shown as the gray line and shaded region. Spearman's rank correlation (ρ) and associated p-value are shown in upper left corner.

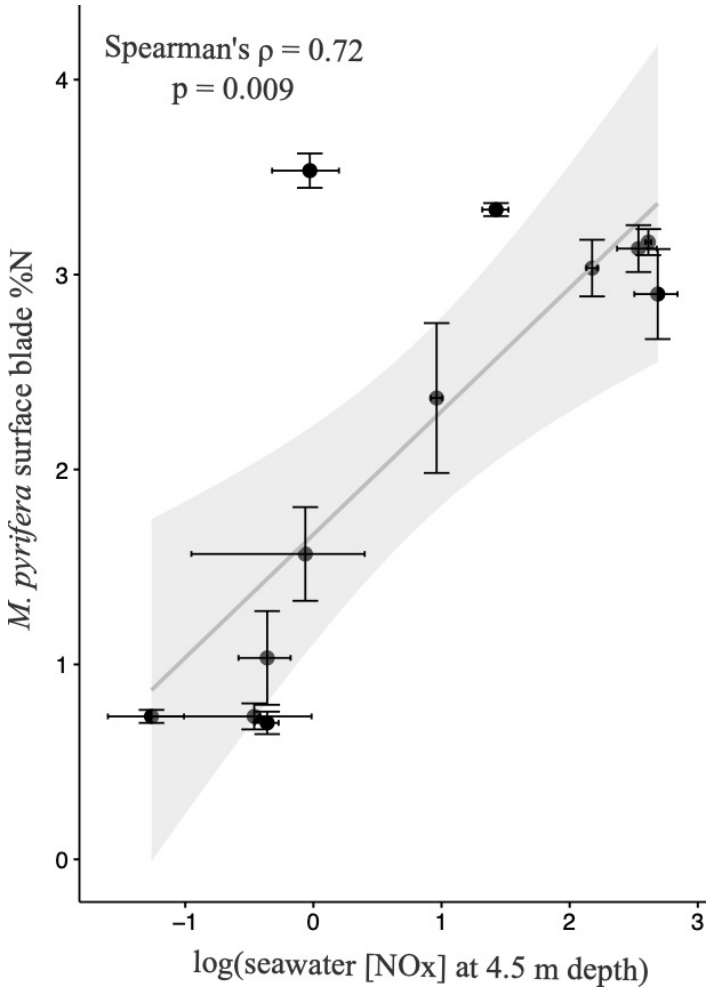

Table S1.1. Regression parameters used to estimate maroalgal wet and dry mass for foliar standing crop determination.

Independent_variable	Dependent_variable	slope	intercept	pvalue	R^2	N	Sample unit
M. pyrifera frond density (all seasons)	*M. pyrifera* wet mass (g; all seasons)	734.9	0	<0.001	0.943	26	individual sporophytes
M. pyrifera frond density (winter only)	*M. pyrifera* wet mass (g; winter only)	748.2	0	<0.001	0.926	10	individual sporophytes
M. pyrifera frond density (summer only)	*M. pyrifera* wet mass (g; summer only)	732.9	0	<0.001	0.941	16	individual sporophytes
M. pyrifera wet mass (g; all tissue samples)	*M. pyrifera* dry mass (g; all tissue samples)	0.103	0	<0.001	0.962	68	tissue samples
M.pyrifera wet mass (g; stipe tissue only)	*M. pyrifera* dry mass (g; stipe tissue only)	0.110	0	<0.001	0.963	36	tissue samples
M.pyrifera wet mass (g; blade tissue only)	*M. pyrifera* dry mass (g; blade tissue only)	0.096	0	<0.001	0.968	32	tissue samples
M.pyrifera wet mass (g; surface tissue only)	*M. pyrifera* dry mass (g; surface tissue only)	0.088	0	<0.001	0.974	23	tissue samples
M.pyrifera wet mass (g; mid-frond tissue only)	*M. pyrifera* dry mass (g; mid-frond tissue only)	0.095	0	<0.001	0.981	24	tissue samples
M.pyrifera wet mass (g; tissue 1m from HF only)	*M. pyrifera* dry mass (g; tissue 1m from HF only)	0.126	0	<0.001	0.988	21	tissue samples
N. fimbriatum blade surface area (cm^2)	*N. fimbriatum* blade wet mass (g)	0.066	0	<0.001	0.962	40	individual sporophytes
H. nigripes blade surface area (cm^2)	*H. nigripes* blade wet mass (g)	0.092	0	<0.001	0.970	41	individual sporophytes
A. clathratum blade surface area (cm^2)	*A. clathratum* blade wet mass (g)	0.131	0	<0.001	0.925	20	individual sporophytes
L. setchellii blade surface area (cm^2)	*L. setchellii* blade wet mass (g)	0.097	0	<0.001	0.983	5	individual sporophytes
P. gardneri blade surface area (cm^2)	*P. gardneri* blade wet mass (g)	0.080	0	0.066	0.801	3	individual sporophytes
N. fimbriatum blade wet mass (g)	*N. fimbriatum* blade dry mass (g)	0.136	0	<0.001	0.994	10	individual sporophytes
H. nigripes blade wet mass (g)	*H. nigripes* blade dry mass (g)	0.190	0	<0.001	0.987	11	individual sporophytes
N. fimbriatum stipe density (# m^{-2}), Jan 2020	*N. fimbriatum* dry biomass (g m-2), Jan 2020	2.505	0	0.007	0.825	5	transects
H. nigripes stipe density (# m^{-2}), Jan 2020	*H. nigripes* dry biomass (g m-2), Jan 2020	5.883	0	0.001	0.971	4	transects
N. fimbriatum stipe density (# m^{-2}), July 2019 & 2020	*N. fimbriatum* dry biomass (g m-2), July 2019 & 2020	17.691	0	0.016	0.525	8	transects
H. nigripes stipe density (# m^{-2}), July 2019 & 2020	*H. nigripes* dry biomass (g m-2), July 2019 & 2020	49.994	0	<0.001	0.982	8	transects

Table S2. Estimated foliar standing crop (g wet mass · m^{-2}) of subtidal understory kelp species by survey site and season from blade morphometric surveys.

	Breast				Harris				Samsing			
	2019		2020		2019		2020		2019		2020	
Species	Spring	Summer	Winter	Summer	Spring	Summer	Winter	Summer	Spring	Summer	Winter	Summer
Hedophyllum nigripes	1.84	0[a]	0	0	2.48	0.49	0	0	17.78	114.74	13.59	86.21
Neoagarum fimbriatum	5.12	22.17	0.36	0.47	19.87	34.97	0.12	0	12.84	60.66	3.89	38.70
Agarum clathratum	0	0	0	0	57.40	82.55	11.34	21.68	33.47	171.51	24.18	107.26
Laminaria setchellii	0	0	0	0	0	0	0	0	0.88	3.17	0.02	3.44
Pleurophycus gardeneri	0	0	0	0	0	0	0	0	0.18	3.33	0	5.11
Total understory kelp biomass (g· m^{-2})	**6.96**	**22.17**	**0.36**	**0.47**	**79.75**	**118.01**	**11.46**	**21.68**	**65.15**	**353.41**	**41.67**	**240.73**

[a]Some plants tagged for productivity measurements did still exist at this site in this season, but were not captured in this particular survey

Table S1.3. Regression parameters used to test the effect of elapsed days in the study on *M. pyrifera* growth rate at two sites

Independent_variable	Dependent_variable	slope	intercept	pvalue	rsquare	N	Sample unit
Number of elapsed days in the study	*M. pyrifera* net growth rate (d^{-1}; Harris Is.)	-0.00003	0.005	<0.001	0.497	16	site surveys
Number of elapsed days in the study	*M. pyrifera* net growth rate (d^{-1}; Breast Is.)	-0.00001	0.00008	0.002	0.442	17	site surveys

Table S1.4. Summary statistics from mixed linear model analysis of monthly seawater NO_x concentrations near Breast Is.
Formula: log(seawater NO_x) ~ depth * location + (1|date)

i. *Variance components for random effects*

Groups	**Variance**	**Std. Dev.**
date	2.244	1.498
residual	0.237	0.487

Number of observations: 104
Groups: date, 13

ii. *ANOVA results from the mixed linear model*

Source	**SS**	**MSE**	**numDF**	**denDF**	**F value**	**Pr(>F)**
depth	3.030	3.030	1	84.020	12.771	<0.001
location	0.480	0.160	3	84.027	0.674	0.570
depth:location	1.057	0.352	3	84.018	1.486	0.224

Table S1.5. Elemental composition (carbon or nitrogen as % dry mass) of subtidal kelp species by collection site and season.

Composition (% dry mass)	Species	Harris		Samsing			
		2018 Summer	2020 Summer	2018 Summer	2019 Winter	2019 Summer	2020 Summer
Carbon	*Macrocystis pyrifera*	29.30 ± 1.90		28.70 ± 1.19	28.22 ± 2.31	32 ± 1.72	
	Hedophyllum nigripes	37.10 ± 1.51		33.10 ± 1.41	29.18 ± 1.13	38.08 ± 0.21	30.44 ± 0.81
	Neoagarum fimbriatum	33.18 ± 0.44		32.02 ± 0.49	32.80 ± 0.32	33.78 ± 0.78	32.38 ± 0.43
	Agarum clathratum		30.14 ± 1.44				36.50 ± 1.41
	Laminaria setchellii						32.02 ± 0.96
	Pleurophycus gardneri						31.60 ± 0.57
Nitrogen	*Macrocystis pyrifera*	0.56 ± 0.25		1.04 ± 0.15	1.6 ± 0.29	1.12 ± 0.39	
	Hedophyllum nigripes	0.74 ± 0.02		1.16 ± 0.07	2.56 ± 0.09	1.24 ± 0.08	1.32 ± 0.06
	Neoagarum fimbriatum	1.46 ± 0.04		1.66 ± 0.08	2.28 ± 0.10	1.94 ± 0.07	1.90 ± 0.10
	Agarum clathratum		1.8 ± 0.12				2.34 ± 0.24
	Laminaria setchellii						0.82 ± 0.04
	Pleurophycus gardneri						0.90 ± 0.06

Table S1.6. Summary statistics for analysis of variance of macroalgal tissue nitrogen concentrations at Samsing Pinnacle

Formula: nitrogen (as % dry mass) ~ season * species

i. *Main effects*

Source	**df**	**SS**	**MSE**	**F value**	**Pr(>F)**
season	1	6.188	6.188	116.26	<0.001
species	2	3.767	1.884	35.380	<0.001
season:species	2	1.646	0.823	15.460	<0.001
residuals	39	2.076	0.053		

ii. *Tukey's post-hoc tests for the effect of species on %N*

Condition1	**Condition2**	**Mean diff**	**95% CI lower**	**95% CI upper**	**P_{tukey}**
H. nigripes	*N. fimbriatum*	-0.307	-0.512	-0.101	0.002
	M. pyrifera	0.400	0.195	0.605	<0.001
M. pyrifera	*N. fimbriatum*	-0.707	-0.912	-0.501	<0.001

ii. *Tukey's post-hoc tests for the effect of the interaction between season and species on %N*

Condition1	**Condition2**	**Mean diff**	**95% CI lower**	**95% CI upper**	**P_{tukey}**
Winter:*N. fimbriatum*	Summer:*N. fimbriatum*	0.480	0.101	0.859	0.006
Summer:*M. pyrifera*	Summer:*N. fimbriatum*	-0.720	-1.029	-0.411	<0.001
Winter:*M. pyrifera*	Summer:*N. fimbriatum*	-0.200	-0.579	0.179	0.614
Summer:*H. nigripes*	Summer:*N. fimbriatum*	-0.600	-0.909	-0.291	<0.001
Winter:*H. nigripes*	Summer:*N. fimbriatum*	0.760	0.381	1.139	<0.001
Summer:*M. pyrifera*	Winter:*N. fimbriatum*	-1.200	-1.579	-0.821	<0.001
Winter:*M. pyrifera*	Winter:*N. fimbriatum*	-0.680	-1.117	-0.243	<0.001
Summer:*H. nigripes*	Winter:*N. fimbriatum*	-1.080	-1.459	-0.701	<0.001
Winter:*H. nigripes*	Winter:*N. fimbriatum*	0.280	-0.157	0.717	0.406
Winter:*M. pyrifera*	Summer:*M. pyrifera*	0.520	0.141	0.899	0.002
Summer:*H. nigripes*	Summer:*M. pyrifera*	0.120	-0.189	0.429	0.851
Winter:*H. nigripes*	Summer:*M. pyrifera*	1.480	1.101	1.859	<0.001
Summer:*H. nigripes*	Winter:*M. pyrifera*	-0.400	-0.779	-0.021	0.033
Winter:*H. nigripes*	Winter:*M. pyrifera*	0.960	0.523	1.397	<0.001
Winter:*H. nigripes*	Summer:*H. nigripes*	1.360	0.981	1.739	<0.001

Table S1.7. Summary statistics for analysis of variance of macroalgal tissue carbon concentrations at Samsing Pinnacle

Formula: carbon (as % dry mass) ~ season * species

i. *Main effects*

Source	df	SS	MSE	F value	Pr(>F)
season	1	82.940	82.940	14.638	<0.001
species	2	126.490	63.240	11.161	<0.001
season:species	2	69.170	34.590	6.104	0.005
residuals	39	220.990	5.670		

ii. *Tukey's post-hoc tests for the effect of species on %N*

Condition1	Condition2	Mean diff	95% CI lower	95% CI upper	P_{tukey}
H. nigripes	*N. fimbriatum*	-3.227	-5.344	-1.109	0.002
	M. pyrifera	0.587	-1.531	2.704	0.779
M. pyrifera	*N. fimbriatum*	3.813	1.696	5.931	<0.001

ii. *Tukey's post-hoc tests for the effect of the interaction between season and species on %N*

Condition1	Condition2	Mean diff	95% CI lower	95% CI upper	P_{tukey}
Winter:*N. fimbriatum*	Summer:*N. fimbriatum*	-0.100	-4.006	3.806	1.000
Summer:*M. pyrifera*	Summer:*N. fimbriatum*	-2.550	-5.739	0.639	0.183
Winter:*M. pyrifera*	Summer:*N. fimbriatum*	-4.680	-8.586	-0.774	0.011
Summer:*H. nigripes*	Summer:*N. fimbriatum*	2.690	-0.499	5.879	0.141
Winter:*H. nigripes*	Summer:*N. fimbriatum*	-3.720	-7.626	0.186	0.070
Summer:*M. pyrifera*	Winter:*N. fimbriatum*	-2.450	-6.356	1.456	0.430
Winter:*M. pyrifera*	Winter:*N. fimbriatum*	-4.580	-9.090	-0.070	0.045
Summer:*H. nigripes*	Winter:*N. fimbriatum*	2.790	-1.116	6.696	0.289
Winter:*H. nigripes*	Winter:*N. fimbriatum*	-3.620	-8.130	0.890	0.180
Winter:*M. pyrifera*	Summer:*M. pyrifera*	-2.130	-6.036	1.776	0.582
Summer:*H. nigripes*	Summer:*M. pyrifera*	5.240	2.051	8.429	<0.001
Winter:*H. nigripes*	Summer:*M. pyrifera*	-1.170	-5.076	2.736	0.945
Summer:*H. nigripes*	Winter:*M. pyrifera*	7.370	3.464	11.276	<0.001
Winter:*H. nigripes*	Winter:*M. pyrifera*	0.960	-3.550	5.470	0.987
Winter:*H. nigripes*	Summer:*H. nigripes*	-6.410	-10.316	-2.504	<0.001

Appendix 2: Supplementary Material for Chapter 2

Figure S2.1. Daily pH variability as a function of daily tidal activity in late winter and spring 2019. Diel variability is shown as the maximum difference in recorded pH_T values at each site (top panel) and the maximum difference in observed tidal heights recorded at the Sitka tidal station (bottom panel).

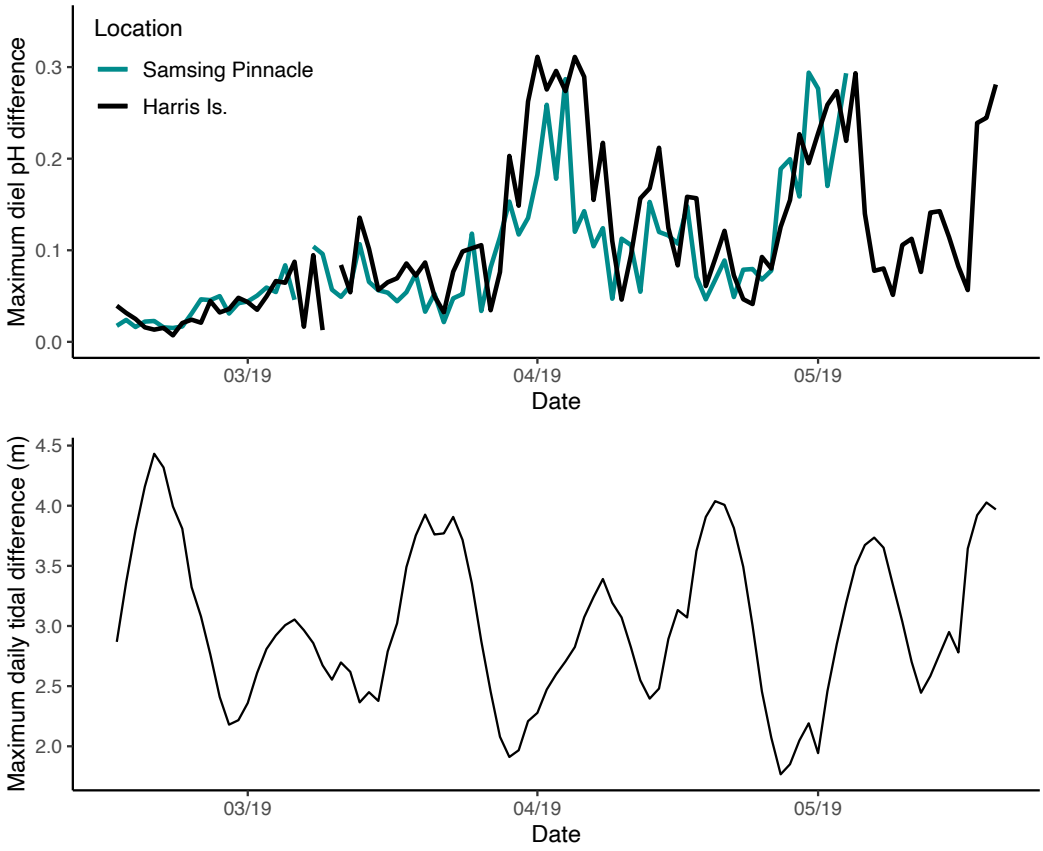

Figure S2.2. Linear blade extension rates (mean ± SE) of understory kelp species by treatment in seasonal experimental conditions (this study) compared to seasonal growth rates observed in situ at kelp forest sites in Sitka Sound (data from Bell and Kroeker 2022).

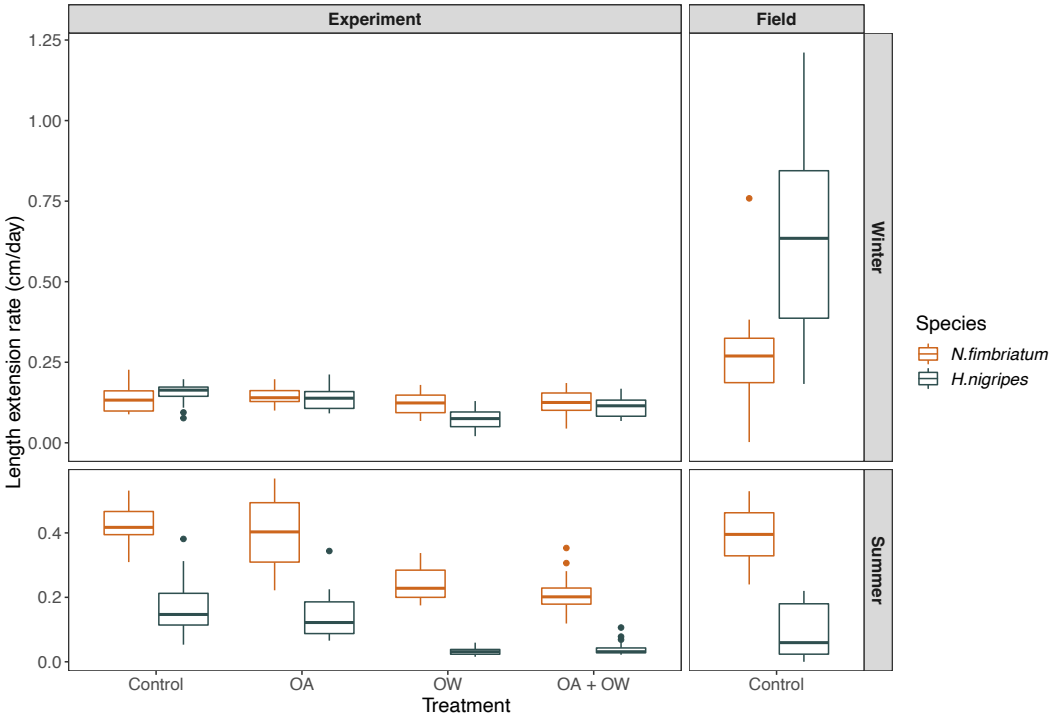

Figure S2.3. Relative consumption (mean ± SE) of experimentally grown *N. fimbriatum* tissue in feeding assays used to test the effects of seasonal pH and temperature treatment on the palatability of algal tissue to a common kelp forest grazer.

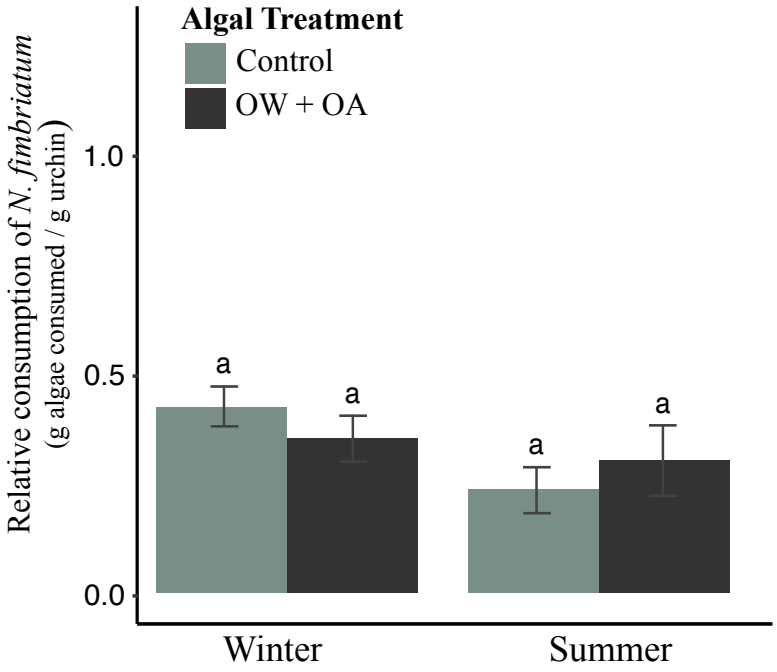

Table S2.1. Summary statistics from mixed linear model analysis of *Hedophyllum nigripes*' relative growth rate as wet mass (d^{-1}) by treatment in winter season experiment.
Formula: *H. nigripes* RGR_{mass} ~ pH * temperature + (1|header/aquaria)

i. *Variance components for random effects*

Groups	**Variance**	**Std. Dev.**
aquaria:header	0.013	0.113
header	0.000	0.000
residual	0.092	0.303

Number of observations: 69
Groups: aquaria:header, 24; header, 8

ii. *Coefficients and statistics for fixed effects*

Fixed Effects	**Estimate**	**SE**	**df**	**t value**	**Pr(>|t|)**
Intercept	1.274	0.085	17.83	14.98	**< 0.001**
OA	-0.052	0.120	17.83	-0.433	0.671
OW	-0.636	0.123	19.26	-5.173	**< 0.001**
OA + OW	0.351	0.173	18.87	2.029	**0.057**

Table S2.2. Summary statistics from mixed linear model analysis of *Hedophyllum nigripes*' relative growth rate as wet mass (d^{-1}) by treatment in summer season experiment.
Formula: *H. nigripes* RGR_{mass} ~ pH * temperature + (1|header/aquaria)

i. *Variance components for random effects*

Groups	**Variance**	**Std. Dev.**
aquaria:header	0.000	0.000
header	0.000	0.000
residual	0.585	0.765

Number of observations: 68
Groups: aquaria:header, 24; header, 8

ii. *Coefficients and statistics for fixed effects*

Fixed Effects	**Estimate**	**SE**	**df**	**t value**	**Pr(>|t|)**
Intercept	1.123	0.180	64	6.229	**< 0.001**
OA	-0.067	0.255	64	-0.262	0.794
OW	-0.763	0.263	64	-2.906	**0.005**
OA + OW	-0.128	0.372	64	-0.344	0.732

Table S2.3. Summary statistics from mixed linear model analysis of *Neoagarum fimbriatum*'s % change in wet mass by treatment in winter season experiment. Formula: *N. fimbriatum* RGR_{mass} ~ pH * temperature + (1|header/aquaria)

i. *Variance components for random effects*

Groups	**Variance**	**Std. Dev.**
aquaria:header	0.000	0.000
header	0.000	0.000
residual	0.124	0.352

Number of observations: 72
Groups: aquaria:header, 24; header, 8

ii. *Coefficients and statistics for fixed effects*

Fixed Effects	**Estimate**	**SE**	**df**	**t value**	**Pr(>|t|)**
Intercept	1.308	0.083	68	15.79	**< 0.001**
OA	0.095	0.117	68	0.813	0.419
OW	-0.079	0.117	68	-0.670	0.505
OA + OW	-0.027	0.166	68	-0.160	0.873

Table S2.4. Summary statistics from mixed linear model analysis of *Neoagarum fimbriatum*'s relative growth rate as wet mass (d^{-1}) by treatment in summer season experiment.
Formula: *N. fimbriatum* RGR_{mass} ~ pH * temperature + (1|header/aquaria)

i. *Variance components for random effects*

Groups	**Variance**	**Std. Dev.**
aquaria:header	0.000	0.000
header	0.000	0.000
residual	0.739	0.860

Number of observations: 63
Groups: aquaria:header, 21; header, 7

ii. *Coefficients and statistics for fixed effects*

Fixed Effects	**Estimate**	**SE**	**df**	**t value**	**Pr(>|t|)**
Intercept	3.654	0.203	59	18.03	**< 0.001**
OA	-0.403	0.287	59	-1.405	0.165
OW	-1.222	0.351	59	-3.481	**< 0.001**
OA + OW	-0.255	0.453	59	0.563	0.575

Table S2.5. Summary statistics from mixed linear model analysis of *Macrocystis pyrifera*'s relative growth rate as wet mass (d^{-1}) by treatment in winter season experiment.
Formula: *M. pyrifera* RGR_{mass} ~ pH * temperature + (1|header/aquaria)

i. *Variance components for random effects*

Groups	**Variance**	**Std. Dev.**
aquaria:header	0.000	0.000
header	0.013	0.114
residual	0.138	0.371

Number of observations: 60
Groups: aquaria:header, 24; header, 8

ii. *Coefficients and statistics for fixed effects*

Fixed Effects	**Estimate**	**SE**	**df**	**t value**	**Pr(>|t|)**
Intercept	0.622	0.121	3.621	5.147	**0.009**
OA	-0.011	0.174	3.893	-0.062	0.953
OW	-0.211	0.182	4.419	-1.161	0.304
OA + OW	0.121	0.253	4.219	0.479	0.656

Table S2.6. Summary statistics from mixed linear model analysis of *Macrocystis pyrifera*'s relative growth rate as wet mass (d^{-1}) by treatment in summer season experiment.
Formula: *M. pyrifera* RGR_{mass} ~ pH * temperature + (1|header/aquaria)

i. *Variance components for random effects*

Groups	**Variance**	**Std. Dev.**
aquaria:header	<0.001	0.013
header	0.000	0.000
residual	0.853	0.924

Number of observations: 70
Groups: aquaria:header, 24; header, 8

ii. *Coefficients and statistics for fixed effects*

Fixed Effects	**Estimate**	**SE**	**df**	**t value**	**Pr(>|t|)**
Intercept	2.906	0.218	19.88	13.35	**<0.001**
OA	-0.214	0.308	19.88	-0.695	0.495
OW	-0.248	0.313	20.69	-0.792	0.437
OA + OW	-0.106	0.442	20.69	-0.241	0.812

Table S2.7. Summary statistics from mixed linear model analysis of *Hedophyllum nigripes*' tissue nitrogen content (as % dry mass) by treatment in winter season experiment.
Formula: *H. nigripes* tissue %N ~ pH * temperature + (1|header)

i. *Variance components for random effects*

Groups	**Variance**	**Std. Dev.**
header	0.0002	0.014
residual	0.019	0.138

Number of observations: 23
Groups: header, 8

ii. *Coefficients and statistics for fixed effects*

Fixed Effects	**Estimate**	**SE**	**df**	**t value**	**Pr(>|t|)**
Intercept	2.667	0.057	3.875	46.738	**<0.001**
OA	0.017	0.081	3.875	0.207	0.847
OW	-0.407	0.085	4.486	-4.809	**0.006**
OA + OW	0.140	0.117	4.179	1.197	0.295

Table S2.8. Summary statistics from mixed linear model analysis of *Hedophyllum nigripes*' tissue nitrogen content (as % dry mass) by treatment in summer season experiment.
Formula: *H. nigripes* tissue %N ~ pH * temperature + (1|header)

i. *Variance components for random effects*

Groups	**Variance**	**Std. Dev.**
header	0.009	0.096
residual	0.057	0.238

Number of observations: 23
Groups: header, 8

ii. *Coefficients and statistics for fixed effects*

Fixed Effects	**Estimate**	**SE**	**df**	**t value**	**Pr(>|t|)**
Intercept	2.400	0.118	2.994	20.26	**<0.001**
OA	-0.083	0.168	2.994	0.497	0.653
OW	0.186	0.174	3.391	1.072	0.354
OA + OW	0.014	0.241	3.191	0.058	0.957

Table S2.9. Summary statistics from mixed linear model analysis of *Neoagarum fimbriatum*'s tissue nitrogen content (as % dry mass) by treatment in winter season experiment.
Formula: *N. fimbriatum* tissue %N ~ pH * temperature + (1|header)

i. *Variance components for random effects*

Groups	**Variance**	**Std. Dev.**
header	0.002	0.049
residual	0.002	0.046

Number of observations: 24
Groups: header, 8

ii. *Coefficients and statistics for fixed effects*

Fixed Effects	**Estimate**	**SE**	**df**	**t value**	**Pr(>|t|)**
Intercept	2.000	0.039	4	51.17	**<0.001**
OA	0.033	0.055	4	0.603	0.579
OW	-0.183	0.055	4	-3.317	**0.030**
OA + OW	-0.067	0.078	4	-0.853	0.442

Table S2.10. Summary statistics from mixed linear model analysis of *Neoagarum fimbriatum*'s tissue nitrogen content (as % dry mass) by treatment in summer season experiment.
Formula: *N. fimbriatum* tissue %N ~ pH * temperature + (1|header)

i. *Variance components for random effects*

Groups	**Variance**	**Std. Dev.**
header	0.003	0.057
residual	0.005	0.068

Number of observations: 24
Groups: header, 8

ii. *Coefficients and statistics for fixed effects*

Fixed Effects	**Estimate**	**SE**	**df**	**t value**	**Pr(>|t|)**
Intercept	2.250	0.049	4	46.305	**<0.001**
OA	-0.050	0.069	4	-0.728	0.507
OW	-0.300	0.069	4	-4.366	**0.012**
OA + OW	0.100	0.097	4	1.029	0.362

Table S2.11. Summary statistics from mixed linear model analysis of *Macrocystis pyrifera*'s tissue nitrogen content (as % dry mass) by treatment in winter season experiment.
Formula: *M. pyrifera* tissue %N ~ pH * temperature + (1|header)

i. *Variance components for random effects*

Groups	**Variance**	**Std. Dev.**
header	0.000	0.000
residual	0.008	0.087

Number of observations: 23
Groups: header, 8

ii. *Coefficients and statistics for fixed effects*

Fixed Effects	**Estimate**	**SE**	**df**	**t value**	**Pr(>|t|)**
Intercept	1.750	0.036	18	49.20	**<0.001**
OA	0.117	0.050	18	2.319	**0.032**
OW	-0.167	0.050	18	-3.313	**0.004**
OA + OW	0.000	0.075	18	0.000	1.000

Table S2.12. Summary statistics from mixed linear model analysis of *Macrocystis pyrifera*'s tissue nitrogen content (as % dry mass) by treatment in summer season experiment.
Formula: *M. pyrifera* tissue %N ~ pH * temperature + (1|header)

i. *Variance components for random effects*

Groups	**Variance**	**Std. Dev.**
header	0.005	0.069
residual	0.021	0.144

Number of observations: 24
Groups: header, 8

ii. *Coefficients and statistics for fixed effects*

Fixed Effects	**Estimate**	**SE**	**df**	**t value**	**Pr(>|t|)**
Intercept	2.000	0.076	4	26.19	**<0.001**
OA	0.000	0.108	4	0.000	1.000
OW	-0.100	-0.108	4	-0.926	0.407
OA + OW	0.067	0.153	4	0.436	0.685

Table S2.13. Summary statistics from mixed linear model analysis of *Hedophyllum nigripes*' tissue $\delta^{13}C$ values by treatment in winter season experiment.
Formula: *H. nigripes* $\delta^{13}C \sim$ pH * temperature + (1|header)

i. *Variance components for random effects*

Groups	**Variance**	**Std. Dev.**
header	0.000	0.000
residual	1.023	1.011

Number of observations: 23
Groups: header, 8

ii. *Coefficients and statistics for fixed effects*

Fixed Effects	**Estimate**	**SE**	**df**	**t value**	**Pr(>|t|)**
Intercept	-27.87	0.413	19	-67.51	**<0.001**
OA	-3.765	0.584	19	-6.448	**<0.001**
OW	0.890	0.612	19	1.453	0.163
OA + OW	0.199	0.846	19	0.235	0.817

Table S2.14. Summary statistics from mixed linear model analysis of *Hedophyllum nigripes*' tissue $\delta^{13}C$ values by treatment in summer season experiment.
Formula: *H. nigripes* $\delta^{13}C \sim$ pH * temperature + (1|header)

i. *Variance components for random effects*

Groups	**Variance**	**Std. Dev.**
header	0.006	0.080
residual	0.825	0.908

Number of observations: 23
Groups: header, 8

ii. *Coefficients and statistics for fixed effects*

Fixed Effects	**Estimate**	**SE**	**df**	**t value**	**Pr(>|t|)**
Intercept	-15.31	0.375	3.582	-40.82	**<0.001**
OA	-3.130	0.531	3.582	-5.900	**0.006**
OW	-2.842	0.556	4.161	-5.112	**0.006**
OA + OW	1.564	0.769	3.870	2.035	0.114

Table S2.15. Summary statistics from mixed linear model analysis of *Neoagarum fimbriatum*'s tissue $\delta^{13}C$ values by treatment in winter season experiment. Formula: *N. fimbriatum* $\delta^{13}C$ ~ pH * temperature + (1|header)

i. *Variance components for random effects*

Groups	**Variance**	**Std. Dev.**
header	0.208	0.456
residual	0.404	0.635

Number of observations: 24
Groups: header, 8

ii. *Coefficients and statistics for fixed effects*

Fixed Effects	**Estimate**	**SE**	**df**	**t value**	**Pr(>|t|)**
Intercept	-28.77	0.414	4	-69.52	**<0.001**
OA	-4.073	0.585	4	-6.959	**0.002**
OW	-0.737	0.585	4	-1.258	0.277
OA + OW	1.315	0.828	4	1.589	0.187

Table S2.16. Summary statistics from mixed linear model analysis of *Neoagarum fimbriatum*'s tissue $\delta^{13}C$ values by treatment in summer season experiment. Formula: *N. fimbriatum* $\delta^{13}C$ ~ pH * temperature + (1|header)

i. *Variance components for random effects*

Groups	**Variance**	**Std. Dev.**
header	0.236	0.486
residual	0.454	0.674

Number of observations: 24
Groups: header, 8

ii. *Coefficients and statistics for fixed effects*

Fixed Effects	**Estimate**	**SE**	**df**	**t value**	**Pr(>|t|)**
Intercept	-17.03	0.440	4	-38.71	**<0.001**
OA	-4.903	0.622	4	-7.880	**0.001**
OW	-0.325	0.622	4	-0.522	0.629
OA + OW	0.958	0.880	4	1.089	0.337

Table S2.17. Summary statistics from mixed linear model analysis of *Macrocystis pyrifera*'s tissue $\delta^{13}C$ values by treatment in winter season experiment.
Formula: *M. pyrifera* $\delta^{13}C$ ~ pH * temperature + (1|header)

i. *Variance components for random effects*

Groups	**Variance**	**Std. Dev.**
header	0.000	0.000
residual	4.927	2.168

Number of observations: 23
Groups: header, 8

ii. *Coefficients and statistics for fixed effects*

Fixed Effects	**Estimate**	**SE**	**df**	**t value**	**Pr(>|t|)**
Intercept	-25.62	0.906	18	-28.27	**<0.001**
OA	0.070	1.282	18	0.055	0.957
OW	0.663	1.282	18	0.518	0.611
OA + OW	-2.443	1.922	18	-1.271	0.220

Table S2.18. Summary statistics from mixed linear model analysis of *Macrocystis pyrifera*'s tissue $\delta^{13}C$ values by treatment in summer season experiment.
Formula: *M. pyrifera* $\delta^{13}C$ ~ pH * temperature + (1|header)

i. *Variance components for random effects*

Groups	**Variance**	**Std. Dev.**
header	0.297	0.545
residual	0.591	0.769

Number of observations: 24
Groups: header, 8

ii. *Coefficients and statistics for fixed effects*

Fixed Effects	**Estimate**	**SE**	**df**	**t value**	**Pr(>|t|)**
Intercept	-17.04	0.497	4	-34.30	**<0.001**
OA	-3.362	0.703	4	-4.784	**0.009**
OW	-0.702	0.703	4	-0.999	0.374
OA + OW	0.988	0.994	4	0.995	0.376

Table S2.19. Summary statistics from analysis of the relative consumption of *H. nigripes* by pH and temperature treatment and seasonal experiment.

i. Two-way ANOVA results for relative consumption

Source	**SS**	**MSE**	**DF**	**F value**	**Pr(>F)**
Treatment	0.831	0.831	1	4.571	**0.036**
Season	1.245	1.245	1	6.848	**0.011**
Treatment:Season	0.720	0.720	1	3.964	**0.051**

ii. Tukey's post-hoc tests comparing the effects of seasonal experiment and combined pH and temperature treatment on relative consumption

Condition1	**Condition2**	**Mean diff**	**95% CI lower**	**95% CI upper**	**P_{tukey}**
Summer OW+OA	*Summer Control*	0.360	0.036	0.685	**0.024**
Winter Control	*Summer Control*	-0.062	-0.485	0.361	0.980
Winter OW+OA	*Summer Control*	-0.146	-0.556	0.263	0.782
Winter Control	*Summer OW+OA*	-0.423	-0.846	0.000	**0.050**
Winter OW+OA	*Summer OW+OA*	-0.507	-0.916	-0.098	**0.009**
Winter OW+OA	*Winter Control*	-0.084	-0.575	0.407	0.969

Table S2.20. Summary statistics from analysis of the relative consumption of *N. fimbriatum* by pH and temperature treatment and seasonal experiment.

i. Two-way ANOVA results for relative consumption

Source	**SS**	**MSE**	**DF**	**F value**	**Pr(>F)**
Treatment	0.001	0.001	1	0.011	0.915
Season	0.163	0.163	1	3.475	0.067
Treatment:Season	0.067	0.067	1	1.421	0.238

Appendix 3: Supplementary Material for Chapter 3

Figure S3.1. Map of rocky reef sites in Sitka Sound, Alaska used in monitoring of seasonal benthic light availability (Breast Is., Harris Is., Samsing Pinnacle, Sandy Cove; 2017-2020), collection of coralline algae for species verification and experiments (Marshall Is.), and in situ study of coralline algal growth rates (Harris Is., 2018-2019).

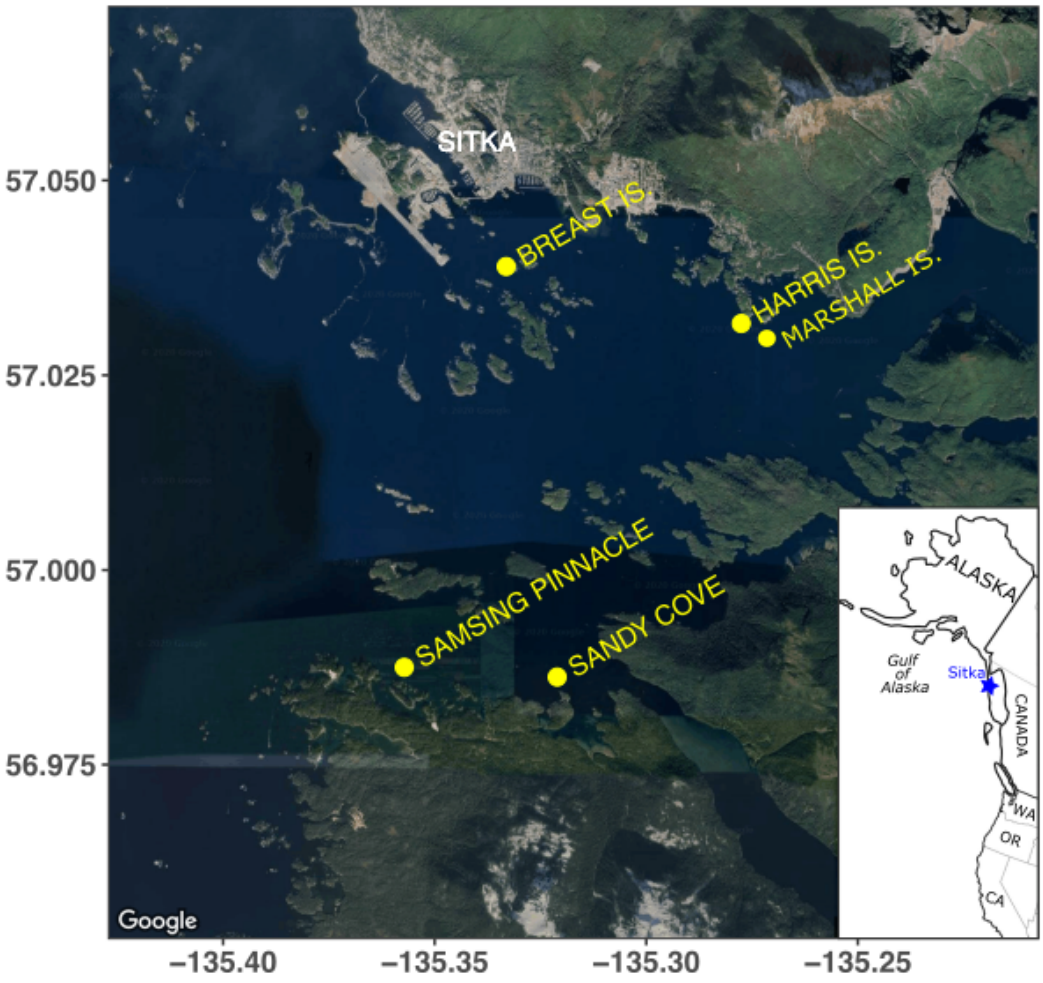

Figure S3.2. Design of the coralline algal laboratory experiment (A) and examples of individuals from either coralline algal morphotype positioned on stands with and without associated *Cryptopleura* (B). A) Incoming seawater from Sitka Sound was first routed into two main sumps, one of which was kept at ambient pH and the other was bubbled continuously with dissolved carbon dioxide gas to decrease pH. Seawater from both sumps was routed into header buckets (n=9) where mixing was controlled via a feedback loop between pH sensors, controllers, and solenoid valves to achieve pre-programmed pH setpoints for experimental treatments (n=3 headers/pH treatment). From each header bucket, seawater flowed into two experimental aquaria assigned either a winter or summer light regime. Each aquaria contained a random arrangement of four *B. orbigniana* ("BO") and four *Crusticorallina* ("C_{sp}") individuals, with half of the individuals within each coralline genus paired with *Cryptopleura ruprechtiana* ("CR"; indicated by red squares). B) Examples of the four within-aquaria red algal species combinations. Individuals were elevated on PVC stands (5cm diameter) to maximize exposure to within-aquaria water flow.

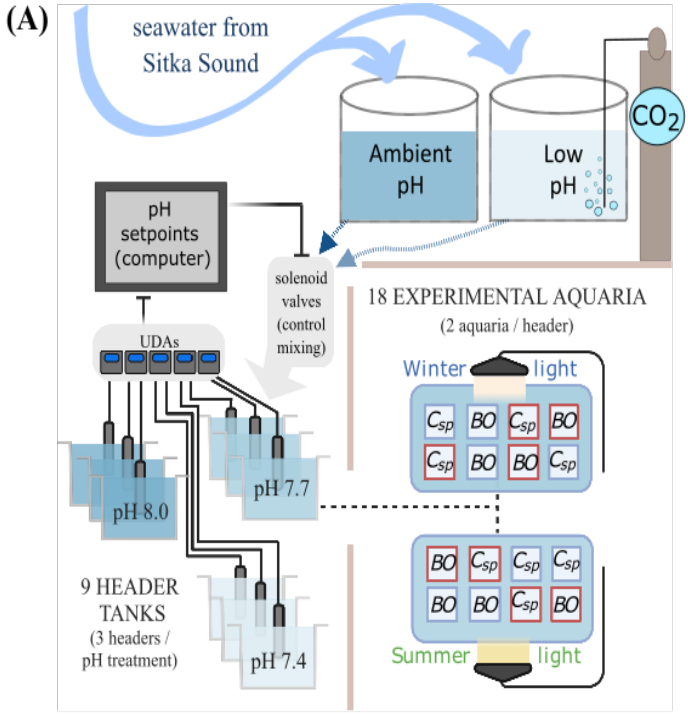

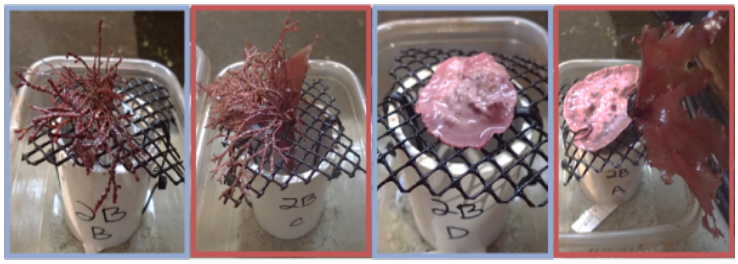

Figure S3.3. Relative growth rate (RGR_{net}) of *Cryptopleura ruprechtiana* exposed to different treatment combinations of pH and light regime during a month-long laboratory experiment (n=12 individuals treatment^{-1}). Lower case letters denote significant differences among treatments.

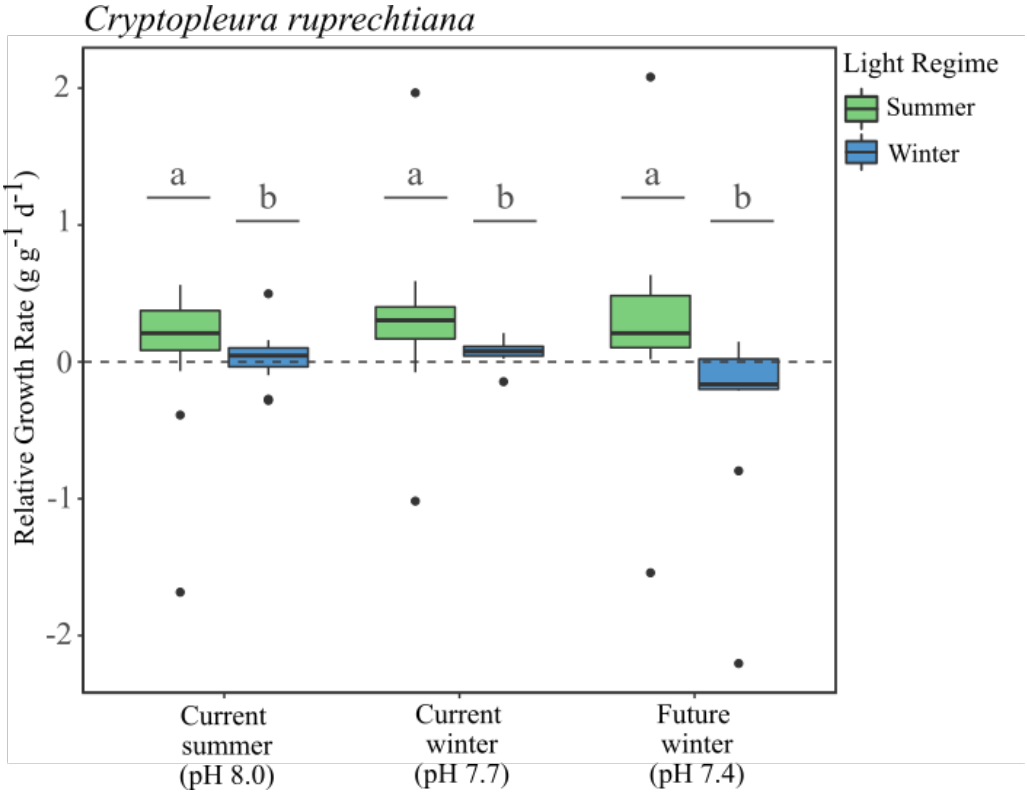

Table S3.1. List of voucher specimens deposited in the University of North Carolina, Chapel Hill herbarium (NCU) with accession number, collection data, and GenBank accession number of the *rbc*L 694 base pair sequence for each.

Taxon Name	Herbarium Accession No.	Collection Data	GenBank Accession No. (*rbc*L)
Bossiella orbigniana	NCU 673983	Marshall Island, Sitka, 57.031844 N, 135.272729 W, 5.viii.2017, on rock reef with *Macrocystis pyrifera*, leg. Lauren Bell	OK430853
Bossiella orbigniana	NCU 673984	Marshall Island, Sitka, 57.031844 N, 135.272729 W, 5.viii.2017, on rock reef with *Macrocystis pyrifera*, leg. Lauren Bell	OK430852
Bossiella orbigniana	NCU 673985	Marshall Island, Sitka, 57.031844 N, 135.272729 W, 5.viii.2017, on rock reef with *Macrocystis pyrifera*, leg. Lauren Bell	OK430857
Bossiella orbigniana	NCU 673986	Marshall Island, Sitka, 57.031844 N, 135.272729 W, 5.viii.2017, on rock reef with *Macrocystis pyrifera*, leg. Lauren Bell	OK430855
Bossiella orbigniana	NCU 673987	Marshall Island, Sitka, 57.031844 N, 135.272729 W, 5.viii.2017, on rock reef with *Macrocystis pyrifera*, leg. Lauren Bell	OK430854
Bossiella orbigniana	NCU 673988	Marshall Island, Sitka, 57.031844 N, 135.272729 W, 5.viii.2017, on rock reef with *Macrocystis pyrifera*, leg. Lauren Bell	OK430858
Bossiella orbigniana	NCU 673989	Marshall Island, Sitka, 57.031844 N, 135.272729 W, 5.viii.2017, on rock reef with *Macrocystis pyrifera*, leg. Lauren Bell	OK430859
Bossiella orbigniana	NCU 673990	Marshall Island, Sitka, 57.031844 N, 135.272729 W, 5.viii.2017, on rock reef with *Macrocystis pyrifera*, leg. Lauren Bell	OK430860
Bossiella orbigniana	NCU 673991	Marshall Island, Sitka, 57.031844 N, 135.272729 W, 5.viii.2017, on rock reef with *Macrocystis pyrifera*, leg. Lauren Bell	OK430861
Bossiella orbigniana	NCU 673992	Marshall Island, Sitka, 57.031844 N, 135.272729 W, 5.viii.2017, on rock reef with *Macrocystis pyrifera*, leg. Lauren Bell	OK430856
Bossiella orbigniana	NCU 673993	Marshall Island, Sitka, 57.031844 N, 135.272729 W, 5.viii.2017, on rock reef with *Macrocystis pyrifera*, leg. Lauren Bell	OK430862
Bossiella orbigniana	NCU 673994	Marshall Island, Sitka, 57.031844 N, 135.272729 W, 5.viii.2017, on rock reef with *Macrocystis pyrifera*, leg. Lauren Bell	OK430863
Crusticorallina adhaerens	NCU 673995	Marshall Island, Sitka, 57.031844 N, 135.272729 W, 5.viii.2017, on rock reef with *Macrocystis pyrifera*, leg. Lauren Bell	OK430869
Crusticorallina muricata	NCU 673996	Marshall Island, Sitka, 57.031844 N, 135.272729 W, 5.viii.2017, on rock reef with *Macrocystis pyrifera*, leg. Lauren Bell	OK430864
Crusticorallina muricata	NCU 674003	Marshall Island, Sitka, 57.031844 N, 135.272729 W, 5.viii.2017, on rock reef with *Macrocystis pyrifera*, leg. Lauren Bell	OK430865
Crusticorallina muricata	NCU 674004	Marshall Island, Sitka, 57.031844 N, 135.272729 W, 5.viii.2017, on rock reef with *Macrocystis pyrifera*, leg. Lauren Bell	OK430866

Crusticorallina muricata	NCU 674005	Marshall Island, Sitka, 57.031844 N, 135.272729 W, 5.viii.2017, on rock reef with *Macrocystis pyrifera*, leg. Lauren Bell	OK430867
Crusticorallina muricata	NCU 674006	Marshall Island, Sitka, 57.031844 N, 135.272729 W, 5.viii.2017, on rock reef with *Macrocystis pyrifera*, leg. Lauren Bell	OK430868
Crusticorallina painei	NCU 673997	Marshall Island, Sitka, 57.031844 N, 135.272729 W, 5.viii.2017, on rock reef with *Macrocystis pyrifera*, leg. Lauren Bell	OK430870
Crusticorallina painei	NCU 673998	Marshall Island, Sitka, 57.031844 N, 135.272729 W, 5.viii.2017, on rock reef with *Macrocystis pyrifera*, leg. Lauren Bell	OK430871
Crusticorallina painei	NCU 673999	Marshall Island, Sitka, 57.031844 N, 135.272729 W, 5.viii.2017, on rock reef with *Macrocystis pyrifera*, leg. Lauren Bell	OK430872
Crusticorallina painei	NCU 674000	Marshall Island, Sitka, 57.031844 N, 135.272729 W, 5.viii.2017, on rock reef with *Macrocystis pyrifera*, leg. Lauren Bell	OK430873
Crusticorallina painei	NCU 674001	Marshall Island, Sitka, 57.031844 N, 135.272729 W, 5.viii.2017, on rock reef with *Macrocystis pyrifera*, leg. Lauren Bell	OK430874
Crusticorallina painei	NCU 674002	Marshall Island, Sitka, 57.031844 N, 135.272729 W, 5.viii.2017, on rock reef with *Macrocystis pyrifera*, leg. Lauren Bell	OK430875
Crusticorallina painei	NCU 674007	Marshall Island, Sitka, 57.031844 N, 135.272729 W, 5.viii.2017, on rock reef with *Macrocystis pyrifera*, leg. Lauren Bell	OK430876
Crusticorallina painei	NCU 674008	Marshall Island, Sitka, 57.031844 N, 135.272729 W, 5.viii.2017, on rock reef with *Macrocystis pyrifera*, leg. Lauren Bell	OK430877

Table S3.2. Results from three Welch's ANOVAs comparing mean coralline algal linear extension rates (mm d^{-1}) in the field by season for each morphotype, and between morphotypes with adjusted p-values for multiple comparisons using Bonferroni corrections.

One-way test	**df_{num}**	**df_{den}**	**F**	**adjusted p-value**
winter vs. summer *(Crusticorallina* spp.)	1	14.967	0.002	1.000
winter vs. summer (*B. orbigniana)*	1	12.957	6.213	0.054
Crusticorallina spp vs. *B. orbigniana* (seasons combined)	1	61.999	79.606	**<0.001***

Table S3.3. Summary statistics from mixed linear model analysis of *B. orbigniana* relative net calcification rate over the duration of the laboratory experiment (RCR_{net}). Formula: *B. orbigniana* RCR_{net} ~ pH * light regime * association with *C. ruprechtiana* + (1|header/aquaria)

i. *Variance components for random effects*

Groups	Variance	Std. Dev.
aquaria:header	0.000	0.000
header	0.000	0.000
residual	0.028	0.168

Number of observations: 53
Groups: aquaria:header, 18; header, 9

ii. *ANOVA results from the mixed linear model*

Source	**SS**	**MSE**	**numDF**	**denDF**	**F value**	**Pr(>F)**
pH	0.551	0.276	2	41	9.72	**<0.001***
light regime	0.059	0.059	1	41	2.08	0.157
C. ruprechtiana association	0.001	0.001	1	41	0.04	0.837
pH:light	0.046	0.023	2	41	0.80	0.455
pH:assoc.	0.011	0.006	2	41	0.20	0.819
light:assoc.	<0.001	<0.001	1	41	0.01	0.934
pH:light:assoc.	0.024	0.012	2	41	0.42	0.662

iii. *Statistics from Tukey's post-hoc tests comparing the effects of pH levels on* B. orbigniana *RCR_{net}.*

Condition1	**Condition2**	**estimate**	**SE**	**z value**	**Pr(>|z|)**
Current summer (8.0)	Current winter (7.7)	-0.147	0.087	-1.70	0.120
	Future winter (7.4)	-0.281	0.075	-3.73	**<0.001***
Current winter (7.7)	Future winter (7.4)	-0.134	0.087	-1.54	0.160

Table S3.4. Summary statistics from mixed linear model analysis of *Crusticorallina* spp. relative net calcification rate over the duration of the laboratory experiment (RCR_{net}).
Formula: *Crusticorallina* spp. RCR_{net} ~ pH * light regime * association with *C. ruprechtiana* + (1|header/aquaria)
i. *Variance components for random effects*

Groups	Variance	Std. Dev.
aquaria:header	0.0001	0.010
header	0.0002	0.013
residual	0.004	0.060

Number of observations: 61
Groups: aquaria:header, 18; header, 9

ii. *ANOVA results from the mixed linear model*

Source	**SS**	**MSE**	**numDF**	**denDF**	**F value**	**Pr(>F)**
pH	0.263	0.132	2	4.719	36.715	**0.001***
light regime	0.007	0.006	1	4.661	1.820	0.239
C. ruprechtiana association	0.010	0.010	1	37.547	2.805	0.102
pH:light	0.002	0.001	2	4.636	0.300	0.754
pH:assoc.	0.005	0.002	2	37.488	0.634	0.526
light:assoc.	0.020	0.020	1	37.547	5.503	**0.024***
pH:light:assoc.	0.015	0.007	2	37.488	2.076	0.140

iii. *Statistics from Tukey's post-hoc tests comparing the effects of pH levels on* Crusticorallina *spp.* RCR_{net}.

Condition1	**Condition2**	**estimate**	**SE**	**z value**	**Pr(>|z|)**
Current summer (8.0)	Current winter (7.7)	-0.028	0.029	-0.97	0.350
	Future winter (7.4)	-0.205	0.033	-6.13	**<0.001***
Current winter (7.7)	Future winter (7.4)	-0.177	0.032	-5.45	**<0.001***

iv. *Statistics from Tukey's post-hoc tests comparing the effects of interactive levels of light regime and* C. ruprechtiana *association on* Crusticorallina *spp.* RCR_{net}.

Condition1	**Condition2**	**estimate**	**SE**	**t value**	**Pr(>|t|)**
summer light, no CR	winter light, no CR	0.059	0.023	2.55	0.077
	summer light, w/ CR	0.063	0.023	2.76	**0.050***
	winter light, w/ CR	0.049	0.023	2.10	0.183
winter light, no CR	summer light, w/ CR	0.004	0.023	0.17	0.998
	winter light, w/ CR	-0.011	0.022	-0.49	0.961
summer light, w/ CR	winter light, w/ CR	-0.015	0.023	-0.64	0.916

Note: CR = Cryptopleura ruprechtiana; w/ = paired with; no = no association

Table S3.5. Summary statistics from mixed linear model analysis of *B. orbigniana* short-term net calcification rate during total alkalinity incubations (G_{net}).
Formula: *B. orbigniana* G_{net} ~ pH * light regime * association with *C. ruprechtiana* + (1|header/aquaria)

i. *Variance components for random effects*

Groups	Variance	Std. Dev.
aquaria:header	0.000	0.000
header	0.000	0.000
residual	1.700	1.310

Number of observations: 34
Groups: aquaria:header, 11; header, 6

ii. *ANOVA results from the mixed linear model*

Source	**SS**	**MSE**	**numDF**	**denDF**	**F value**	**Pr(>F)**
pH	25.080	12.540	2	22	7.36	**0.004***
light regime	0.420	0.430	1	22	0.25	0.621
C. ruprechtiana association	10.05	10.040	1	22	5.89	**0.024**
pH:light	0.350	0.180	2	22	0.10	0.902
pH:assoc.	4.650	2.330	2	22	1.36	0.276
light:assoc.	0.500	0.500	1	22	0.29	0.593
pH:light:assoc.	2.660	1.330	2	22	0.78	0.471

iii. *Statistics from Tukey's post-hoc tests comparing the effects of pH levels on* B. orbigniana *G_{net}.*

Condition1	**Condition2**	**estimate**	**SE**	**z value**	**Pr(>|z|)**
Current summer (8.0)	Current winter (7.7)	1.239	0.730	1.70	0.999
	Future winter (7.4)	-1.163	0.754	-1.54	0.150
Current winter (7.7)	Future winter (7.4)	-2.402	0.730	-3.29	**0.001***

Table S3.6. Summary statistics from mixed linear model analysis of *Crusticorallina* spp. short-term net calcification rate during total alkalinity incubations (G_{net}). Formula: *Crusticorallina* spp. G_{net} ~ pH * light regime * association with *C. ruprechtiana* + (1|header/aquaria)

i. *Variance components for random effects*

Groups	Variance	Std. Dev.
aquaria:header	0.199	0.447
header	0.130	0.369
residual	0.216	0.465

Number of observations: 27
Groups: aquaria:header, 10; header, 5

ii. ANOVA results from the mixed linear model

Source	**SS**	**MSE**	**numDF**	**denDF**	**F value**	**Pr(>F)**
pH	0.435	0.218	2	2.24	1.01	0.487
light regime	1.796	1.796	1	2.64	8.31	0.074
C. ruprechtiana association	0.016	0.016	1	12	0.08	0.787
pH:light	0.338	0.169	2	2.54	0.78	0.544
pH:assoc.	0.537	0.269	2	12	1.24	0.323
light:assoc.	0.107	0.107	1	12	0.49	0.496
pH:light:assoc.	0.228	0.228	1	12	1.06	0.325

Table S3.7. Summary statistics from mixed linear model analysis of *Cryptopleura ruprechtiana* relative net growth rate over the duration of the laboratory experiment (RGR_{net}).
Formula: *C. ruprechtiana* RCR_{net} ~ pH * light regime + (1|header/aquaria)
i. *Variance components for random effects*

Groups	Variance	Std. Dev.
aquaria:header	0.000	0.000
header	0.000	0.000
residual	0.328	0.573

Number of observations: 70
Groups: aquaria:header, 18; header, 9

ii.ANOVA results from the mixed linear model

Source	**SS**	**MSE**	**numDF**	**denDF**	**F value**	**Pr(>F)**
pH	0.582	0.291	2	64	0.89	0.417
light regime	1.456	1.456	1	64	4.44	**0.039***
pH:light	0.914	0.457	2	64	1.39	0.256

Table S3.8. Statistics of parameter estimates for photosynthesis-irradiance curves for *B. orbigniana* and *Crusticorallina* spp., pooled across all treatments by morphotype. Formula: Net production ~(Pmax) * (1 - exp(-((alpha) * I)/(Pmax))) * (exp(-((beta) * I)/(Pmax)))

	Parameter	Estimate	SE	t-value	Pr(>|t|)
Bossiella orbigniana	Pmax	23.793	5.906	4.029	**<0.001***
	alpha	0.135	0.009	15.209	**<0.001***
	beta	0.050	0.022	2.295	**0.023***
Crusticorallina spp.	Pmax	16.918	0.421	40.170	**<0.001***
	alpha	0.039	0.002	22.090	**<0.001***
	beta	0.070†			

† insufficient data to constrain beta parameter for Crusticorallina *spp. Beta of 0.07 used to estimate Pmax and alpha parameters for curve fit.*

Table S3.9. Statistics of parameter estimates for *Cryptopleura ruprechtiana* photosynthesis-irradiance curves, by pH treatment. The final row indicates the significant effect of pH (as represented in model by parameter "C" multiplied by a binary pH_code representing pH treatment) on the Pmax parameter.
Formula: Net production ~(Pmax+(C*pH_code)) * (1 - exp(-((alpha) * I)/(Pmax+(C*pH_code)))) * (exp(-((beta) * I)/(Pmax+(C*pH_code))))

	Parameter	Estimate	SE	t-value	Pr(>|t|)
C. ruprechtiana (pH 7.4) (pH_code = 1)	Pmax	38.246	4.631	8.259	**<0.001***
	alpha	0.597	0.066	9.107	**<0.001***
	beta	0.070	0.020	3.561	**<0.001***
C. ruprechtiana (pH 8.0) (pH_code = 0)	Pmax	23.928	3.588	6.668	**<0.001***
	alpha	0.471	0.087	5.431	**<0.001***
	beta	0.035	0.014	2.478	**0.019***
pH effect on Pmax	*parameter "C"*	*7.232*	*1.330*	*5.439*	***<0.001****

Table S3.10. Statistics from an F test comparing modeled P-E curves for *C. ruprechtiana* by pH treatment.
Formula: Net production ~(Pmax) * (1 - exp(-((alpha) * I)/(Pmax))) * (exp(-((beta) * I)/(Pmax)))
Group parameters used for comparison: *C.ruprechtiana* (pH 7.4) & *C. ruprechtiana* (pH 8.0)

	Res.df	**Res. SS**	**df**	**SS**	**F-value**	**Pr(>F)**
null model (pooled data)	101	2073.2				
model parameterized by group	98	1491.4	3	581.720	12.742	**<0.001***

REFERENCES

Ainsworth, E. A., & Long, S. P. (2004). What have we learned from 15 years of free-air CO_2 enrichment (FACE)? A meta-analytic review of the responses of photosynthesis, canopy properties and plant production to rising CO_2. *New Phytologist, 165*, 351–372. https://doi.org/10.1111/j.1469-8137.2004.01224.x

Alstyne, K. L. V., McCarthy III, J. J., Hustead, C. L., & Kearns, L. J. (1999). Phlorotannin allocation among tissues of Northeastern Pacific kelps and rockweeds. *Journal of Phycology*, *35*, 483–92. https://doi.org/10.1046/j.1529-8817.1999.3530483.x

Amsler, C. D., Iken, K., McClintock, J. B., Amsler, M. O., Peters, K. J., Hubbard, J. M., Furrow, F. B., & Baker, B. J. (2005). Comprehensive evaluation of the palatability and chemical defenses of subtidal macroalgae from the Antarctic Peninsula. *Marine Ecology Progress Series, 294*, 141–159. https://doi.org/10.3354/meps294141

AMTF. (2018). *Alaska Mariculture Development Plan*. Alaska Mariculture Task Force, State of Alaska, 82 pp.

Andersen, G. S., Pedersen, M. F., & Nielsen, S. L. (2013). Temperature acclimation and heat tolerance of photosynthesis in Norwegian *Saccharina latissima* (Laminariales, Phaeophyceae). *Journal of Phycology, 49*, 689–700. https://doi.org/10.1111/jpy.12077

Andersson A. J., Mackenzie, F.T., & Bates, N.R. (2008). Life on the margin: implications of ocean acidification on Mg-calcite, high latitude and cold-water marine calcifiers, *Marine Ecology Progress Series, 373*, 265–273. https://doi.org/10.3354/meps07639

Arnold, T., Mealey, C., Leahey, H., Miller, A. W., Hall-Spencer, J. M., Milazzo, M., & Maers, K. (2012). Ocean acidification and the loss of phenolic substances in marine plants. *PLoS ONE, 7*(4), e35107. https://doi.org/10.1371/journal.pone.0035107

Attwood, C. G., Lucas, M. I., Probyn, T. A., McQuaid, C. D., & Fielding, P. J. (1991). Production and standing stocks of the kelp *Macrocystis laevis* Hay at the Prince Edward Islands, Subantarctic. *Polar Biology*, *11*, 129–33. https://doi.org/10.1007/BF00234275

Bach, L. T., Tamsitt, V., Gower, J., Hurd, C. L., Raven, J. A., & Boyd, P. W. (2021). Testing the climate intervention potential of ocean afforestation using the Great Atlantic *Sargassum* Belt. *Nature Commun*ications, *12*, 2556. https://doi.org/10.1038/s41467-021-22837-2

Barner A. K., Chan, F., Hettinger, A., Hacker, S. D., Marshall, K., & Menge, B. A. (2018). Generality in multispecies responses to ocean acidification revealed through multiple hypothesis testing. *Global Change Biology, 24*, 4464–4477. https://doi.org/10.1111/gcb.14372

Becheler, R., Haverbeck, D., Clerc, C., Montecinos, G., Valero, M., Mansilla, A., & Faugeron, S. (2022). Variation in thermal tolerance of the giant kelp's gametophytes: suitability of habitat, population quality or local adaptation? *Frontiers in Marine Science, 9*, 802535. https://doi.org/10.3389/fmars.2022.802535

Beer D. D., & Larkum, A.W.D. (2001). Photosynthesis and calcification in the calcifying algae *Halimeda discoidea* studied with microsensors. *Plant, Cell & Environment, 24*, 1209–1217. https://doi.org/10.1046/j.1365-3040.2001.00772.x

Bell, L. E., Gómez, J. B., Donham, E., Steller, D. L., Gabrielson, P. W., & Kroeker, K. J. (2022). High-latitude calcified coralline algae exhibit seasonal vulnerability to acidification despite physical proximity to a non-calcified alga. *Climate Change Ecology*, *3*, 100049. https://doi.org/10.1016/j.ecochg.2022.100049

Bell, L. E., & Kroeker, K. J. (2022). Standing crop, turnover, and production dynamics of *Macrocystis pyrifera* and understory species *Hedophyllum nigripes* and *Neoagarum fimbriatum* in high latitude giant kelp forests. *Journal of Phycology, 58*(6), 773–788. https://doi.org/10.1111/jpy.13291

Bergstrom E., Ordoñez, A., Ho, M., Hurd, C., Fry, B., & Diaz-Pulido, G. (2020). Inorganic carbon uptake strategies in coralline algae: plasticity across evolutionary lineages under ocean acidification and warming. *Marine Environmental Research, 161*, 105107. https://doi.org/10.1016/j.marenvres.2020.105107

Bernhardt, J. R., & Leslie, H. M. (2013). Resilience to climate change in coastal marine ecosystems. *Annual Review of Marine Sci*ence, *5*, 371–92. https://doi.org/10.1146/annurev-marine-121211-172411

Bilan, M. I., & Usov, A. I. (2001). Polysaccharides of calcareous algae and their effect on the calcification process. *Russian Journal of Bioorganic Chemistry, 27*(1), 2–16. https://doi.org/10.1023/A:1009584516443

Bolton, J. J. (2016). What is aquatic botany? - And why algae are plants: the importance of non-taxonomic terms for groups of organisms. *Aquatic Bot*any, 132, 1–4. https://doi.org/10.1016/j.aquabot.2016.02.006

Bresnahan, P. J., Martz, T. R., Takeshita, Y., Johnson, K. S., & LaShomb, M. (2014). Best practices for autonomous measurement of seawater pH with the Honeywell Durafet. *Methods in Oceanography, 9*, 44–60. https://doi.org/10.1016/j.mio.2014.08.003

Briggs, A.A., & Carpenter, R.C. (2019). Contrasting responses of photosynthesis and photochemical efficiency to ocean acidification under different light environments in a calcifying alga. *Science Reports, 9*, 3986. https://doi.org/10.1038/s41598-019-40620-8

Britton, D., Cornwall, C.E., Revill, A.T., Hurd, C.L., & Johnson, C.R. (2016). Ocean acidification reverses the positive effects of seawater pH fluctuations on growth and photosynthesis of the habitat-forming kelp, *Ecklonia radiata*. *Science Reports, 6*, 26036. https://doi.org/10.1038/srep26036

Britton, D., Schmid, M., Noisette, F., Havenhand, J. N., Paine, E. R., McGraw, C. M., Revill, A. T., Virtue, P., Nichols, P. D., Mundy, C. N., & Hurd, C. L. (2020). Adjustments in fatty acid composition is a mechanism that can explain resilience to marine heatwaves and future ocean conditions in the habitat-forming seaweed *Phyllospora comosa* (Labillardière) C.Agardh. *Global Change Biology, 26*(6), 3512–3524. https://doi.org/10.1111/gcb.15052

Brown, M. B., Edwards, M. S., & Kim, K. Y. (2014). Effects of climate change on the physiology of giant kelp, *Macrocystis pyrifera*, and grazing by purple urchin, *Strongylocentrotus purpuratus. Algae, 29*(3), 203–215. http://dx.doi.org/10.4490/algae.2014.29.3.203

Brown, M. T., Nyman, M. A., Keogh, J. A., & Chin, N. K. M. (1997). Seasonal growth of the giant kelp *Macrocystis pyrifera* in New Zealand. *Marine Biology, 129*, 417–24. https://doi.org/10.1007/s002270050182

Bruno, J. F., Carr, L. A., & O'Connor, M. I. (2015). Exploring the role of temperature in the ocean through metabolic scaling. *Ecology, 96*, 3126–3140. https://doi.org/10.1890/14-1954.1

Brzezinski, M. A, Reed, D. C., Harrer, S., Rassweiler, A., Melack, J. M., Goodridge, B. M., & Dugan, J. E. (2013). Multiple sources and forms of nitrogen sustain year-round kelp growth on the inner continental shelf of the Santa Barbara Channel. *Oceanography*, 26, 114–23. https://www.jstor.org/stable/24862072

Bulleri, F. (2006). Duration of overgrowth affects survival of encrusting coralline algae. *Marine Ecology Progress Series, 321*, 79–85. https://doi.org/10.3354/meps321079

Burek, K. A., Gulland, F. M. D., & O'Hara, T. M. (2008). Effects of climate change on arctic marine mammal health. *Ecological Applications, 18*(2), S126–S134. https://doi.org/10.1890/06-0553.1

Burnell, O. W., Russell, B. D., Irving, A. D., & Connell, S. D. (2014). Seagrass response to CO_2 contingent on epiphytic algae: indirect effects can overwhelm direct effects. *Oecologia, 176*, 871–882. https://doi.org/10.1007/s00442-014-3054-z

Burt, J. M., Tinker, M. T., Okamoto, D. K., Demes, K. W., Holmes, K., & Salomon, A. K. (2018). Sudden collapse of a mesopredator reveals its complementary role in mediating rocky reef regime shifts. *Proceedings of the Royal Society B, 285*, 20180553. https://doi.org/10.1098/rspb.2018.0553

Buschmann, A. H., Camus, C., Infante, J., Neori, A., Israel, Á., Hernàndez-González, M. C., Pereda, S. V., Gomez-Pinchetti, J. L., Golberg, A., Tadmor-Shalev, N., Critchley, & A. T. (2017). Seaweed production: overview of the global state of exploitation, farming and emerging research activity. *European Journal of Phycology, 52*(4), 391–406. http://doi.org/10.1080/09670262.2017.1365175

Cai, J., Lovatelli, A., Aguilar-Manjarrez, J., Cornish, L., Dabbadie, L., Desrochers, A., Diffey, S., Garrido Gamarro, E., Geehan, J., Hurtado, A., Lucente, D., Mair, G., Miao, W., Potin, P., Przybyla, C., Reantaso, M., Roubach, R., Tauati, M., & Yuan, X. (2021). Seaweeds and microalgae: an overview for unlocking their potential in global aquaculture development. FAO Fisheries and Aquaculture Circular No. 1229. Rome, FAO. https://doi.org/10.4060/cb5670en

Calvin, N. I., & Ellis, R. J. (1981). Growth of subtidal *Laminaria groenlandica* in Southeastern Alaska. *Botanica Marina*, *24*, 107–14. https://doi.org/10.1515/botm.1981.24.2.107

Campanyà-Llovet, N., Snelgrove, P. V. R., & Parrish, C. C. (2017). Rethinking the importance of food quality in marine benthic food webs. *Progress in Oceanography, 156*, 240–251. https://doi.org/10.1016/j.pocean.2017.07.006

Castorani, M. C. N., Harrer, S. L., Miller, R. J., & Reed, D. C. (2021). Disturbance structures canopy and understory productivity along an environmental gradient. *Ecology Lett*ers, *24*, 2192–206. https://doi.org/10.1111/ele.13849

Cavicchioli, R., Ripple, W. J., Timmis, K. N., Azam, F., Bakken, L. R., Baylis, M., Behrenfeld, M. J., Boetius, A., Boyd, P. W., Classen, A. T., Crowther, T. W., Danovaro, R., Foreman, C. M., Huisman, J., Hutchins, D. A., Jansson, J. K., Karl, D. M., Koskella, B., Mark Welch, D. B., Martiny, J. B. H., Moran, M. A., Orphan, V. J., Reay, D. S., Remais, J. V., Rich, V. I., Singh, B. K., Stein,

L. Y., Stewart, F. J., Sullivan, M. B., van Oppen, M. J. H., Weaver, S. C., Webb, E. A., Webster, N. S. (2019). Scientists' warning to humanity: microorganisms and climate change. *Nature Reviews Microbiology, 17*, 569–586. https://doi.org/10.1038/s41579-019-0222-5

Cebrian, J., Shurin, J. B., Borer, E. T., Cardinale, B. J., Ngai, J. T., Smith, M. D., & Fagan, W. F. (2009). Producer nutritional quality controls ecosystem trophic structure. *PLoS ONE, 4*(3), e4929. https://doi.org/10.1371/journal.pone.0004929

Cedeno, T. H., Brzezinski, M. A., Miller, R. J., & Reed, D. C. (2021). An evaluation of surge uptake capability in the giant kelp (*Macrocystis pyrifera*) in response to pulses of three different forms of nitrogen. *Marine Biology, 168*(11), 166. https://doi.org/10.1007/s00227-021-03975-z

Celis-Plá, P. S. M., Hall-Spencer, J. M., Horta, P. A., Milazzo, M., Korbee, N., Cornwall, C. E., & Figueroa, F. L. (2015). Macroalgal responses to ocean acidification depend on nutrient and light levels. *Frontiers in Marine Science, 2*, 26. https://doi.org/10.3389/fmars.2015.00026

Chan, F., Barth, J. A., Blanchette, C. A., Byrne, R. H., Chavez, F., Cheriton, O., Feely, R. A., Friederich, G., Gaylord, B., Gouhier, T., Hacker, S., Hill, T., Hofmann, G., McManus, M. A., Menge, B. A., Nielsen, K. J., Russell, A., Sanford, E., Sevadjian, J., & Washburn, L. (2017). Persistent spatial structuring of coastal ocean acidification in the California Current System. *Science Reports, 7*, 2526. https://doi.org/10.1038/s41598-017-02777-y

Chenelot, H., Jewett, S. C., & Hoberg, M. K. (2011). Macrobenthos of the nearshore Aleutian Archipelago, with emphasis on invertebrates associated with *Clathromorphum nereostratum* (Rhodophyta, Corallinaceae). *Marine Biodiversity, 41*, 413–424. https://doi.org/10.1007/s12526-010-0071-y

Cheng, L., Abraham, J., Hausfather, Z., & Trenberth, K. E. (2019). How fast are the oceans warming? *Science, 363*, 128–129. https://doi.org/10.1126/science.aav7619.

Cherry, J. E., Walker, S., Fresco, N., Trainor, S., & Tidwell, A. (2010). Impacts of climate change and variability on hydropower in southeast Alaska: planning for a robust energy future. National Oceanic and Atmospheric Administration, National Marine Fisheries Service Report, 17388. https://repository.library.noaa.gov/view/noaa/17388

Clark, R. P., Edwards, M. S., & Foster, M.S. (2004). Effects of shade from multiple kelp canopies on an understory algal assemblage. *Marine Ecology Progress Series, 267*, 107–119. https://doi.org/10.3354/meps267107

Close, S. L., Hacker, S. D., Menge, B. A., Chan, F., & Nielsen, K. J. (2020). Biogeography of macrophyte elemental composition: spatiotemporal modification of species-level traits. *Ecosystems*, 23, 1494–522. https://doi.org/10.1007/s10021-020-00484-w

Comeau S., Carpenter, R. C., & Edmunds, P. J. (2013). Coral reef calcifiers buffer their response to ocean acidification using both bicarbonate and carbonate. *Proceedings of the Royal Society B Biological Sciences, 280*, 20122374. https://doi.org/10.1098/rspb.2012.2374

Comeau S., Carpenter, R. C., & Edmunds, P. J. (2014). Effects of irradiance on the response of the coral *Acropora pulchra* and the calcifying alga *Hydrolithon reinboldii* to temperature elevation and ocean acidification. *Journal of Experimental Marine Biology and Ecology, 453*, 28–35. https://doi.org/10.1016/j.jembe.2013.12.013

Comeau S., Cornwall, C. E., Pupier, C. A., DeCarlo, T. M., Alessi, C., Trehern, R., & McCulloch, M. T. (2019). Flow-driven micro-scale pH variability affects the physiology of corals and coralline algae under ocean acidification. *Science Reports, 9*, 12829. https://doi.org/10.1038/s41598-019-49044-w

Connell, S. D., Kroeker, K. J., Fabricius, K. E., Kline, D. I., & Russell, B. D. (2013). The other ocean acidification problem: CO_2 as a resource among competitors for ecosystem dominance. *Philosophical Transactions of the Royal Society B, 368*, 20120442. http://dx.doi.org/10.1098/rstb.2012.0442

Cornwall, C. E., Boyd, P. W., McGraw, C. M., Hepburn, C. D., Pilditch, C. A., Morris, J. N., Smith, A. M., & Hurd, C. L. (2014). Diffusion boundary layers ameliorate the negative effects of ocean acidification on the temperate coralline macroalga *Arthrocardia corymbosa*. *PLoS One, 9*, e97235. https://doi.org/10.1371/journal.pone.0097235

Cornwall, C. E., Comeau, S., DeCarlo, T. M., Larcombe, E., Moore, B., Giltrow, K., Puerzer, F., D'Alexis, Q., & McCulloch, M. T. (2020). A coralline alga gains tolerance to ocean acidification over multiple generations of exposure. *Nature Climate Change, 10*, 143–146. https://doi.org/10.1038/s41558-019-0681-8

Cornwall, C. E., Comeau, S., Kornder, N. A., Perry, C. T., van Hooidonk, R., DeCarlo, T. M., Pratchett, M. S., Anderson, K.D., Browne, N., Carpenter, R., Diaz-Pulido, G., D'Olivo, J. P., Doo, S. S., Figueiredo, J., Fortunato, S. A. V., Kennedy, E., Lantz, C. A., McCulloch, M. T., González-Rivero, M., Schoepf, V., Smithers, S. G., & Lowe, R. J. (2021a). Global declines in coral reef calcium carbonate production under ocean acidification and warming. *Proceedings of the National Academy of Science, 118,* e2015265118. https://doi.org/10.1073/pnas.2015265118

Cornwall, C. E., Comeau, S., & McCulloch, M. T. (2017). Coralline algae elevate pH at the site of calcification under ocean acidification, Global Change Biology, 23, 4245–4256. https://doi.org/10.1111/gcb.13673.

Cornwall, C. E., Diaz-Pulido, G., & Comeau, S. (2019). Impacts of ocean warming on coralline algal calcification: meta-analysis, knowledge gaps, and key recommendations for future research. *Frontiers in Marine Science, 6*, 186. https://doi.org/10.3389/fmars.2019.00186

Cornwall, C. E., Harvey, B. P., Comeau, S., Cornwall, D. L., Hall-Spencer, J. M., Peña, V., Wada, S., & Porzio, L. (2021b). Understanding coralline algal responses to ocean acidification: meta-analysis and synthesis. *Global Change Biology, 28*(2), 362–374. https://doi.org/10.1111/gcb.15899

Cornwall, C. E., Hepburn, C. D., McGraw, C. M., Currie, K. I., Pilditch, C. A., Hunter, K. A., Boyd, P. W., & Hurd, C. L. (2013a). Diurnal fluctuations in seawater pH influence the response of a calcifying macroalga to ocean acidification. *Proceedings of the Royal Society B Biological Sciences,* 280, 20132201. https://doi.org/10.1098/rspb.2013.2201

Cornwall, C. E., Hepburn, C. D., Pilditch, C. A., & Hurd, C. L. (2013b). Concentration boundary layers around complex assemblages of macroalgae: implications for the effects of ocean acidification on understory coralline algae. *Limnology and Oceanography, 58*, 121–130. https://doi.org/10.4319/lo.2013.58.1.0121

Cornwall, C. E., Hepburn, C. D., Pritchard, D., Currie, K. I., McGraw, C. M., Hunter, K. A., & Hurd, C. L. (2012). Carbon-use strategies in macroalgae: differential responses to lowered pH and implications for ocean acidification. *Journal of Phycology, 48*(1), 137–144. https://doi.org/10.1111/j.1529-8817.2011.01085.x

Cornwall, C. E., & Hurd, C. L. (2016). Experimental design in ocean acidification research: problems and solutions. *ICES Journal of Marine Science, 73*(3), 572–581. https://doi.org/10.1093/icesjms/fsv118

Cornwall, C. E., Pilditch, C. A., Hepburn, C. D., & Hurd, C. L. (2015a). Canopy macroalgae influence understorey corallines' metabolic control of near-surface pH and oxygen concentration. *Marine Ecology Progress Series, 525*, 81–95. https://doi.org/10.3354/meps11190

Cornwall, C. E., Revill, A. T., & Hurd, C. L. (2015b). High prevalence of diffusive uptake of CO_2 by macroalgae in a temperate subtidal ecosystem. *Photosynthesis Research, 124*(2), 181–190. https://doi.org/10.1007/s11120-015-0114-0

Cruz-Rivera, E., & Hay, M. E. (2000). Can quantity replace quality? Food choice, compensatory feeding, and fitness of marine mesograzers. *Ecology, 81*(1), 201–219. https://doi.org/10.2307/177144

Dankworth, M., Heinrich, S., Fredriksen, S., & Bartsch, I. (2020). DNA barcoding and mucilage ducts in the stipe reveal the presence of *Hedophyllum nigripes* (Laminariales, Phaeophyceae) in Kongsfjorden (Spitsbergen). *Journal of Phycology, 56*(5), 1245–1254. https://doi.org/10.1111/jpy.13012

de Coninck, H., Revi, A., Babiker, M., Bertoldi, P., Buckeridge, M., Cartwright, A., Dong, W., Ford, J., Fuss, S., Hourcade, J.-C., Ley, D., Mechler, R., Newman, P., Revokatova, A., Schultz, S., Steg, L., & Sugiyama, T. (2018). Strengthening and implementing the global response. *In:* Masson-Delmotte, V., Zhai, P., Pörtner, H.-O., Roberts, D., Skea, J., Shukla, P. R., Pirani, A., Moufouma-Okia, W., Péan, C., Pidcock, R., Connors, S., Matthews, J. B. R., Chen, Y., Zhou, X., Gomis, M. I., Lonnoy, E., Maycock, T., Tignor, M., & Waterfield, T. [Eds.] *Global Warming of 1.5°C. An IPCC Special Report on the impacts of global warming of 1.5°C above pre-industrial levels and related global greenhouse gas emission pathways, in the context of strengthening the global response to the threat of climate change, sustainable development, and efforts to eradicate poverty.* Geneva, Switzerland, Intergovernmental Panel on Climate Change. pp. 313–443.

Demko, A. M., Amsler, C. D., Hay, M. E., Long, J. D., McClintock, J. B., Paul, V. J., & Sotka, E. E. (2017). Declines in plant palatability from polar to tropical latitudes depend on herbivore and plant identity. *Ecology, 98*(9), 2312–2321. https://doi.org/10.1002/ecy.1918

Dickson, A. G. (1993). pH buffers for sea water media based on the total hydrogen ion concentration scale. *Deep Sea Research Part I: Oceanographic Research Papers, 40*(1), 107–118. https://doi.org/10.1016/0967-0637(93)90055-8

Dickson, A. G., & Millero, F. J. (1987). A comparison of the equilibrium constants for the dissociation of carbonic acid in seawater media. *Deep Sea Research Part A, 34*, 1733–1743. https://doi.org/10.1016/01980149(87)90021-5

Dickson A. G., Sabine, C. L., & Christian, J. R. (2007). Guide to best practices for ocean CO_2 measurements. PICES Special Publication 3, pp. 1–191. http://dx.doi.org/10.25607/OBP-1342

Doney, S. C., Busch, D. S., Cooley, S. R., & Kroeker, K. J. (2020). The impacts of ocean acidification on marine ecosystems and reliant human communities. *Annual Review of Environmental Resources, 45*, 83–112. https://doi.org/10.1146/annurev-environ-012320-083019

Doney, S. C., Fabry, V. J., Feely, R. A., & Kleypas, J. A. (2009). Ocean acidification: the other CO_2 problem. *Annual Reviews of Marine Science, 1*, 169–192. https://doi.org/10.1146/annurev.marine.010908.163834

Donham, E. M., Strope, L. T., Hamilton, S. L., & Kroeker, K. J. (2021). Coupled changes in pH, temperature, and dissolved oxygen impact the physiology and ecology of herbivorous kelp forest grazers. *Global Change Biology, 28*, 3023–3039. http://doi.org/10.1111/gcb.16125

Doubleday, Z. A., Nagelkerken, I., Coutts, M. D., Goldenberg, S. U., & Connell, S. D. (2019). A triple trophic boost: how carbon emissions indirectly change a marine food chain. *Global Change Biology, 25*(3), 978–984. https://doi.org/10.1111/gcb.14536

Druehl, L. D. (1967). Distribution of two species of *Laminaria* as related to some environmental factors. *Journal of Phycology, 3(*2), 103–108. https://doi.org/10.1111/j.1529-8817.1967.tb04641.x

Druehl, L. D. (1970). The pattern of Laminariales distribution in the northeast Pacific. *Phycologia, 9*, 237–247. https://doi.org/10.2216/i0031-8884-9-3-237.1

Druehl, L. D. (1981). Geographic distribution. *In:* Lobban, C. R., & Wynne, M. J. [Eds.] *The Biology of Seaweeds.* Vol. 17. University of California Press, pp. 306–325.

Druehl, L. D., Cabot, E. L., & Lloyd, K. E. (1987). Seasonal growth of *Laminaria groenlandica* as a function of plant age. *Canadian Journal of Botany, 65*, 1599–604. https://doi.org/10.1139/b87-219

Druehl, L. D., & Wheeler, W. N. (1986). Population biology of *Macrocystis integrifolia* from British Columbia, Canada. *Marine Biology, 90*, 173–9. https://doi.org/10.1007/BF00569124

Duarte, C. M., Bruhn, A., & Krause-Jensen, D. (2022a). A seaweed aquaculture imperative to meet global sustainability targets. *Nature Sustainability, 5*, 185–93. https://doi.org/10.1038/s41893-021-00773-9

Duarte, C. M.. Gattuso, J.-P., Hancke, K., Gundersen, H., Filbee-Dexter, K., Pedersen, M. F., Middelburg, J. J., Burrows, M. T., Krumhansl, K. A., Wernberg, T., Moore, P., Pessarrodona, A., Ørberg, S. B., Pinto, I. S., Assis, J., Queirós, A. M., Smale, D. A., Bekkby, T., Serrão, E. A., & Krause-Jensen, D. (2022b). Global estimates of the extent and production of macroalgal forests. *Global Ecology and Biogeography, 31*, 1422–1439. https://doi.org/10.1111/geb.13515

Duarte, C., López, J., Benítez, S., Manríquez, P. H., Navarro, J. M., Bonta, C. C., Torres, R., & Quijón, P. (2016). Ocean acidification induces changes in algal palatability and herbivore feeding behavior and performance. *Oecologia, 180*(2), 453–462. https://doi.org/10.1007/s00442-015-3459-3

Dubois, A., & Iken, K. (2012). Seasonal variation in kelp phlorotannins in relation to grazer abundance and environmental variables in the Alaskan sublittoral zone. *Algae*, *27*, 9–19.

Duffy, J. E., & Paul, V. J. (1992). Prey nutritional quality and the effectiveness of chemical defenses against tropical reef fishes. *Oecologia, 90*(3), 333–339. https://doi.org/10.1007/BF00317689

Durack, P. J., Gleckler, P. J., Purkey, S. G., Johnson, G. C., Lyman, J. M., & Boyer, T. P. (2018). Ocean warming: from the surface to the deep in observations and models. *Oceanography, 31*, 41–51. https://www.jstor.org/stable/26542650

Edwards, M., & Richardson, A. J. (2004). Impact of climate change on marine pelagic phenology and trophic mismatch. *Nature, 430*, 881–884. https://doi.org/10.1038/nature02808

Eggert, A. (2012). Seaweed responses to temperature. *In:* Wiencke C., & Bischof, K. [Eds.], *Seaweed Biology.* Springer, Berlin, Heidelberg, pp. 47–66. https://doi.org/10.1007/978-3-642-28451-9_3

Endo, H., Suehiro, K., Gao, X., & Agatsuma, Y. (2017). Interactive effects of elevated summer temperature, nutrient availability, and irradiance on growth and chemical compositions of juvenile kelp, *Eisenia bicyclis. Phycological Research, 65*(2), 118–126. https://doi.org/10.1111/pre.12170

Evans W., Mathis, J. T., Ramsay, J., Hetrick, J. (2015). On the frontline: tracking ocean acidification in an Alaskan shellfish hatchery. *PLoS ONE, 10*, e0130384. https://doi.org/10.1371/journal.pone.0130384

Fabricius, K. E., Noonan, S. H. C., Abrego, D., Harrington, L., & De'ath, G. (2017). Low recruitment due to altered settlement substrata as primary constrain for coral communities under ocean acidification. *Proceedings of the Royal Society B, 284*, 20171536. http://dx.doi.org/10.1098/rspb.2017.1536

Fabry, V. J., McClintock, J. B., Mathis, J. T., & Grebmeier, J. M. (2009). Ocean acidification at high latitudes: the bellweather. *Oceanography*, *22*, 160–71. https://www.jstor.org/stable/24861032

Facey, S. L., Ellsworth, D. S., Staley, J. T., Wright, D. J., & Johnson, S. N. (2014). Upsetting the order: how climate and atmospheric change affects herbivore–

enemy interactions. *Current Opinion in Insect Science, 5*, 66–74. https://doi.org/10.1016/j.cois.2014.09.015

Falkenberg, L. J., Connell, S. D., & Russell, B. D. (2014). Herbivory mediates the expansion of an algal habitat under nutrient and CO_2 enrichment. *Marine Ecology Progress Series, 497*, 87–92. https://doi.org/10.3354/meps10557

Falkenberg, L. J., Russell, B. D., & Connell, S. D. (2013). Future herbivory: the indirect effects of enriched CO_2 may rival its direct effects. *Marine Ecology Progress Series, 492*, 85–95. https://doi.org/10.3354/meps10491

Feely, R. A., Byrne, R. H., Acker, J. G., Betzer, P. R., Chen, C. -T. A., Gendron, J. F., & Lamb, M. F. (1988). Winter-summer variations of calcite and aragonite saturation in the Northeast Pacific. *Marine Chemistry, 25*, 227–241. https://doi.org/10.1016/0304-4203(88)90052-7

Feely, R. A., Sabine, C. L., Lee, K., Berelson, W., Kleypas, J., Fabry, V.J., & Millero F.J. (2004). Impact of anthropogenic CO_2 on the $CaCO_3$ system in the oceans. *Science, 305*, 362–366. https://doi.org/10.1126/science.1097329

Fernández, P. A., Gaitán-Espitia, J. D., Leal, P. P., Schmid, M., Revill, A. T., & Hurd, C. L. (2020). Nitrogen sufficiency enhances thermal tolerance in habitat-forming kelp: implications for acclimation under thermal stress. *Scientific Reports, 10*, 3186. https://doi.org/10.1038/s41598-020-60104-4

Fietzke J., Ragazzola, F., Halfar, J., Dietze, H., Foster, L. C., Hansteen, T. H., Eisenhauer, A., & Steneck, R. S. (2015). Century-scale trends and seasonality in pH and temperature for shallow zones of the Bering Sea. *Proceedings of the National Academy of Sciences, 112*, 2960–2965. https://doi.org/10.1073/pnas.1419216112

Filbee-Dexter, K., & Wernberg, T. (2020). Substantial blue carbon in overlooked Australian kelp forests. *Scientific Rep*orts, 10, 12341. https://doi.org/10.1038/s41598-020-69258-7

Franke, K., Liesner, D., Heesch, S., & Bartsch, I. (2021). Looks can be deceiving: contrasting temperature characteristics of two morphologically similar kelp species co-occurring in the Arctic. *Botanica Marina, 64*(3), 163–175. https://doi.org/10.1515/bot-2021-0014

Franklin, J., Serra-Diaz, J. M., Syphard, A. D., & Regan, H. M. (2016). Global change and terrestrial plant community dynamics. *Proceedings of the National Academy of Sciences, 113*(14), 3725–3734. https://doi.org/10.1073/pnas.1519911113

Freiwald A., & Henrich, R. (1994). Reefal coralline algal build-ups within the Arctic Circle: morphology and sedimentary dynamics under extreme environmental seasonality. *Sedimentology, 41*, 963–984. https://doi.org/10.1111/j.1365-3091.1994.tb01435.x

Freshwater D.W., & Rueness, J. (1994). Phylogenetic relationships of some European *Gelidium* (Gelidiales, Rhodophyta) species, based on *rbcL* nucleotide sequence analysis. *Phycologia, 33*, 187–194. https://doi.org/10.2216/i0031-8884-33-3-187.1

Gabrielson, P.W., Miller, K.A., & Martone, P.T. (2011). Morphometric and molecular analyses confirm two distinct species of *Calliarthron* (Corallinales, Rhodophyta), a genus endemic to the northeast Pacific. *Phycologia, 50*, 298–316. https://doi.org/10.2216/10-42.1

Gagné, J. A., & Mann, K. H. (1987). Evaluation of four models used to estimate kelp productivity from growth measurements. *Marine Ecology Progress Series, 37*, 35–44. https://www.jstor.org/stable/24825489

Gagné, J. A., Mann, K. H., & Chapman, A. R. O. (1982). Seasonal patterns of growth and storage in *Laminaria longicruris* in relation to differing patterns of availability of nitrogen in the water. *Marine Biology, 69*, 91–101. https://doi.org/10.1007/BF00396965

Gallagher, J. B., Shelamoff, V., & Layton, C. (2022). Seaweed ecosystems may not mitigate CO_2 emissions. *ICES Journal of Marine Sci*ence, *79*, 585–92. https://doi.org/10.1093/icesjms/fsac011

Galloway, A. W. E., Schram, J. B., Bell, L. E., Yoshioka, R. M., & Kroeker, K. J. (in prep). Fatty acid trophic markers track seasonal physiological and trophic dynamics in seaweeds and benthic herbivores in a temperate coastal ecosystem. Manuscript in preparation.

Gao, G., Zhao, X., Jiang, M., & Gao, L. (2021). Impacts of marine heatwaves on algal structure and carbon sequestration in conjunction with ocean warming and acidification. *Frontiers in Marine Science, 8*, 758651. https://doi.org/10.3389/fmars.2021.758651

Gattuso J.-P., Magnan, A., Billé, R., Cheung, W. W. L., Howes, E. L., Joos, F., Allemand, D., Bopp, L., Cooley, S. R., Eakin, C. M., Hoegh-Guldberg, O., Kelly, R. P., Pörtner, H.-O., Rogers, A. D., Baxter, J. M., Laffoley, D., Osborn, D., Rankovic, A., Rochette, J., Sumaila, U. R., Treyer, S., & Turley, C. (2015). Contrasting futures for ocean and society from different anthropogenic CO_2 emissions scenarios. *Science, 349*, aac4722. http://dx.doi.org/10.1126/science.aac4722

Gaylord, B., Kroeker, K. J., Sunday, J. M., Anderson, K. M., Barry, J. P., Brown, N. E., Connell, S. D., Dupont, S., Fabricius, K. E., Hall-Spencer, J. M., Klinger, T., Milazzo, M., Munday, P. L., Russell, B. D., Sanford, E., Schreiber, S. J., Thiyagarajan, V., Vaughn, M. L. H., Widdicombe, S., & Harley, C. D. G. (2015). Ocean acidification through the lens of ecological theory. *Ecology*, *96*, 3–15. https://doi.org/10.1890/14-0802.1

Gaylord B., Rosman, J. H., Reed, D. C., Koseff, J. R., Fram, J., MacIntyre, S., Arkema, K., McDonald, C., Brzezinski, M. A., Largier, J. L., Monismith, S. G., Raimondi, P. T., & Mardian, B. (2007). Spatial patterns of flow and their modification within and around a giant kelp forest. *Limnology and Oceanography, 52*, 1838–1852. https://doi.org/10.4319/lo.2007.52.5.1838

Gerard, V.A. (1976). Some aspects of material dynamics and energy flow in a kelp forest in Monterey Bay, California. Ph.D. dissertation, University of California Santa Cruz, 185 pp.

Gerard, V. A. (1982a). In situ rates of nitrate uptake by giant kelp, *Macrocystis pyrifera* (L.) C. Agardh: tissue differences, environmental effects, and predictions of nitrogen-limited growth. *Journal of Experimental Marine Biology and Ecology, 62*, 211–24. https://doi.org/10.1016/0022-0981(82)90202-7

Gerard, V. A. (1982b). In situ water motion and nutrient uptake by the giant kelp *Macrocystis pyrifera*. *Marine Biology,* 69, 51–4. https://doi.org/10.1007/BF00396960

Gerard, V. A. (1997). The role of nitrogen nutrition in high-temperature tolerance of the kelp, *Laminaria saccharina* (Chromophyta). *Journal of Phycology, 33*(5), 800–810. https://doi.org/10.1111/j.0022-3646.1997.00800.x

Gevaert, F., Davoult, D., Creach, A., Kling, R., Janquin, M.-A., Seuront, L., & Lemoine, Y. (2001). Carbon and nitrogen content of *Laminaria saccharina* in the eastern English Channel: biometrics and seasonal variations. *Journal of the Marine Biological Association of the United Kingdom,* 81, 727–34. https://doi.org/10.1017/S0025315401004532

Gilbert, B., MacDougall, A. S., Kadoya, T., Akasaka, M., Bennett, J. R., Lind, E. M., Flores-Moreno, H., Firn, J., Hautier, Y., Borer, E. T., Seabloom, E. W., Adler, P. B., Cleland, E. E., Grace, J. B., Harpole, W. S., Esch, E. H., Moore, J. L., Knops, J., McCulley, R., Mortensen, B., Bakker, J., & Fay, P. A. (2020). Climate and local environment structure asynchrony and the stability of primary production in grasslands. *Global Ecology and Biogeography, 29*(7), 1177–1188. https://doi.org/10.1111/geb.13094

Gilson, A. R., Smale, D. A., & O'Connor, N. (2021). Ocean warming and species range shifts affect rates of ecosystem functioning by altering consumer–resource interactions. *Ecology*, *102*, e03341. https://doi.org/10.1002/ecy.3341

Gomez-Lemos, L. A., & Diaz-Pulido, G. (2017). Crustose coralline algae and associated microbial biofilms deter seaweed settlement on coral reefs. *Coral Reefs, 36*, 453–462. https://doi.org/10.1007/s00338-017-1549-x

Gómez, I., & Wiencke, C. (1998). Seasonal changes in C, N and major organic compounds and their significance to morpho-functional processes in the endemic Antarctic brown alga *Ascoseira mirabilis. Polar Biol*ogy, *19*, 115–24. https://doi.org/10.1007/s003000050222

Gómez, I., Wulff, A., Roleda, M. Y., Huovinen, P., Karsten, U., Quartino, M. L., Dunton, K., & Wiencke, C. (2009). Light and temperature demands of marine benthic microalgae and seaweeds in polar regions. *Botanica Marina, 52*(6), 593–608. https://doi.org/10.1515/BOT.2009.073

Gorra, T. R., Garcia, S. C. R., Langhans, M. R., Hoshijima, U., Estes, J. A., Raimondi, P. T., Tinker, M. T., Kenner, M. C., & Kroeker, K. J. (2022). Southeast Alaskan kelp forests: inferences of process from large-scale patterns of variation in space and time. *Proceedings of the Royal Society B Biological Sciences, 289*, 20211697. https://doi.org/10.1098/rspb.2021.1697

Graba-Landry, A., Hoey, A. S., Matley, J. K., Sheppard-Brennand, H., Poore, A. G. B., Byrne, M., & Dworjanyn, S. A. (2018). Ocean warming has greater and more consistent negative effects than ocean acidification on the growth and health of subtropical macroalgae. *Marine Ecology Progress Series, 595*, 55–69. https://doi.org/10.3354/meps12552

Graham, M. H. (2004). Effects of local deforestation on the diversity and structure of southern California giant kelp forest food webs. *Ecosystems, 7*, 341–357. https://doi.org/10.1007/s10021-003-0245-6

Graham, M. H., Vasquez, J. A., & Buschmann, A. H. (2007). Global ecology of the giant kelp *Macrocystis*: from ecotypes to ecosystems. *Oceanography and Marine Biology, 45*, 39–88.

Graiff, A., Bartsch, I., Ruth, W., Wahl, M., & Karsten, U. (2015). Season exerts differential effects of ocean acidification and warming on growth and carbon metabolism of the seaweed *Fucus vesiculosus* in the western Baltic Sea. *Frontiers in Marine Science, 2*, 112. https://doi.org/10.3389/fmars.2015.00112

Granado, I., & Caballero, P. (2001). Feeding rates of *Littorina striata* and *Osilinus atratus* in relation to nutritional quality and chemical defenses of seaweeds. *Marine Biology, 138*(6), 1213–1224. https://doi.org/10.1007/s002270100544

Grant, W. S., Lydon, A., & Bringloe, T. T. (2020). Phylogeography of split kelp *Hedophyllum nigripes*: northern ice-age refugia and trans-Arctic dispersal. *Polar Biol*ogy, *43*, 1829–41. https://doi.org/10.1007/s00300-020-02748-6

Gunderson, A. R., Armstrong, E. J., & Stillman, J. H. (2016). Multiple stressors in a changing world: the need for an improved perspective on physiological responses to the dynamic marine environment. *Annual Review of Marine Science, 8(*1), 357–378. https://doi.org/10.1146/annurev-marine-122414-033953

Guy-Haim T., Silverman, J., Wahl, M., Aguirre, J., Noisette, F., & Rilov, G. (2020). Epiphytes provide microscale refuge from ocean acidification. *Marine Environmental Research, 161*, 105093. https://doi.org/10.1016/j.marenvres.2020.105093

Harley, C. D. G., Anderson, K. M., Demes, K. W., Jorve, J. P., Kordas, R. L., Coyle, T. A., & Graham, M. H. (2012). Effects of climate change on global seaweed communities. *Journal of Phycology, 48*(5), 1064–1078. https://doi.org/10.1111/j.1529-8817.2012.01224.x

Harley, C. D. G., Connell, S. D., Doubleday, Z. A., Kelaher, B., Russell, B. D., Sarà, G., & Helmuth, B. (2017). Conceptualizing ecosystem tipping points within a physiological framework. *Ecology and Evolution, 7*(15), 6035–6045. https://doi.org/10.1002/ece3.3164

Harley, C. D. G., Hughes, A. R., Hultgren, K. M., Miner, B. G., Sorte, C. J. B., Thornber, C. S., Rodriguez, L. F., Tomanek, L., & Williams, S. L. (2006). The impacts of climate change in coastal marine systems. *Ecology Letters, 9*, 228–241. https://doi.org/10.1111/j.1461-0248.2005.00871.x

Harmon, M. E., Phillips, D. L., Battles, J. J., Rassweiler, A., Hall Jr., R. O., & Lauenroth, W. K. (2007). Quantifying uncertainty in net primary production measurements. *In:* Fahey, T. J., & Knapp, A. K. [Eds.] *Principles and Standards for Measuring Primary Production*. Oxford University Press, pp. 238–60.

Harrison, P. J., Druehl, L. D., Lloyd, K. E., & Thompson, P. A. (1986). Nitrogen uptake kinetics in three year-classes of *Laminaria groenlandica* (Laminariales: Phaeophyta). *Marine Biology, 93*(1), 29–35. https://doi.org/10.1007/BF00428652

Hauri, C., Schultz, C., Hedstrom, K., Danielson, S., Irving, B., Doney, S. C., Dussin, R., Curchitser, E. N., Hill, D. F., & Stock, C. A. (2020). A regional hindcast model simulating ecosystem dynamics, inorganic carbon chemistry, and ocean acidification in the Gulf of Alaska. *Biogeosciences, 17*(14), 3837–3857. https://doi.org/10.5194/bg-17-3837-2020

Hay, M. E., Kappel, Q. E., & Fenical, W. (1994). Synergisms in plant defenses against herbivores: interactions of chemistry, calcification, and plant quality. *Ecology, 75*(6), 1714–1726. https://doi.org/10.2307/1939631

Helmuth, B., Harley, C. D. G., Halpin, P. M., O'Donnell, M., Hofmann, G. E., & Blanchette, C. A. (2002). Climate change and latitudinal patterns of intertidal thermal stress. Science, 298, 1015–1017. https://doi.org/10.1126/science.1076814

Hemmi, A., & Jormalainen, V. (2002). Nutrient enhancement increases performance of a marine herbivore via quality of its food alga. *Ecology, 83*, 1052–1064. https://doi.org/10.2307/3071913

Hepburn, C. D., Pritchard, D. W., Cornwall, C. E., McLeod, R. J., Beardall, J., Raven, J. A., & Hurd, C. L. (2011). Diversity of carbon use strategies in a kelp forest community: implications for a high CO_2 ocean. *Global Change Biology, 17*(7), 2488–2497. https://doi.org/10.1111/j.1365-2486.2011.02411.x

Hermann, A. J., Hinckley, S., Dobbins, E. L., Haidvogel, D. B., Bond, N. A., Mordy, C., Kachel, N., & Stabeno, P. J. (2009). Quantifying cross-shelf and vertical nutrient flux in the coastal Gulf of Alaska with a spatially nested, coupled biophysical model. *Deep Sea Research Part II: Topical Studies in Oceanography, 56*(24), 2474–2486. https://doi.org/10.1016/j.dsr2.2009.02.008

Hillebrand, H., Worm, B., & Lotze, H. K. (2000). Marine microbenthic community structure regulated by nitrogen loading and grazing pressure. *Marine Ecology Progress Series, 204*, 27–38. https://doi.org/10.3354/meps204027

Himes-Cornell, A., & Kasperski, S. (2015). Assessing climate change vulnerability in Alaska's fishing communities. Fisheries Research, 162, 1–11. https://doi.org/10.1016/j.fishres.2014.09.010

Hirsh, H. K., Nickols, K. J., Takeshita, Y., Traiger, S. B., Mucciarone, D. A., Monismith, S., & Dunbar, R. B. (2020). Drivers of biogeochemical variability in a central California kelp forest: implications for local amelioration of ocean acidification. *Journal of Geophysical Research: Oceans, 125*, e2020JC016320. https://doi.org/10.1029/2020JC016320

Hofmann, G. E., Smith, J. E., Johnson, K. S., Send, U., Levin, L. A., Micheli, F., Paytan, A., Price, N. N., Peterson, B., Takeshita, Y., Matson, P. G., Crook, E. D., Kroeker, K. J., Gambi, M. C., Rivest, E. B., Frieder, C. A., Yu, P. C., & Martz, T. R. (2011). High-frequency dynamics of ocean pH: a multi-ecosystem comparison. *PLoS ONE, 6*, e28983. https://doi.org/10.1371/journal.pone.0028983

Hofmann, L. C., & Bischof, K. (2014). Ocean acidification effects on calcifying macroalgae, *Aquatic Biology, 22*, 261–279. https://doi.org/10.3354/ab00581

Hofmann, L. C., & Heesch, S. (2018). Latitudinal trends in stable isotope signatures and carbon-concentrating mechanisms of northeast Atlantic rhodoliths, Biogeosciences, 15, 6139–6149. https://doi.org/10.5194/bg-15-6139-2018

Hofmann, L. C., Schoenrock, K., & de Beer, D. (2018). Arctic coralline algae elevate surface pH and carbonate in the dark. *Frontiers in Plant Science, 9*, 1496. https://doi.org/10.3389/fpls.2018.01416

Hofmann, L. C., Straub, S., & Bischof, K. (2012). Competition between calcifying and noncalcifying temperate marine macroalgae under elevated CO_2 levels. *Marine Ecology Progress Series, 464*, 89–105. https://doi.org/10.3354/meps09892

Hollarsmith, J. A., Buschmann, A. H., Camus, C., & Grosholz, E. D. (2020). Varying reproductive success under ocean warming and acidification across giant kelp (*Macrocystis pyrifera*) populations. *Journal of Experimental Marine Biology and Ecology, 522*, 151247. https://doi.org/10.1016/j.jembe.2019.151247

Hollowed, A. B., Haynie, A. C., Hermann, A. J., Holsman, K. K., Punt, A. E., & Szuwalski, C. S. (2022). Implications of climate change on the Bering Sea and other cold water systems. *Deep Sea Research Part II: Topical Studies in Oceanography, 201*, 105110. https://doi.org/10.1016/j.dsr2.2022.105110.

Holsman, K., Hollowed, A., Ito, S.I., Bograd, S., Hazen, E., King, J., Mueter, F., & Perry, R.I. (2019). Climate change impacts, vulnerabilities and adaptations: North Pacific and Pacific Arctic marine fisheries. *In:* Barange, M., Bahri, T., Beveridge, M. C. M., Cochrane, K. L., Funge-Smith, S., & Poulain, F. [Eds.], *Impacts of climate change on fisheries and aquaculture,* Rome: Food and Agriculture Organization of the United Nations, pp.113-138.

Hood, E., & Scott, D. (2008). Riverine organic matter and nutrients in southeast Alaska affected by glacial coverage. *Nature Geoscience, 1*(9), 583–587. https://doi.org/10.1038/ngeo280

Hughey, J. R., Silva, P. C., & Hommersand, M. H. (2001). Solving taxonomic and nomenclatural problems in Pacific Gigartinaceae (Rhodophyta) using DNA from type material. Journal of Phycology, 37, 1091–1109. https://doi.org/10.1046/j.1529-8817.2001.01048.x

Hurd, C. L. (2015). Slow-flow habitats as refugia for coastal calcifiers from ocean acidification. Journal of Phycology, 51, 599–605. https://doi.org/10.1111/jpy.12307

Hurd, C. L., Beardall, J., Comeau, S., Cornwall, C. E., Havenhand, J. N., Munday, P. L., Parker, L. M., Raven, J. A., & McGraw, C. M. (2020). Ocean acidification as a multiple driver: how interactions between changing seawater carbonate parameters affect marine life. *Marine and Freshwater Research, 71*(3), 263. https://doi.org/10.1071/MF19267

Hurd, C. L., Durante, K. M., Chia, F.-S., & Harrison, P. J. (1994). Effect of bryozoan colonization on inorganic nitrogen acquisition by the kelps *Agarum fimbriatum* and *Macrocystis integrifolia*. *Marine Biology,* 121, 167–73. https://doi.org/10.1007/BF00349486

Hurd, C. L., Harrison, P. J., Bischof, K., & Lobban, C. S. (2014). Seaweed Ecology and Physiology. 2nd Ed. Cambridge University Press, 567 pp.

Hurd, C. L., Law, C. S., Bach, L. T., Britton, D., Hovenden, M., Paine, E. R., Raven, J. A., Tamsitt, V., & Boyd, P. W. (2022). Forensic carbon accounting: assessing the role of seaweeds for carbon sequestration. *Journal of Phycology, 58,* 347–63. https://doi.org/10.1111/jpy.13249

IPCC. (2018). Summary for Policymakers. *In:* Masson-Delmotte, V., Zhai, P., Pörtner, H.-O., Roberts, D., Skea, J., Shukla, P. R., Pirani, A., Moufouma-Okia, W., Péan, C., Pidcock, R., Connors, S., Matthews, J. B. R., Chen, Y., Zhou, X., Gomis, M. I., Lonnoy, E., Maycock, T., Tignor, M., & Waterfield, T. [Eds.] *Global Warming of 1.5°C. An IPCC Special Report on the impacts of global warming of 1.5°C above pre-industrial levels and related global greenhouse gas emission pathways, in the context of strengthening the global response to the threat of climate change, sustainable development, and efforts to eradicate poverty.* Geneva, Switzerland, Intergovernmental Panel on Climate Change, 32 pp.

Ji, R., Edwards, M., Mackas, D. L., Runge, J. A., & Thomas, A. C. (2010). Marine plankton phenology and life history in a changing climate: current research and future directions. *Journal of Plankton Research, 32*(10), 1355–1368. https://doi.org/10.1093/plankt/fbq062

Jin, P., & Gao, K. (2021). Effects of ocean acidification on marine primary producers and related ecological processes under multiple stressors. *In:* Häder, D.-P., Helbling, E. W., & Villafañe, V. E. [Eds.], *Anthropogenic Pollution of Aquatic Ecosystems*. Springer International Publishing, pp. 401–426. https://doi.org/10.1007/978-3-030-75602-4_18

Jin, P., Hutchins, D. A., & Gao, K. (2020). The impacts of ocean acidification on marine food quality and its potential food chain consequences. *Frontiers in Marine Science, 7*, 543979. https://doi.org/10.3389/fmars.2020.543979

Johnson M. D., Rodriguez Bravo, L. M., O'Connor, S. E., Varley, N. F., & Altieri, A. H. (2019). pH variability exacerbates effects of ocean acidification on a Caribbean crustose coralline alga. *Frontiers in Marine Science, 6*, 150. https://doi.org/10.3389/fmars.2019.00150

Jokiel, P. L., Maragos, J. E., & Franzisket, L. (1978). Coral growth: buoyant weight technique. *In:* Stoddart, D. R., & Johannes, R. E. [Eds.], *Coral Reefs: Research Methods,* UNESCO, Paris, 1978, pp. 529–542.

Kavanaugh, M. T., Nielsen, K. J ., Chan, F. T., Menge, B. A., Letelier, R. M., & Goodrich, L. M. (2009). Experimental assessment of the effects of shade on an intertidal kelp: do phytoplankton blooms inhibit growth of open coast macroalgae? *Limnology and Oceanography, 54*, 276–88. https://doi.org/10.4319/lo.2009.54.1.0276

King, N. G., McKeown, N. J., Smale, D. A., & Moore, P. J. (2017). The importance of phenotypic plasticity and local adaptation in driving intraspecific variability in thermal niches of marine macrophytes. *Ecography, 41*(9), 1469–1484. https://doi.org/10.1111/ecog.03186

King, N. G., Moore, P. J., Pessarrodona, A., Burrows, M. T., Porter, J., Bue, M., & Smale, D. A. (2020). Ecological performance differs between range centre and trailing edge populations of a cold-water kelp: implications for estimating net primary productivity. *Marine Biology, 167*(9), 137. https://doi.org/10.1007/s00227-020-03743-5

Kinnby, A., Toth, G. B., & Pavia, H. (2021). Climate change increases susceptibility to grazers in a foundation seaweed. *Frontiers in Marine Science, 8*, 688406. https://doi.org/10.3389/fmars.2021.688406

Koch, M., Bowes, G., Ross, C., & Zhang, X.-H. (2013). Climate change and ocean acidification effects on seagrasses and marine macroalgae. *Global Change Biology, 19*(1), 103–132. https://doi.org/10.1111/j.1365-2486.2012.02791.x

Korb, R. E., & Gerard, V. A. (2000). Effects of concurrent low temperature and low nitrogen supply on polar and temperate seaweeds. *Marine Ecology Progress Series, 198*, 73–82. https://doi.org/10.3354/meps198073

Koweek, D. A., Nickols, K. J., Leary, P. R., Litvin, S. Y., Bell, T. W., Luthin, T., Lummis, S., Mucciarone, D. A., & Dunbar, R. B. (2017). A year in the life of a central California kelp forest: physical and biological insights into biogeochemical variability. *Biogeosciences, 14*(1), 31–44. https://doi.org/10.5194/bg-14-31-2017

Kram, S. L., Price, N. N., Donham, E. M., Johnson, M. D., Kelly, E. L. A., Hamilton, S. L., & Smith, J. E. (2016). Variable responses of temperate calcified and fleshy macroalgae to elevated pCO_2 and warming. *ICES Journal of Marine Science, 73*(3), 693–703. https://doi.org/10.1093/icesjms/fsv168

Krause-Jensen, D., & Duarte, C. M. (2014). Expansion of vegetated coastal ecosystems in the future Arctic. *Frontiers in Marine Science, 1*(77), 1–10. http://doi.org/10.3389/fmars.2014.00077

Krause-Jensen, D., & Duarte, C. M. (2016). Substantial role of macroalgae in marine carbon sequestration. *Nature Geosciences, 9*, 737–42. https://doi.org/10.1038/ngeo2790

Krause-Jensen, D., Archambault, P., Assis, J., Bartsch, I., Bischof, K., Filbee-Dexter, K., Dunton, K. H., Maximova, O., Ragnarsdóttir, S. B., Sejr, M. K., Simakova, U., Spiridonov, V., Wegeberg, S., Winding, M. H. S., & Duarte, C. M. (2020). Imprint of climate change on pan-arctic marine vegetation. *Frontiers in Marine Science, 7*, 617324. http://doi.org/10.3389/fmars.2020.617324

Krause-Jensen, D., Lavery, P., Serrano, O., Marbà, N., Masque, P., & Duarte, C. M. (2018). Sequestration of macroalgal carbon: the elephant in the Blue Carbon room. *Biology Letters, 14*, 20180236. https://doi.org/10.1098/rsbl.2018.0236

Krause-Jensen, D., Marbà, N., Sanz-Martin, M., Hendriks, I. E., Thyrring, J., Carstensen, J., Sejr, M. K., & Duarte, C. M. (2016). Long photoperiods sustain high pH in Arctic kelp forests. *Science Advances, 2*, e1501938. https://doi.org/10.1126/sciadv.1501938

Kroeker, K. J., Bell, L. E., Donham, E. M., Hoshijima, U., Lummis, S., Toy, J. A., & Willis-Norton, E. (2020). Ecological change in dynamic environments: accounting for temporal environmental variability in studies of ocean change biology. *Global Change Biology, 26*(1), 54–67. https://doi.org/10.1111/gcb.14868

Kroeker, K. J., Kordas, R. L., Crim, R. N., Hendriks, I. E., Ramajo, L., Singh, G. S., Duarte, C. M., Gattuso, J. -P. (2013a). Impacts of ocean acidification on marine organisms: quantifying sensitivities and interaction with warming. *Global Change Biology, 19,* 1884–1896. https://doi.org/10.1111/gcb.12179

Kroeker, K. J., Kordas, R. L, Crim, R. N., & Singh, G. G. (2010). Meta-analysis reveals negative yet variable effects of ocean acidification on marine organisms. *Ecology Letters, 13*, 1419–1434. https://doi.org/j.1461-0248.2010.01518.x

Kroeker, K. J., Kordas, R. L., & Harley, C. D. G. (2017). Embracing interactions in ocean acidification research: confronting multiple stressor scenarios and context dependence. *Biology Letters, 13*, 20160802. https://doi.org/10.1098/rsbl.2016.0802

Kroeker, K. J., Micheli, F. & Gambi, M. C. (2013b). Ocean acidification causes ecosystem shifts via altered competitive interactions. *Nature Climate Change, 3,* 156–159. https://doi.org/10.1038/nclimate1680

Kroeker, K. J., Powell, C., & Donham, E. M. (2021). Windows of vulnerability: seasonal mismatches in exposure and resource identity determine ocean acidification's effect on a primary consumer at high latitude. *Global Change Biology, 27*(5), 1042–1051. https://doi.org/10.1111/gcb.15449

Krumhansl, K. A., Okamoto, D. K., Rassweiler, A., Novak, M., Bolton, J. J., Cavanaugh, K. C., Connell, S. D., Johnson, C. R., Konar, B., Ling, S. D., Micheli, F., Norderhaug, K. M., Pérez-Matus, A., Sousa-Pinto, I., Reed, D. C., Salomon, A. K., Shears, N. T., Wernberg, T., Anderson, R. J., Barrett, N. S., Buschmann, A. H., Carr, M. H., Caselle, J. E., Derrien-Courtel, S., Edgar, G. J., Edwards, M., Estes, J. A., Goodwin, C., Kenner, M. C., Kushner, D. J., Moy, F. E., Nunn, J., Steneck, R. S., Vásquez, J., Watson, J., Witman, J. D., & Byrnes, J. E. K. (2016). Global patterns of kelp forest change over the past half-century. *Proceedings of the National Academy of Sciences, 113*, 13785–90. https://doi.org/10.1073/pnas.1606102113

Kübler, J. E., Johnston, A. M., & Raven, J. A. (1999). The effects of reduced and elevated CO_2 and O_2 on the seaweed *Lomentaria articulata*. *Plant Cell and Environment, 22*, 1303–1310. https://doi.org/10.1046/j.1365-3040.1999.00492.x

Kuffner, I. B., Andersson, A. J., Jokiel, P. L., Rodgers, K. S., & Mackenzie, F. T. (2008). Decreased abundance of crustose coralline algae due to ocean acidification. *Nature Geoscience, 1*, 114–117. https://doi.org/10.1038/ngeo100

Kumar, A., AbdElgawad, H., Castellano, I., Selim, S., Beemster, G. T. S., Asard, H., Buia, M. C., & Palumbo, A. (2018). Effects of ocean acidification on the levels of primary and secondary metabolites in the brown macroalga *Sargassum vulgare* at different time scales. *Science of The Total Environment, 643*, 946–956. https://doi.org/10.1016/j.scitotenv.2018.06.176

Kumar, A., Buia, M. C., Palumbo, A., Mohany, M., Wadaan, M. A. M., Hozzein, W. N., Beemster, G. T. S., & AbdElgawad, H. (2020). Ocean acidification affects biological activities of seaweeds: a case study of *Sargassum vulgare* from Ischia volcanic CO_2 vents. *Environmental Pollution, 259*, 113765. https://doi.org/10.1016/j.envpol.2019.113765

Kwiatkowski, L., Gaylord, B., Hill, T., Hosfelt, J., Kroeker, K. J., Nebuchina, Y., Ninokawa, A., Russell, A. D., Rivest, E. B., Sesboüé, M., & Caldeira, K. (2016). Nighttime dissolution in a temperate coastal ocean ecosystem increases under acidification. *Science Reports, 6*, 22984. https://doi.org/10.1038/srep22984

Ladah, L. B., & Zertuche-González, J. A. (2022). Local adaptation of juvenile giant kelp, *Macrocystis pyrifera*, from their southern limit in the northern hemisphere explored using reciprocal transplantation. *European Journal of Phycology, 57*(3), 357–366. https://doi.org/10.1080/09670262.2021.2007543

Ladd, C., & Cheng, W. (2016). Gap winds and their effects on regional oceanography Part I: Cross Sound, Alaska. *Deep Sea Research Part II: Topical Studies in Oceanography, 132*, 41–53. https://doi.org/10.1016/j.dsr2.2015.08.006

Laurens, L. M. L., Lane, M., & Nelson, R. S. (2020). Sustainable seaweed biotechnology solutions for carbon capture, composition, and deconstruction. *Trends in Biotechnology, 38*, 1232–44. https://doi.org/10.1016/j.tibtech.2020.03.015

Lecocq, F., Winkler, H., Daka, J. P., Fu, S., Gerber, J. S., Kartha, S., Krey, V., Lofgren, H., Masui, T., Mathur, R., Portugal-Pereira, J., Sovacool, B. K., Vilariño, M. V., & Zhou, N. (2022). Mitigation and development pathways in the near- to mid-term. *In:* Shukla, P. R., Skea, J., Slade, R., Al Khourdajie, A., van Diemen, R., McCollum, D., Pathak, M., Some, S., Vyas, P., Fradera, R., Belkacemi, M., Hasija, A., Lisboa, G., Luz, S., & Malley, J. [Eds.]. *Climate Change 2022: Mitigation of Climate Change. Contribution of Working Group III to the Sixth Assessment Report of the Intergovernmental Panel on Climate Change.* IPCC, Cambridge University Press, Cambridge, UK and New York, USA.

Lewis, B., & Diaz-Pulido, G. (2017). Suitability of three fluorochrome markers for obtaining in situ growth rates of coralline algae. *Journal of Experimental*

Marine Biology and Ecology, 490, 64–73. https://doi.org/10.1016/j.jembe.2017.02.004

Lewis, E. R., & Wallace, D. W. R. (1998). Program developed for CO_2 system calculations. Carbon Dioxide Information Analysis Center, managed by Lockheed Martin Energy Research Corporation for the U.S. Department of Energy, Tennessee. https://doi.org/10.15485/1464255

Liu, H., Mi, Z., Lin, L., Wang, Y., Zhang, Z., Zhang, F., Wang, H., Liu, L., Zhu, B., Cao, G., Zhao, X., Sanders, N. J., Classen, A. T., Reich, P. B., & He, J.-S. (2018). Shifting plant species composition in response to climate change stabilizes grassland primary production. *Proceedings of the National Academy of Sciences, 115*(16), 4051–4056. https://doi.org/10.1073/pnas.1700299114

Longtin, C. M., & Saunders, G. W. (2016). The relative contribution of *Saccharina nigripes* (Phaeophyceae) to the Bay of Fundy Laminariaceae: spatial and temporal variability. *Marine Ecology Progress Series, 543*, 153–162. https://doi.org/10.3354/meps11566

Lotze, H. K., Tittensor, D. P., Bryndum-Buchholz, A., Eddy, T. D., Cheung, W. W. L., Galbraith, E. D., Barange, M., Barrier, N., Bianchi, D., Blanchard, J. L., Bopp, L., Büchner, M., Bulman, C. M., Carozza, D. A., Christensen, V., Coll, M., Dunne, J. P., Fulton, E. A., Jennings, S., Jones, M. C., Mackinson, S., Maury, O., Niiranen, S., Oliveros-Ramos, R., Roy, T., Fernandes, J. A., Schewe, J., Shin, Y.-J., Silva, T. A. M., Steenbeek, J., Stock, C. A., Verley, P., Volkholz, J., Walker, N. D., & Worm, B. (2019). Global ensemble projections reveal trophic amplification of ocean biomass declines with climate change. *Proceedings of the National Academy of Sciences,* 116(26), 12907–12912. http://www.doi.org/10.1073/pnas.1900194116.

Lüning, K. (1990). Seaweeds: Their Environment, Biogeography, and Ecophysiology. John Wiley & Sons, New York, 544 pp.

Lüning, K. (1993). Environmental and internal control of seasonal growth in seaweeds. *In:* Chapman, A. R. O., Brown, M. T., & Lahaye, M. [Eds.], *Fourteenth International Seaweed Symposium.* Developments in Hydrobiology, vol. 85. Springer, Dordrecht, pp. 1–14. https://doi.org/10.1007/978-94-011-1998-6_1

Mabin, C. J. T., Johnson, C. R., & Wright, J. T. (2019). Physiological response to temperature, light, and nitrates in the giant kelp *Macrocystis pyrifera* from Tasmania, Australia. *Marine Ecology Progress Series, 614,* 1–19. https://doi.org/10.3354/meps12900

Macreadie, P. I., Anton, A., Raven, J. A., Beaumont, N., Connolly, R. M., Friess, D. A., Kelleway, J. J., Kennedy, H., Kuwae, T., Lavery, P. S., Lovelock, C. E., Smale, D. A., Apostolaki, E. T., Atwood, T. B., Baldock, J., Bianchi, T. S., Chmura, G. L., Eyre, B. D., Fourqurean, J. W., Hall-Spencer, J. M., Huxham, M., Hendriks, I. E., Krause-Jensen, D., Laffoley, D., Luisetti, T., Marbà, N., Masque, P., McGlathery, K. J., Megonigal, J. P., Murdiyarso, D., Russell, B. D., Santos, R., Serrano, O., Silliman, B. R., Watanabe, K., & Duarte, C. M. (2019). The future of Blue Carbon science. *Nature Communications, 10*, 3998. https://doi.org/10.1038/s41467-019-11693-w

Markon, C. J., Trainor, S. F., & Chapin, F. S. III (2012). The United States National Climate Assessment—Alaska Technical Regional Report. U. S. Geological Survey Circular 1379, 148 pp. https://doi.org/10.3133/cir1379

Martin S., Castets, M. -D., & Clavier, J. (2006). Primary production, respiration and calcification of the temperate free-living coralline alga *Lithothamnion corallioides*. Aquatic Botany, 85, 121–128. https://doi.org/10.1016/j.aquabot.2006.02.005

Martin S., & Gattuso, J. -P. (2009). Response of Mediterranean coralline algae to ocean acidification and elevated temperature. *Global Change Biology, 15*, 2089–2100. https://doi.org/10.1111/j.1365-2486.2009.01874.x

Maschler, J., Bialic-Murphy, L., Wan, J., Andresen, L. C., Zohner, C. M., Reich, P. B., Lüscher, A., Schneider, M. K., Müller, C., Moser, G., Dukes, J. S., Schmidt, I. K., Bilton, M. C., Zhu, K., & Crowther, T. W. (2022). Links across ecological scales: plant biomass responses to elevated CO_2. *Global Change Biology, 28*(21), 6115–6134. https://doi.org/10.1111/gcb.16351

Mathis, J. T., Cooley, S. R., Lucey, N., Colt, S., Ekstrom, J., Hurst, T., Hauri, C., Evans, W., Cross, J. N., & Feely, R. A. (2015). Ocean acidification risk assessment for Alaska's fishery sector. *Progress in Oceanography, 136*, 71–91. https://doi.org/10.1016/j.pocean.2014.07.001

McCoy, S. J. (2013). Morphology of the crustose coralline alga *Pseudolithophyllum muricatum* (Corallinales, Rhodophyta) responds to 30 years of ocean acidification in the Northeast Pacific. *Journal of Phycology, 49*, 830–837. https://doi.org/10.1111/jpy.12095

McCoy, S. J., & Kamenos, N. A. (2015). Coralline algae (Rhodophyta) in a changing world: integrating ecological, physiological, and geochemical responses to global change. *Journal of Phycology, 51*, 6–24. https://doi.org/10.1111/jpy.12262

McCoy, S. J., & Pfister, C. A. (2014). Historical comparisons reveal altered competitive interactions in a guild of crustose coralline algae. *Ecology Letters, 17*, 475–483. https://doi.org/10.1111/ele.12247

McCoy, S. J., & Ragazzola, F. (2014). Skeletal trade-offs in coralline algae in response to ocean acidification. *Nature Climate Change, 4*, 719–723. https://doi.org/10.1038/nclimate2273

McDevit, D. C., & Saunders, G. W. (2010). A DNA barcode examination of the Laminariaceae (Phaeophyceae) in Canada reveals novel biogeographical and evolutionary insights. *Phycologia, 49*(3), 235–248. https://doi.org/10.2216/PH09-36.1

McNicholl, C., Koch, M. S., & Hofmann, L. C. (2019). Photosynthesis and light-dependent proton pumps increase boundary layer pH in tropical macroalgae: a proposed mechanism to sustain calcification under ocean acidification. *Journal of Experimental Marine Biology and Ecology, 521*, 151208. https://doi.org/10.1016/j.jembe.2019.151208

Mehrbach, C., Culberson, C. H., Hawley, J. E., & Pytkowicx, R. M. (1973). Measurement of the apparent dissociation constants of carbonic acid in seawater at atmospheric pressure. *Limnology and Oceanography, 18*(6), 897–907. https://doi.org/10.4319/lo.1973.18.6.0897

Menge, B. A., Close, S. L., Hacker, S. D., Nielsen, K. J., & Chan, F. (2021). Biogeography of macrophyte productivity: effects of oceanic and climatic regimes across spatiotemporal scales. *Limnology and Oceanography, 66*, 711–726. http://doi.org/10.1002/lno.11635.

Menge, B. A., Lubchenco, J., Bracken, M. E. S., Chan, F., Foley, M. M., Freidenburg, T. L., Gaines, S. D., Hudson, G., Krenz, C., Leslie, H., Menge, D. N. L., Russell, R., & Webster, M. S. (2003). Coastal oceanography sets the pace of rocky intertidal community dynamics. *Proceedings of the National Academy of Sciences, 100*, 12229–12234. https://doi.org/10.1073/pnas.1534875100

Miller, R. J., Reed, D. C., & Brzezinski, M. A. (2011). Partitioning of primary production among giant kelp (*Macrocystis pyrifera*), understory macroalgae, and phytoplankton on a temperate reef. *Limnology and Oceanography, 56,* 119–32. https://doi.org/10.4319/lo.2011.56.1.0119

Moore, B., Comeau, S., Bekaert, M., Cossais, A., Purdy, A., Larcombe, E., Puerzer, F., McCulloch, M. T., & Cornwall, C. E. (2021). Rapid multi-generational acclimation of coralline algal reproductive structures to ocean acidification. *Proceedings of the Royal Society B, 288*, 20210130. https://doi.org/10.1098/rspb.2021.0130

Morse, A. N. C., & Morse, D. E. (1996). Flypapers for coral and other planktonic larvae. *Bioscience, 46*, 254–262. https://doi.org/10.2307/1312832

Nash, M. C., Diaz-Pulido, G., Harvey, A. S., & Adey, W. (2019). Coralline algal calcification: a morphological and process-based understanding. *PLoS ONE, 14*, e0221396. https://doi.org/10.1371/journal.pone.0221396

Nejrup, L. B., Staehr, P. A., & Thomsen, M. S. (2013). Temperature- and light-dependent growth and metabolism of the invasive red algae *Gracilaria vermiculophylla* – a comparison with two native macroalgae. *European Journal of Phycology, 48*(3), 295–308. https://doi.org/10.1080/09670262.2013.830778

Nelson, W. A. (2009). Calcified macroalgae - critical to coastal ecosystems and vulnerable to change: a review. *Marine Freshwater Research, 60*, 787–801. https://doi.org/10.1071/MF08335

Nielsen, M. M., Krause-Jensen, D., Olesen, B., Thinggaard, R., Christensen, P. B., & Bruhn, A. (2014). Growth dynamics of *Saccharina latissima* (Laminariales, Phaeophyceae) in Aarhus Bay, Denmark, and along the species' distribution range. *Marine Biology, 161*, 2011–22. https://doi.org/10.1007/s00227-014-2482-y

Noisette, F., Egilsdottir, H., Davoult, D., & Martin, S. (2013). Physiological responses of three temperate coralline algae from contrasting habitats to near-future ocean acidification. *Journal of Experimental Marine Biology and Ecology, 448*, 179–187. https://doi.org/10.1016/j.jembe.2013.07.006

Noisette, F., & Hurd, C. L. (2018). Abiotic and biotic interactions in the diffusive boundary layer of kelp blades create a potential refuge from ocean acidification. *Functional Ecology, 32*, 1329–1342. https://doi.org/10.1111/1365-2435.13067

Olischläger, M., Iñiguez, C., Gordillo, F. J. L., & Wiencke, C. (2014). Biochemical composition of temperate and Arctic populations of *Saccharina latissima* after exposure to increased pCO_2 and temperature reveals ecotypic variation. *Planta, 240*(6), 1213–1224. https://doi.org/10.1007/s00425-014-2143-x

Orr, J. C., Fabry, V. J., Aumont, O., Bopp, L., Doney, S. C., Feely, R. A., Gnanadesikan, A., Gruber, N., Ishida, A., Joos, F., Key, R. M., Lindsay, K., Maier-Reimer, E., Matear, R., Monfray, P., Mouchet, A., Najjar, R. G., Plattner, G.-K., Rodgers, K. B., Sabine, C. L., Sarmiento, J. L., Schlitzer, R., Slater, R. D., Totterdell, I. J., Weirig, M.-F., Yamanaka, Y., Yool, A. (2005). Anthropogenic ocean acidification over the twenty-first century and its impact

on calcifying organisms. *Nature, 437,* 681–686. https://doi.org/10.1038/nature04095

Ortega, A., Geraldi, N. R., Alam, I., Kamau, A. A., Acinas, S. G., Logares, R., Gasol, J. M., Massana, R., Krause-Jensen, D., & Duarte, C. M. (2019). Important contribution of macroalgae to oceanic carbon sequestration. *Nature Geoscience, 12*, 748–54. https://doi.org/10.1038/s41561-019-0421-8

Paine, E. R., Britton, D., Schmid, M., Brewer, E. A., Diaz-Pulido, G., Boyd, P. W., & Hurd, C. L. (2023). No effect of ocean acidification on growth, photosynthesis, or dissolved organic carbon release by three temperate seaweeds with different dissolved inorganic carbon uptake strategies. *ICES Journal of Marine Science, 0*, 1–10. https://doi.org/10.1093/icesjms/fsac221

Paine, E. R., Schmid, M., Boyd, P. W., Diaz-Pulido, G., & Hurd, C. L. (2021). Rate and fate of dissolved organic carbon release by seaweeds: a missing link in the coastal ocean carbon cycle. *Journal of Phycology,* 57, 1375–91. https://doi.org/10.1111/jpy.13198

Parke, M. (1948). Studies on British Laminariaceae. I. Growth in *Laminaria Saccharina* (L.) Lamour. *Journal of the Marine Biological Association of the United Kingdom, 27*, 651–709. https://doi.org/10.1017/S0025315400056071

Pearson, R. K. (2011). Exploring Data in Engineering, the Sciences, and Medicine. Oxford University Press. 770 pp.

Pedersen, M. F., Filbee-Dexter, K., Norderhaug, K. M., Fredriksen, S., Frisk, N. L., Fagerli, C. W., & Wernberg, T. (2020). Detrital carbon production and export in high latitude kelp forests. *Oecologia*, *192*, 227–39. https://doi.org/10.1007/s00442-019-04573-z

Pentecost, A. (1978). Calcification and photosynthesis in *Corallina officinalis* L. using the $^{14}CO_2$ method. *British Phycological Journal, 13*, 383–390. https://doi.org/10.1080/00071617800650431

Pessarrodona, A., Filbee-Dexter, K., Krumhansl, K. A., Moore, P. J., & Wernberg, T. (2022). A global dataset of seaweed net primary productivity. *Scientific Data*, *9*, 484. https://doi.org/10.1038/s41597-022-01554-5

Pessarrodona, A., Foggo, A., & Smale, D. A. (2019). Can ecosystem functioning be maintained despite climate-driven shifts in species composition? Insights from novel marine forests. *Journal of Ecology, 107*, 91–104. https://doi.org/10.1111/1365-2745.13053

Pessarrodona, A., Moore, P. J., Sayer, M. D. J., & Smale, D. A. (2018). Carbon assimilation and transfer through kelp forests in the NE Atlantic is diminished under a warmer ocean climate. *Global Change Biology, 24*, 4386–98. https://doi.org/10.1111/gcb.14303

Pfister, C. A., Altabet, M. A., & Weigel, B. L. (2019). Kelp beds and their local effects on seawater chemistry, productivity, and microbial communities. *Ecology, 100*, e02798. https://doi.org/10.1002/ecy.2798

Phelps, C. M., Boyce, M. C., & Huggett, M. J. (2017). Future climate change scenarios differentially affect three abundant algal species in southwestern Australia. *Marine Environmental Research, 126*, 69–80. https://doi.org/10.1016/j.marenvres.2017.02.008

Pierrot, D., Lewis, E., & Wallace, D. W. R. (2006). MS Excel program developed for CO_2 system calculations. ORNL/CDIAC-105. Carbon Dioxide Information Analysis Center, Oak Ridge National Laboratory, US Department of Energy, Oak Ridge, Tennessee.

Platt, T., Gallegos, C. L., & Harrison, W. G. (1980). Photoinhibition of photosynthesis in natural assemblages of marine phytoplankton. *Journal of Marine Research, 38*, 687–701.

Poloczanska, E. S., Brown, C. J., Sydeman, W. J., Kiessling, W., Schoeman, D. S., Moore, P. J., Brander, K., Bruno, J. F., Buckley, L. B., Burrows, M. T., Duarte, C. M., Halpern, B. S., Holding, J., Kappel, C. V., O'Connor, M. I., Pandolfi, J. M., Parmesan, C., Schwing, F., Thompson, S. A., & Richardson, A. J. (2013). Global imprint of climate change on marine life. *Nature Climate Change, 3*, 919–925. http://doi.org/10.1038/nclimate1958

Poorter, H. (1988). Interspecific variation in the growth response of plants to an elevated ambient CO_2 concentration. *In:* Rozema, J., Lambers, H., van de Geijn, S. C., & Cambridge, M. L. [Eds.], *CO_2 and Biosphere.* Advances in Vegetation Science, vol. 14. Springer, Dordrecht, pp. 77-97. https://doi.org/10.1007/978-94-011-1797-5_6

Porzio, L., Buia, M. C., Hall-Spencer, J. M. (2011). Effects of ocean acidification on macroalgal communities. *Journal of Experimental Marine Biology and Ecology, 400*, 278–287. https://doi.org/10.1016/j.jembe.2011.02.011

Pueschel, C. M., & Korb, R. E. (2001). Storage of nitrogen in the form of protein bodies in the kelp *Laminaria solidungula*. *Marine Ecology Progress Series, 218*, 107–14. https://doi.org/10.3354/meps218107

Queirós, A. M., Stephens, N., Widdicombe, S., Tait, K., McCoy, S. J., Ingels, J., Rühl, S., Airs, R., Beesley, A., Carnovale, G., Cazenave, P., Dashfield, S., Hua, E., Jones, M., Lindeque, P., McNeill, C. L., Nunes, J., Parry, H., Pascoe, C., Widdicombe, C., Smyth, T., Atkinson, A., Krause-Jensen, D., & Somerfield, P. J. (2019). Connected macroalgal-sediment systems: blue carbon and food webs in the deep coastal ocean. *Ecological Monographs, 89*, e01366. https://doi.org/10.1002/ecm.1366

R Core Team. (2022). R: A language and environment for statistical computing. R Foundation for Statistical Computing, Vienna, Austria. https://www.R-project.org/

Ragazzola, F., Foster, L. C., Form, A., Anderson, P. S. L., Hansteen, T. H., & Fietzke, J. (2012). Ocean acidification weakens the structural integrity of coralline algae. *Global Change Biology, 18*, 2804–2812. https://doi.org/10.1111/j.1365-2486.2012.02756.x

Ragazzola, F., Foster, L. C., Form, A., Büscher, J., Hansteen, T. H., & Fietzke, J. (2013). Phenotypic plasticity of coralline algae in a high CO_2 world. *Ecology and Evolution, 3*, 3436–3446. https://doi.org/10.1002/ece3.723

Ragazzola, F., Foster, L. C., Jones, C. J., Scott, T. B., Fietzke, J., Kilburn, M. R., & Schmidt, D. N. (2016). Impact of high CO_2 on the geochemistry of the coralline algae *Lithothamnion glaciale*. *Science Reports, 6,* 20572. https://doi.org/10.1038/srep20572

Rassweiler, A., Arkema, K. K., Reed, D. C., Zimmerman, R. C., & Brzezinski, M. A. (2008). Net primary production, growth, and standing crop of *Macrocystis pyrifera* in Southern California: *Ecological Archives* E089-119. *Ecology*, *89*, 2068. https://doi.org/10.1890/07-1109.1

Rassweiler, A., Reed, D. C., Harrer, S. L., & Nelson, J. C. (2018). Improved estimates of net primary production, growth, and standing crop of *Macrocystis pyrifera* in Southern California. *Ecology, 99*, 2132. https://doi.org/10.1002/ecy.2440

Raven, J. A., & Geider, R. J. (1988). Temperature and algal growth. *New Phytologist, 110*(4), 441–461. https://doi.org/10.1111/j.1469-8137.1988.tb00282.x

Raven, J. A., Johnston, A. M., Kübler, J. E., Korb, R., McInroy, S. G., Handley, L. L., Scrimgeour, C. M., Walker, D. I., Beardall, J., Vanderklift, M., Fredriksen, S., & Dunton, K. H. (2002). Mechanistic interpretation of carbon isotope discrimination by marine macroalgae and seagrasses. *Functional Plant Biology, 29*(3), 355–378. https://doi.org/10.1071/pp01201

Raymond, W. W., Tinker, M. T., Kissling, M. L., Benter, B., Gill, V. A., & Eckert G. L. (2019). Location-specific factors influence patterns and effects of subsistence sea otter harvest in Southeast Alaska. *Ecosphere, 10*, e02874. https://doi.org/10.1002/ecs2.2874

Reed, D. C., & Brzezinski, M. A. (2009). Kelp forests. *In:* Laffoley, D. & Grimsditch, G. [Eds.] *The Management of Natural Coastal Carbon Sinks*. IUCN, Gland, Switzerland. pp. 31-7.

Reed, D. C., & Foster, M. S. (1984). The effects of canopy shadings on algal recruitment and growth in a giant kelp forest. *Ecology, 65*, 937–948. https://doi.org/10.2307/1938066

Reed, D. C., Rassweiler, A., & Arkema, K. K. (2008). Biomass rather than growth rate determines variation in net primary production by giant kelp. *Ecology*, 89, 2493–505. https://doi.org/10.1890/07-1106.1

Reed, D., Rassweiler, A., & Arkema, K. K. (2009). Density derived estimates of standing crop and net primary production in the giant kelp *Macrocystis pyrifera*. *Marine Biology, 156*(10), 2077–2083. https://doi.org/10.1007/s00227-009-1238-6

Ries, J. B. (2011). Skeletal mineralogy in a high-CO_2 world. *Journal of Experimental Marine Biology and Ecology, 403*, 54–64. https://doi.org/10.1016/j.jembe.2011.04.006

Roberts, R. D., Kühl, M., Glud, R. N., & Rysgaard, S. (2002). Primary production of crustose coralline red algae in a high Arctic fjord. *Journal of Phycology, 38*, 273–283. https://doi.org/10.1046/j.1529-8817.2002.01104.x

Rodríguez, A., Clemente, S., Brito, A., & Hernández, J. C. (2018). Effects of ocean acidification on algae growth and feeding rates of juvenile sea urchins. *Marine Environmental Research, 140*, 382–389. https://doi.org/10.1016/j.marenvres.2018.07.004

Rodriguez, G. E., Reed, D. C., & Holbrook, S. J. (2016). Blade life span, structural investment, and nutrient allocation in giant kelp. *Oecologia*, 182, 397–404. https://doi.org/10.1007/s00442-016-3674-6

Roleda, M. Y., Boyd, P. W., & Hurd, C. L. (2012). Before ocean acidification: calcified chemistry lessons. *Journal of Phycology, 48*, 840–843. https://doi.org/10.1111/j.1529-8817.2012.01195.x.

Roleda, M. Y., Cornwall, C. E., Feng, Y., McGraw, C. M., Smith, A. M., & Hurd, C. L. (2015). Effect of ocean acidification and pH fluctuations on the growth and

development of coralline algal recruits, and an associated benthic algal assemblage. *PLoS ONE, 10*, e0140394. https://doi.org/10.1371/journal.pone.0140394

Roleda, M. Y., & Hurd, C. L. (2019). Seaweed nutrient physiology: application of concepts to aquaculture and bioremediation. *Phycologia, 58*(5), 552–562. https://doi.org/10.1080/00318884.2019.1622920

Rosenblatt, A. E., & Schmitz, O. J. (2016). Climate change, nutrition, and bottom-up and top-down food web processes. *Trends in Ecology & Evolution, 31*(12), 965–975. https://doi.org/10.1016/j.tree.2016.09.009

Ross, F., Tarbuck, P., & Macreadie, P. I. (2022). Seaweed afforestation at large-scales exclusively for carbon sequestration: critical assessment of risks, viability and the state of knowledge. *Frontiers in Marine Science, 9*, 1015612. http://doi.org/10.3389/fmars.2022.1015612

Ross, R., Jackson, J., & Hannah, C. (2021). The northeast pacific: update on marine heatwave status and trends. *PICES Press, 29*, 46–48.

Russell, B. D., & Connell, S. D. (2007). Response of grazers to sudden nutrient pulses in oligotrophic versus eutrophic conditions. *Marine Ecology Progress Series, 349*, 73–80. https://doi.org/10.3354/meps07097

Russell, B. D., Passarelli, C. A., & Connell, S. D. (2011). Forecasted CO_2 modifies the influence of light in shaping subtidal habitat. *Journal of Phycology, 47*, 744–752. https://doi.org/10.1111/j.1529-8817.2011.01002.x

Sanford, E., Roth, M. S., Johns, G. C., Wares, J. P., & Somero, G. N. (2003). Local selection and latitudinal variation in a marine predator-prey interaction. *Science, 300*, 1135–1137. https://doi.org/10.1126/science.1083437

Scheschonk, L., Becker, S., Hehemann, J.-H., Diehl, N., Karsten, U., & Bischof, K. (2019). Arctic kelp eco-physiology during the polar night in the face of global warming: a crucial role for laminarin. *Marine Ecology Progress Series, 611*, 59–74. https://doi.org/10.3354/meps12860

Schiel, D. R., & Foster, M. S. (2015). *The Biology and Ecology of Giant Kelp Forests*. University of California Press, Oakland. 412 pp.

Schlenger, A. J., Beas-Luna, R., & Ambrose, R. F. (2021). Forecasting ocean acidification impacts on kelp forest ecosystems. *PLoS ONE, 16*(4), e0236218. https://doi.org/10.1371/journal.pone.0236218

Schmid, M., Fernández, P. A., Gaitán-Espitia, J. D., Virtue, P., Leal, P. P., Revill, A. T., Nichols, P. D., & Hurd, C. L. (2020). Stress due to low nitrate availability reduces the biochemical acclimation potential of the giant kelp *Macrocystis pyrifera* to high temperature. *Algal Research, 47*, 101895. https://doi.org/10.1016/j.algal.2020.101895

Schoenrock, K. M., Schram, J. B., Amsler, C. D., McClintock, J. B., Angus, R. A., & Vohra, Y. K. (2016). Climate change confers a potential advantage to fleshy Antarctic crustose macroalgae over calcified species. *Journal of Experimental Marine Biology and Ecology, 474*, 58–66. https://doi.org/10.1016/j.jembe.2015.09.009

Seibold, S., Cadotte, M. W., MacIvor, J. S., Thorn, S., & Müller, J. (2018). The necessity of multitrophic approaches in community ecology. *Trends in Ecology & Evolution, 33*(10), 754–764. https://doi.org/10.1016/j.tree.2018.07.001

Shanley, C. S., Pyare, S., Goldstein, M. I., Alaback, P. B., Albert, D. M., Beier, C. M., Brinkman, T. J., Edwards, R. T., Hood, E., MacKinnon, A., McPhee, M. V., Patterson, T. M., Suring, L. H., Tallmon, D. A., & Wipfli, M. S. (2015). Climate change implications in the northern coastal temperate rainforest of North America. *Climatic Change, 130*(2), 155–170. https://doi.org/10.1007/s10584-015-1355-9

Shears, N. T., & Babcock, R. C. (2007). Quantitative Description of Mainland New Zealand's Shallow Subtidal Reef Communities, Science for Conservation 280, Department of Conservation, Wellington.

Short, J. A., Kendrick, G. A., Falter, J., McCulloch, M. T. (2014). Interactions between filamentous turf algae and coralline algae are modified under ocean acidification. *Journal of Experimental Marine Biology and Ecology, 456*, 70–77. https://doi.org/10.1016/j.jembe.2014.03.014

Short, J. A., Pedersen, O., & Kendrick, G. A. (2015). Turf algal epiphytes metabolically induce local pH increase, with implications for underlying coralline algae under ocean acidification. *Estuarine and Coastal Shelf Science, 164*, 463–470. https://doi.org/10.1016/j.ecss.2015.08.006

Siedlecki, S. A., Pilcher, D. J., Hermann, A. J., Coyle, K., & Mathis, J. (2017). The importance of freshwater to spatial variability of aragonite saturation state in the Gulf of Alaska. *Journal of Geophysical Research Oceans, 122*, 8482–8502. https://doi.org/10.1002/2017JC012791

Smale, D. A. (2020). Impacts of ocean warming on kelp forest ecosystems. *New Phytologist, 225*, 1447–54. https://doi.org/10.1111/nph.16107

Smale, D. A., Pessarrodona, A., King, N., & Moore, P. J. (2021). Examining the production, export, and immediate fate of kelp detritus on open-coast subtidal reefs in the Northeast Atlantic. *Limnology and Oceanography, 9999*, 1–14. https://doi.org/10.1002/lno.11970

Smith, S. V., & Key, G. S. (1975). Carbon dioxide and metabolism in marine environments. *Limnology and Oceanography, 20*, 493–495. https://doi.org/10.4319/lo.1975.20.3.0493

Stabeno, P. J., Bond, N. A., Kachel, N. B., Ladd, C., Mordy, C. W., & Strom, S. L. (2016). Southeast Alaskan shelf from southern tip of Baranof Island to Kayak Island: currents, mixing and chlorophyll-a. *Deep Sea Research Part II: Topical Studies in Oceanography, 132*, 6–23. https://doi.org/10.1016/j.dsr2.2015.06.018

Steinacher, M., Joos, F., Frolicher, T. L., Plattner, G.-K., Doney, S.C. (2009). Imminent ocean acidification in the Arctic projected with the NCAR global coupled carbon cycle-climate model. *Biogeoscience, 6*, 515-533. https://doi.org/10.5194/bg-6-515-2009

Steinberg, P. D. (1985). Feeding preferences of *Tegula funebralis* and chemical defenses of marine brown algae. *Ecological Monographs, 55*(3), 333–349. https://doi.org/10.2307/1942581

Stekoll, M. S. (2019). The seaweed resources of Alaska. *Botanica Marina*, 62, 227–35. https://doi.org/10.1515/bot-2018-0064

Stekoll, M. S., & Else, P. V. (1990). Cultivation of *Macrocystis integrifolia* (Laminariales, Phaeophyta) in southeastern Alaskan waters. *Hydrobiologia, 204/205*, 445–51. https://doi.org/10.1007/BF00040269

Stekoll, M. S., Peeples, T. N., & Raymond, A. E. T. (2021). Mariculture research of *Macrocystis pyrifera* and *Saccharina latissima* in Southeast Alaska. *Journal of the World Aquaculture Society*. 52:1031–46. https://doi.org/10.1111/jwas.12765

Steneck, R. S., Graham, M. H., Bourque, B. J., Corbett, D., Erlandson, J. M., Estes, J. A., & Tegner, M. J. (2002). Kelp forest ecosystems: biodiversity, stability, resilience and future. *Environmental Conservation, 29*, 436–459. https://doi.org/10.1017/S0376892902000322

Stephens, T. A., & Hepburn, C. D. (2016). A kelp with integrity: *Macrocystis pyrifera* prioritises tissue maintenance in response to nitrogen fertilisation. *Oecologia*, 182, 71–84. https://doi.org/10.1007/s00442-016-3641-2

Stewart, H. L., Fram, J. P., Reed, D. C., Williams, S. L., Brzezinski, M. A., MacIntyre, S., & Gaylord, B. (2009). Differences in growth, morphology and tissue carbon and nitrogen of *Macrocystis pyrifera* within and at the outer edge of a giant kelp forest in California, USA. *Marine Ecology Progress Series, 375*, 101–12. https://doi.org/10.3354/meps07752

Strom, S. L., Fredrickson, K. A., & Bright, K. J. (2016). Spring phytoplankton in the eastern coastal Gulf of Alaska: photosynthesis and production during high and low bloom years. *Deep Sea Research Part II: Topical Studies in Oceanography, 132*, 107–121. https://doi.org/10.1016/j.dsr2.2015.05.003

Suggitt, A. J., Gillingham, P. K., Hill, J. K., Huntley, B., Kunin, W. E., Roy, D. B., & Thomas, C. D. (2011). Habitat microclimates drive fine-scale variation in extreme temperatures. *Oikos, 120*, 1–8. https://doi.org/10.1111/j.1600-0706.2010.18270.x

Swanson, A. K., & Fox, C. H. (2007). Altered kelp (Laminariales) phlorotannins and growth under elevated carbon dioxide and ultraviolet-B treatments can influence associated intertidal food webs. *Global Change Biology, 13*(8), 1696–1709. https://doi.org/10.1111/j.1365-2486.2007.01384.x

Sydeman, W. J., & Bograd, S. J. (2009). Marine ecosystems, climate and phenology: introduction. *Marine Ecology Progress Series, 393*, 185–188. https://doi.org/10.3354/meps08382

Takahashi, T., Olafsson, J., Goddard, J. G., Chipman, D. W., & Sutherland, S. C. (1993). Seasonal variation of CO_2 and nutrients in the high-latitude surface oceans: a comparative study. *Global Biogeochemical Cycles, 7*(4), 843–878. https://doi.org/10.1029/93GB02263

Tebben, J., Motti, C. A., Siboni, N., Tapiolas, D. M., Negri, A. P., Schupp, P. J., Kitamura, M., Hatta, M., Steinberg, P. D., & Harder, T. (2015). Chemical mediation of coral larval settlement by crustose coralline algae. *Scientific Reports, 5*, 10803. https://doi.org/10.1038/srep10803

Teichert, S., & Freiwald, A. (2014). Polar coralline algal $CaCO_3$-production rates correspond to intensity and duration of the solar radiation. Biogeoscience, 11, 833–842. https://doi.org/10.5194/bg-11-833-2014

Terrer, C., Jackson, R. B., Prentice, I. C., Keenan, T. F., Kaiser, C., Vicca, S., Fisher, J. B., Reich, P. B., Stocker, B. D., Hungate, B. A., Peñuelas, J., McCallum, I., Soudzilovskaia, N. A., Cernusak, L. A., Talhelm, A. F., Van Sundert, K., Piao, S., Newton, P. C. D., Hovenden, M. J., Blumenthal, D. M., Liu, Y. Y., Müller, C., Winter, K., Field, C. B., Viechtbauer, W., Van Lissa, C. J., Hoosbeek, M. R., Watanabe, M., Koike, T., Leshyk, V. O., Polley, H. W.,

Franklin, O. (2019). Nitrogen and phosphorus constrain the CO_2 fertilization of global plant biomass. *Nature Climate Change, 9*(9), 684–689. https://doi.org/10.1038/s41558-019-0545-2

Thiers, B. (2021). Index Herbariorum: a global directory of public herbaria and associated staff, New York Botanical Garden Virtual Herbarium, accessed May 25, 2021. http://sweetgum.nybg.org/ih/

Tian, R. C., Vézina, A. F., Starr, M., & Saucier, F. (2001). Seasonal dynamics of coastal ecosystems and export production at high latitudes: a modeling study. *Limnology and Oceanography, 46*(8), 1845–1859. https://doi.org/10.4319/lo.2001.46.8.1845

Twist, B. A., Cornwall, C., McCoy, S., Gabrielson, P., Martone, P., & Nelson, W. (2020). The need to employ reliable and reproducible species identifications in coralline algal research. *Marine Ecology Progress Series, 654*, 225–231. https://doi.org/10.3354/meps13506

Twist, B. A., Neill, K. F., Bilewitch, J., Jeong, S. Y., Sutherland, J. E., & Nelson, W. A. (2019). High diversity of coralline algae in New Zealand revealed: knowledge gaps and implications for future research. *PLoS ONE, 14*, e0225645. https://doi.org/10.1371/journal.pone.0225645

Ullah, H., Nagelkerken, I., Goldenberg, S. U., & Fordham, D. A. (2018). Climate change could drive marine food web collapse through altered trophic flows and cyanobacterial proliferation. *PLoS Biology, 16*(1), e2003446. https://doi.org/10.1371/journal.pbio.2003446

Umanzor, S., Sandoval-Gil, J., Sánchez-Barredo, M., Ladah, L. B., Ramírez-García, M.-M., & Zertuche-González, J. A. (2021). Short-term stress responses and recovery of giant kelp (*Macrocystis pyrifera*, Laminariales, Phaeophyceae) juvenile sporophytes to a simulated marine heatwave and nitrate scarcity. *Journal of Phycology, 57*(5), 1604–1618. https://doi.org/10.1111/jpy.13189

van Tussenbroek, B. I. (1989). Seasonal growth and composition of fronds of *Macrocystis pyrifera* in the Falkland Islands. *Marine Biology,* 100, 419–30. https://doi.org/10.1007/BF00391158

Vásquez-Elizondo, R. M., & Enríquez, S. (2016). Coralline algal physiology is more adversely affected by elevated temperature than reduced pH. *Scientific Reports, 6*, 19030. https://doi.org/10.1038/srep19030

Vizzini, S., Martínez-Crego, B., Andolina, C., Massa-Gallucci, A., Connell, S. D., Gambi, M. C. (2017). Ocean acidification as a driver of community simplification via the collapse of higher-order and rise of lower-order

consumers. *Scientific Reports, 7*, 4018. https://doi.org/10.1038/s41598-017-03802-w

von Biela, V. R., Newsome, S. D., Bodkin, J. L., Kruse, G. H., & Zimmerman, C. E. (2016) Widespread kelp-derived carbon in pelagic and benthic nearshore fishes suggested by stable isotope analysis. *Estuarine, Coastal and Shelf Science, 181*, 364–374. https://doi.org/10.1016/j.ecss.2016.08.039

Wahl, M., Werner, F. J., Buchholz, B., Raddatz, S., Graiff, A., Matthiessen, B., Karsten, U., Hiebenthal, C., Hamer, J., Ito, M., Gülzow, E., Rilov, G., & Guy-Haim, T. (2020). Season affects strength and direction of the interactive impacts of ocean warming and biotic stress in a coastal seaweed ecosystem. *Limnology and Oceanography, 65*(4), 807–827. https://doi.org/10.1002/lno.11350

Walker, A. P., De Kauwe, M. G., Bastos, A., Belmecheri, S., Georgiou, K., Keeling, R. F., McMahon, S. M., Medlyn, B. E., Moore, D. J. P., Norby, R. J., Zaehle, S., Anderson-Teixeira, K. J., Battipaglia, G., Brienen, R. J. W., Cabugao, K. G., Cailleret, M., Campbell, E., Canadell, J. G., Ciais, P., Craig, M. E., Ellsworth, D. S., Farquhar, G. D., Fatichi, S., Fisher, J. B., Frank, D. C., Graven, H., Gu, L., Haverd, V., Heilman, K., Heimann, M., Hungate, B. A., Iversen, C. M., Joos, F., Jiang, M., Keenan, T. F., Knauer, J., Körner, C., Leshyk, V. O., Leuzinger, S., Liu, Y., MacBean, N., Malhi, Y., McVicar, T. R., Penuelas, J., Pongratz, J., Shafer Powell, A., Riutta, T., Sabot, M. E. B., Schleucher, J., Sitch, S., Smith, W. K., Sulman, B., Taylor, B., Terrer, C., Torn, M. S., Treseder, K. K., Trugman, A. T., Trumbore, S. E., van Mantgem, P. J., Voelker, S. L., Whelan, M. E., Zuidema, P. A. (2021). Integrating the evidence for a terrestrial carbon sink caused by increasing atmospheric CO_2. *New Phytologist, 229*(5), 2413–2445. https://doi.org/10.1111/nph.16866

Wei, Z., Long, C., Yang, F., Long, L., Huo, Y., Ding, D., & Mo, J. (2020). Increased irradiance availability mitigates the physiological performance of species of the calcifying green macroalga *Halimeda* in response to ocean acidification. *Algal Research, 48*, 101906. https://doi.org/10.1016/j.algal.2020.101906

Weigel, B. L., & Pfister, C. A. (2021). The dynamics and stoichiometry of dissolved organic carbon release by kelp. *Ecology*, *102*, e03221. https://doi.org/10.1002/ecy.3221

Werner, F. J., Graiff, A., & Matthiessen, B. (2016). Temperature effects on seaweed-sustaining top-down control vary with season. *Oecologia, 180*, 889–901. http://doi.org/10.1007/s00442-015-3489-x

Wheeler, W. N., & Druehl, L. D. (1986). Seasonal growth and productivity of *Macrocystis integrifolia* in British Columbia, Canada. *Marine Biology, 90*, 181–6. https://doi.org/10.1007/BF00569125

Wheeler, W. N., & Srivastava, L. M. (1984). Seasonal nitrate physiology of *Macrocystis integrifolia* Bory. *Journal of Experimental Marine Biology and Ecology, 76*(1), 35–50. https://doi.org/10.1016/0022-0981(84)90015-7

Whitehead, C., Evans, W., Lanphier, K., Peterson, W., Kennedy, E., & Hales, B. (2022). High-resolution record of surface seawater CO_2 content from June 2017 to April 2021 collected in Sitka Harbor, Alaska, USA. (NCEI Accession 0247208). NOAA National Centers for Environmental Information. Dataset. https://doi.org/10.25921/9vnv-0g64

Wickham, S. B., Darimont, C. T., Reynolds, J. D., & Starzomski, B. M. (2019). Species-specific wet-dry mass calibrations for dominant Northeastern Pacific Ocean macroalgae and seagrass. *Aquatic Botany, 152*, 27–31. https://doi.org/10.1016/j.aquabot.2018.09.006

Wiencke, C., Gómez, I., & Dunton, K. (2009). Phenology and seasonal physiological performance of polar seaweeds. *Botanica Marina, 52*(6), 585–592. https://doi.org/10.1515/BOT.2009.078

Wilmers, C. C., Estes, J. A., Edwards, M., Laidre, K. L., & Konar, B. (2012). Do trophic cascades affect the storage and flux of atmospheric carbon? An analysis of sea otters and kelp forests. *Frontiers in Ecology and the Environment, 10*, 409–15. https://doi.org/10.1890/110176

Winter, B. (2013). Linear models and linear mixed effects models in R with linguistic applications. *arXiv*, 1308.5499. http://arxiv.org/abs/1308.5499

Wright, L., Pessarrodona, A., & Foggo, A. (2022). Climate-driven shifts in kelp forest composition reduce carbon sequestration potential. *Global Change Biol*ogy, *28*, 5514–5531. https://doi.org/10.1111/gcb.16299

Wulff, A., Iken, K., Quartino, M. L., Al-Handal, A., Wiencke, C., & Clayton, M. N. (2009). Biodiversity, biogeography and zonation of marine benthic micro- and macroalgae in the Arctic and Antarctic. *Botanica Marina,* 52, 491–507. https://doi.org/10.1515/BOT.2009.072

Yong, W. T. L, Thien, V. Y., Rupert, R., & Rodrigues, K. F. (2022). Seaweed: a potential climate change solution. *Renewable and Sustainable Energy Reviews, 159*, 112222. https://doi.org/10.1016/j.rser.2022.112222.

Zhang, X., Xu, D., Han, W., Wang, Y., Fan, X., Loladze, I., Gao, G., Zhang, Y., Tong, S., & Ye, N. (2021). Elevated CO_2 affects kelp nutrient quality: a case study of *Saccharina japonica* from CO_2 -enriched coastal mesocosm systems. *Journal of Phycology, 57*(1), 379–391. https://doi.org/10.1111/jpy.13097